European Commission

JRC SCIENTIFIC AND POLICY REPORTS

Methodology for systemic seismic vulnerability assessment of buildings, infrastructures, networks and socio-economic impacts

SYNER-G Reference Report 1

Editors: Paolo Franchin

Reviewers: Amr Elnashai

Publishing Editors: Fabio Taucer and Ufuk Hancilar

2013

Report EUR 25884 EN

Joint Research Centre

European Commission
Joint Research Centre
Institute for the Protection and Security of the Citizen

Contact information
Fabio Taucer
Address: Joint Research Centre, Via Enrico Fermi 2749, TP 480, 21027 Ispra (VA), Italy
E-mail: fabio.taucer@jrc.ec.europa.eu
Tel.: +39 0332 78 5886
Fax: +39 0332 78 9049

http://elsa.jrc.ec.europa.eu/
http://www.jrc.ec.europa.eu/

JRC80613

EUR 25884 EN

ISBN 978-92-79-28975-0

ISSN 1831-9424

doi:10.2788/69238

Luxembourg: Publications Office of the European Union, 2013

Printed in Ispra (Va) - Italy

D 8.7

DELIVERABLE

PROJECT INFORMATION

Project Title:	**Systemic Seismic Vulnerability and Risk Analysis for Buildings, Lifeline Networks and Infrastructures Safety Gain**
Acronym:	SYNER-G
Project N°:	244061
Call N°:	FP7-ENV-2009-1
Project start:	01 November 2009
Duration:	36 months

DELIVERABLE INFORMATION

Deliverable Title:	**D8.7 - Methodology for systemic seismic vulnerability assessment of buildings, infrastructures, networks and socio-economic impacts**
Date of issue:	31 March 2013
Work Package:	WP8 – Guidelines, recommendations and dissemination
Deliverable/Task Leader:	Joint Research Centre
Editor:	Paolo Franchin (UROMA)
Reviewer:	Amr Elnashai (UILLINOIS)

REVISION: Final

SEVENTH FRAMEWORK PROGRAMME

Project Coordinator:	Prof. Kyriazis Pitilakis
Institution:	Aristotle University of Thessaloniki
e-mail:	kpitilak@civil.auth.gr
fax:	+ 30 2310 995619
telephone:	+ 30 2310 995693

The SYNER-G Consortium

Aristotle University of Thessaloniki (Co-ordinator) (AUTH)

Vienna Consulting Engineers (VCE)

Bureau de Recherches Geologiques et Minieres (BRGM)

European Commission – Joint Research Centre (JRC)

Norwegian Geotechnical Institute (NGI)

University of Pavia (UPAV)

University of Roma “La Sapienza” (UROMA)

Middle East Technical University (METU)

Analysis and Monitoring of Environmental Risks (AMRA)

University of Karlsruhe (KIT-U)

University of Patras (UPAT)

Willis Group Holdings (WILLIS)

Mid-America Earthquake Center, University of Illinois (UILLINOIS)

Kobe University (UKOBE)

Foreword

SYNER-G is a European collaborative research project funded by European Commission (Seventh Framework Program, Theme 6: Environment) under Grant Agreement no. 244061. The primary purpose of SYNER-G is to develop an integrated methodology for the systemic seismic vulnerability and risk analysis of buildings, transportation and utility networks and critical facilities, considering for the interactions between different components and systems. The whole methodology is implemented in an open source software tool and is validated in selected case studies. The research consortium relies on the active participation of twelve entities from Europe, one from USA and one from Japan. The consortium includes partners from the consulting and the insurance industry.

SYNER-G developed an innovative methodological framework for the assessment of physical as well as socio-economic seismic vulnerability and risk at the urban/regional level. The built environment is modelled according to a detailed taxonomy, grouped into the following categories: buildings, transportation and utility networks, and critical facilities. Each category may have several types of components and systems. The framework encompasses in an integrated fashion all aspects in the chain, from hazard to the vulnerability assessment of components and systems and to the socio-economic impacts of an earthquake, accounting for all relevant uncertainties within an efficient quantitative simulation scheme, and modelling interactions between the multiple component systems.

The methodology and software tools are validated in selected sites and systems in urban and regional scale: city of Thessaloniki (Greece), city of Vienna (Austria), harbour of Thessaloniki, gas system of L'Aquila in Italy, electric power network, roadway network and hospital facility again in Italy.

The scope of the present series of Reference Reports is to document the methods, procedures, tools and applications that have been developed in SYNER-G. The reports are intended to researchers, professionals, stakeholders as well as representatives from civil protection, insurance and industry areas involved in seismic risk assessment and management.

Prof. Kyriazis Pitilakis
Aristotle University of Thessaloniki, Greece
Project Coordinator of SYNER-G

Fabio Taucer and Ufuk Hancilar
Joint Research Centre
Publishing Editors of the SYNER-G Reference Reports

Abstract

The SYNER-G project aims at developing a methodology to evaluate the vulnerability to earthquakes of a complex system of interconnected infrastructural systems of regional/urban extension. This report describes the developed methodology, which is based on smart simulation of an object-oriented model of the system to account for the uncertainties involved (in the hazard, as well as in the system) and to tackle the complexity of the interactions existing within each system between its components, and across the systems. The methodology integrates within the same framework the hazard, the physical vulnerability and the social consequences/impact. The strength of the object-oriented foundation of the model is that it can be easily expanded and developed step-wise, allowing for multiple choices for each intermediate model. This allows also the integration of previous research results and models within a larger simulation framework for distributed infrastructural systems. The developed methodology is implemented in the SYNER-G software toolbox.

Keywords: infrastructural systems, interdependence, uncertainty, vulnerability, impact, object-oriented model, fragility models, distributed hazard, lifelines, networks, critical facilities, casualties, displaced population, emergency planning

Acknowledgments

The research leading to these results has received funding from the European Community's Seventh Framework Programme [FP7/2007-2013] under grant agreement n° 244061

Deliverable Contributors

AMRA	Iunio Iervolino	Sections 1.6.8, 1.6.9, 2.4.5
	Simona Esposito	Sections 1.6.8, 1.6.9, 2.4.5
AUTH	Sotiris Argyroudis	Sections 1.6.3, 1.6.5, 1.6.6, 2.3.3
	Kalliopi Kakderi	Sections 1.6.3, 1.6.5, 1.6.6, 2.3.3
	Jacapo Selva	Sections 2.5.1
BRGM	Pierre Gehl	Sections 1.6.1, 2.3.2, 2.3.4
KIT-U	Bijan Khazai	Sections 2.3.1, 2.3.4
UPAV	Helen Crowley	Sections 2.3.4
	Graeme Weatherill	Sections 2.4.4, 2.4.5
UROMA	Paolo Pinto	Sections 1.2, 1.3, 1.4
	Paolo Franchin	Sections 1, 2, 3
	Francesco Cavalieri	Sections 1.6, 2.3.4, 2.3.6, 2.3.7, 3
	Alessio Lupoi	Sections 1.6.2

Table of Contents

Foreword ..... **i**
Abstract ..... **iii**
Acknowledgments ..... **v**
Deliverable Contributors ..... **vii**
Table of Contents ..... **ix**
List of Figures ..... **xiii**
List of Tables ..... **xvii**
1 Introduction **1**
1.1 CONTENT OF THE REPORT 1
1.2 DEFINITIONS 1
1.3 TIME, SPACE AND STAKEHOLDER DIMENSIONS IN A SYSTEMIC STUDY 4
1.4 SPATIAL CHARACTERISATION AND APPROACH LEVEL 5
1.5 THE SYNER-G TAXONOMY 6
1.5.1 System 1 - Building aggregates (BDG) 6
1.5.2 System 2 – Health-care system (HCS) 6
1.5.3 System 3 – Harbour (HBRS) 7
1.5.4 System 4 – Road network (RDN) 7
1.5.5 System 5 – Railway network (RWN) 8
1.5.6 System 6 – Water-supply network (WSN) 8
1.5.7 System 7 – Waste-water network (WWN) 9
1.5.8 System 8 – Fire-fighting system (HCS) 9
1.5.9 System 9 – Electric power network (EPN) 9
1.5.10 System 10 – Natural gas system (GAS) 10
1.5.11 System 11 – Oil system (OIL) 10
1.6 A SELECTED LITERATURE REVIEW 11
1.6.1 Buildings (BDG) 11
1.6.2 Health-care system (HCS) 15
1.6.3 Harbour (HBR) 17
1.6.4 Road network (RDN) 20
1.6.5 Water-supply network (WSN) 22
1.6.6 Waste-water network (WWN) 25

1.6.7 Fire-fighting system (FFS) 29
1.6.8 Electric power network (EPN) 30
1.6.9 Natural Gas system (GAS) 33
1.6.10 Oil system (OIL) 34
2 The SYNER-G methodology 35
2.1 INTRODUCTION 35
2.2 OBJECT-ORIENTED MODEL: GENERAL 38
2.2.1 A brief overview of basic concepts in OO modelling 38
2.2.2 Fundamentals of the Unified Modelling Language (UML) 40
2.2.3 Class diagrams of the SYNER-G model 43
2.2.4 Sample object diagrams 49
2.3 INFRASTRUCTURE MODEL 50
2.3.1 Introduction 50
2.3.2 Interdependencies 50
2.3.3 Deterministic link vs. non-deterministic links 54
2.3.4 Selected systems: Buildings (the Region class) 54
2.3.5 Selected systems: The Network, Node and Edge abstract classes 65
2.3.6 Selected systems: Water supply system (the WSS class) 69
2.3.7 Selected systems: Electric power network (the EPN class) 75
2.3.8 Performance indicators 84
2.4 SEISMIC HAZARD MODEL 89
2.4.1 Introduction 89
2.4.2 Model for event generation 90
2.4.3 Model for the spatially distributed intensities (ShakeFields) on rock 90
2.4.4 Modelling of site effects 93
2.4.5 Geotechnical hazards 96
2.5 PROBABILISTIC ANALYSIS 100
2.5.1 Uncertainty modelling 100
2.5.2 Simulation methods 105
2.5.3 Non-simulation methods 111
3 A pilot application 113
3.1 THE TEST CASE 113
3.1.1 Seismic hazard 114
3.1.2 Cities (BDG) 114

3.1.3 The water supply system (WSS) 117
3.1.4 The electric power network (EPN) 118
3.2 VULNERABILITY ANALYSIS 119
3.2.1 Introduction 119
3.2.2 Echo of the input 119
3.2.3 Demand under reference non-seismic conditions 121
3.2.4 Response under seismic conditions 122
References 135

List of Figures

Fig. 1.1 Abstract representation of the Infrastructure 4

Fig. 1.2 The three dimensions in an Infrastructure vulnerability study 5

Fig. 1.3 Illustration of the different categories of components/sub-systems of the Infrastructure 6

Fig. 1.4 Debris obstruction (collapsed RC buildings) 14

Fig. 1.5 Debris obstruction (collapsed buildings confined in two opposite sides, debris volume is 30% of initial volume, friction angle 45°) 14

Fig. 1.6 Example of application, number of obstructed streets by district 15

Fig. 1.7 Demand and capacity “distribution” as a function of peak ground acceleration 16

Fig. 2.1 Integrated evaluation of physical and socio-economic performance indicators 36

Fig. 2.2 The class icon (left) and abstract classes (right) 41

Fig. 2.3 Relationships between classes 42

Fig. 2.4 Highest level class diagram for the Infrastructural vulnerability assessment problem (the grey hatch, as indicated, denotes classes that have been included at the conceptual level but have not yet been implemented; the orange hatch indicates classes that are detailed in the following) 44

Fig. 2.5 Class diagram for the Hazard class (the grey hatch, as indicated, denotes classes that have been included at the conceptual level but have not yet been implemented) 45

Fig. 2.6 Class diagram for the LocalIntensity class (the grey hatch denotes classes that have been included at the conceptual level but have not yet been implemented) 46

Fig. 2.7 Class diagram for the Infrastructure portion of the model (the grey hatch denotes classes included at the conceptual level but not yet implemented) 47

Fig. 2.8 Class diagram for the WSS and EPN classes (the grey hatch denotes classes included at the conceptual level but not yet implemented) 48

Fig. 2.9 Sample WSS (top) and corresponding object-diagram (bottom) 49

Fig. 2.10 Sample EPN (top) and corresponding object-diagram (bottom) 50

Fig. 2.11 State diagram to model the inter-dependencies: sequence in the evaluation of states of the objects and messages (quantities) transmitted between objects .. 53

Fig. 2.12 Raster approach to the discretization of the study region (the region is that of the illustrative example presented in Chapter 3) 56

Fig. 2.13 The evaluateBuildingDamage method of the Region class 58

Fig. 2.14 Mean and individual curves for the (a) yielding and (b) collapse limit states, for low rise bearing wall un-reinforced masonry buildings 59

Fig. 2.15 Mean and individual curves for the (a) yielding and (b) collapse limit states, for RC moment-resisting frame, mid rise, seismically designed, bare, non ductile buildings 60

Fig. 2.16 The evaluateBuildingHabitability method of the Region class 61

Fig. 2.17 Typical topological structures, grid-like (on the left) and tree-like (on the right) 69

Fig. 2.18 High voltage transformer 76

Fig. 2.20 Sketch of a T&D system for an EPN (TL = Transmission Lines, D = Distribution lines, TD [HV→MV] = Transformation (from high to medium voltage) and Distribution station, TD [MV→LV] = Transformation (from medium to low voltage) and Distribution station, L = Load) 76

Fig. 2.23 Fragility functions for three failure modes of 230 kV circuit breakers 83

Fig. 2.24 (from D2.13) Overview of the Shakemap process for strong motion on rock: attenuation of median ground motion (top), generation of field of spatially correlated ground motion residuals (middle) and calculation of ground motion on rock (bottom). Fault source indicated by black line, target sites indicated by black circles 92

Fig. 2.25 The network of random variables modelling the uncertainty in the regional seismic vulnerability assessment problem 102

Fig. 2.26 The sequence of models with associated input and output quantities 103

Fig. 2.27 Sample physical system for Fig. 2.25 104

Fig. 2.28 Sampling densities for the magnitude and intra-event errors/residuals (from Jayaram and baker 2010) 109

Fig. 3.1 The ideal Infrastructure 113

Fig. 3.2 The three cities in the idealized infrastructure 115

Fig. 3.3 The WSS of the idealized Infrastructure (legend in Fig. 3.1) 118

Fig. 3.4 The EPN of the idealized infrastructure (legend in Fig. 3.1) 118

Fig. 3.5 Echo of the input: sub-city districts of each city (see Fig. 3.2), also shown the discretization of the study region into geo-cells with variable size 119

Fig. 3.6 Echo of the input: land-use plan of each city (see Fig. 3.2), also shown the discretization of the study region into geo-cells with variable size 120

Fig. 3.7 Input echo: Building census (BC) areas of each city (see Fig. 3.2) 120

Fig. 3.8 Input echo: population density after projection onto the grid (see Fig. 3.2) 121

Fig. 3.9 WSS: water demand in each cell after projection onto the grid. Dashed lines show relationship between demand nodes and the tributary grid cells 122

Fig. 3.10 EPN: power demand in each cell after projection onto the grid. Dashed lines show relationship between demand nodes and the tributary grid cells 122

Fig. 3.11 Sample simulation of the primary IM (PGA) for a magnitude 7 event in zone 2: (a) circular decay of the 'average' value (ten to the power of μlog+η); (b) field of intra-event residuals, note the clusters of close values caused by spatial

correlation; (c) total shake field; (d) plot of primary IM versus epicentral distance. 123

Fig. 3.12 DamageMap to Masonry buildings for one simulation of a M=7 event 124

Fig. 3.13 DamageMap to RC buildings for one simulation of a M=7 event 124

Fig. 3.14 DamageMap to the WSS for one simulation of a M=7 event..... 125

Fig. 3.15 DamageMap to the EPN for one simulation of a M=7 event: Voltage ratio VR in the grid cells (inactive lines are removed from the plot). Damage level is severe . 126

Fig. 3.16 DamageMap to the EPN for one simulation of a M=7 event: Voltage ratio VR in the grid cells (inactive lines are removed from the plot). Damage level is less severe than in Fig. 3.15 126

Fig. 3.17 Number of deaths for one simulation of a M=7 event..... 127

Fig. 3.18 Number of displaced people (good weather conditions) for one simulation of a M=7 event..... 127

Fig. 3.19 Displaced population in the study area: and close-up on city B (same color code as in Fig. 3.18) for good/bad weather and utility loss present/not present, for the same simulation run as in Fig. 3.18..... 128

Fig. 3.20 Validation of the event generation portion of the seismic hazard model: top left, relative frequency of activation of the three faults from the simulation (light grey) and as specified in the input (black); top right and bottom plots, magnitude PDF from the Gutenberg-Richter law and the histogram of relative frequencies as obtained from simulation 129

Fig. 3.21 Head ratio for all nodes, values averaged on a 10,000 run simulation: independent lifelines (left) and interdependent lifelines (right) 130

Fig. 3.22 Evolution of the mean of the average head ratio (left) and the system serviceability index (right) vs number of samples/runs (interdependent lifelines). 131

Fig. 3.23 Evolution of the mean of the average head ratio (left) and the system serviceability index (right) vs number of samples/runs (independent lifelines) 131

Fig. 3.24 Expected VR contour map; the blue zones indicate the generators' positions ... 132

Fig. 3.25 Mean Annual Frequency (MAF) of exceedance curves of AHR (left) and SSI (right), for both cases of dependent and independent lifelines 132

Fig. 3.26 DCI (left) and UBI (right) indexes for the pipes in WSS 133

Fig. 3.27 Summary results for the whole simulation (10,000 runs). Mean annual rate of exceedance of (a) fatalities and (b) displaced population, as a ratio of total population; (c) different mean annual rates of exceedance obtained considering various levels of interaction of the normalized displaced population (curves refer to city B)..... 134

List of Tables

Table 2.1 Interdependencies for sample system from the Taxonomy 52

Table 2.2 Mean and CoV of the lognormal fragility parameters for low rise bearing wall unreinforced masonry buildings 60

Table 2.3 Correlation coefficient matrix for low rise bearing wall masonry 60

Table 2.4 Mean and CoV of the lognormal fragility parameters for low rise bearing wall unreinforced masonry buildings 60

Table 2.5 Correlation coefficient matrix for reinforced concrete with moment resisting frame buildings, mid rise, seismically designed, bare non ductile model building type 61

Table 2.6 Lethality Ratios by damage level and building type, adapted from (Zuccaro and Cacace, 2011) where five damage states were used 63

Table 2.7 Usability percentages by damage level 63

Table 2.8 Default values proposed for Utility Loss Tolerance Thresholds 64

Table 2.9 Defaults weights proposed for each utility system 64

Table 3.1 Building population distribution in the BC areas, per typology 115

Table 3.2 Fragility curves parameters for each building typology (the IM is PGA) 116

Table 3.3 Socio-economic data (part 1) 116

Table 3.4 Socio-economic data (part 2) 117

Table 3.5 Land Use Plan 117

1 Introduction

1.1 CONTENT OF THE REPORT

This report presents the general methodology developed within the SYNER-G project for the assessment of the seismic vulnerability of an Infrastructure (see definition in Section 1.2). This report starts with an introduction of definitions, terms of reference, the identified taxonomy of infrastructural systems and a brief, non exhaustive review of available technical literature in chapter 1. It them presents in more detail the modelling of a subset of the complete set of infrastructural systems included in the SYNER-G Taxonomy (see Section 1.5) in Chapter 2, and illustrates the methodology with reference to a simple example in Chapter 3.

1.2 DEFINITIONS

The following is a list of definitions employed consistently throughout the SYNER-G set of projects outputs.

- Hazard (seismic)
  - A probabilistic model describing the occurrence (in space/time) of earthquakes, and/or the corresponding intensity at a site. When dealing with a single site the hazard is often represented by the final outcome of a probabilistic seismic hazard analysis, PSHA, (where the above model is the input), i.e. a seismic hazard curve (or surface). The latter yields the annual rate of exceedance of a scalar (or vector) measure of local intensity above (outside) any given threshold. When dealing with a distributed system where the simultaneous intensity at several sites is of interest (conceptually a vector of random, statistically dependent intensity values), the complete model is used (i.e. seismic sources characterization in terms of geometry and activity, plus attenuation laws and a model for spatial correlation amongst intensity measures at different sites).
- Hazard map
  - A map of uniform-hazard or iso-probable intensity values (often, but not exclusively, peak ground acceleration or a spectral ordinate) over a region. Used for design purposes, it cannot be employed in systemic studies since the intensity values are not simultaneous.
- Scenario (seismic)
  - It refers to a single seismic event. It can be presented in terms of the event location, magnitude, faulting style, etc., or in terms of the corresponding distribution of local intensity (e.g. a “shake map”), or, finally, in terms of the event consequences (e.g. a damage map).
- Limit state (or Damage state, or Performance level)

- The state when a demand quantity reaches a corresponding threshold/capacity. It is not limited to extreme states (such as collapse of a structure or structural element), but it can be formulated for any intermediate state of performance/damage, e.g. continued functionality/operativity, light, medium or severe structural and non-structural damage. It can be expressed in terms of different performance measures, such as physical, structural quantities (drift, shear), or socio-economic ones (number of casualties, economic value of loss, downtime, number of unfed users on a network, etc).

- Fragility
  - A function representing the conditional probability of a component or system (component fragility, system fragility) exceeding a pre-defined limit-state as a function of a parameter. The latter is most commonly a scalar (or vector) measure of seismic intensity, but it can also be a structural response parameter (such as floor acceleration or interstorey drift) e.g. for non-structural components' fragility.
- Risk
  - A probabilistic measure of the consequence of a probabilistically defined hazardous event. It is often the unconditional probability or the mean annual frequency (probabilistic measure) of a component or system exceeding a pre-defined limit-state (consequence). Risk is also used to indicate the expected value, and possibly variance (within the reference time frame) of: Economic value of physical damage; Casualties/fatalities; Downtime; Economic loss: direct (physical damage/lives) + indirect (downtime, etc).
- System
  - A set of connected parts (components) interacting to perform a function, such as producing or transporting goods or services.
- Component
  - A basic part of a system. Its definition depends on the resolution of the study. It can be a single non-reducible item, or it can be itself a sub-system within the larger system.
- Network
  - In Mathematics, a weighted directed graph (digraph) made up of vertices (nodes) connected by edges (arcs, links). The weights may represent the links' capacity to accommodate flows between vertices. The in-coming and out-going flows in vertices usually sum up to zero, unless the vertex is a source or a sink.
  - A network is a system and any system can be represented as a network.
- Lifeline
  - See network. Usually employed with reference to Utilities networks.
- Infrastructure
  - A network of distinct man-made systems and processes that function collaboratively and synergistically to produce and distribute a continuous flow of

essential goods and services[1]. In this sense the Infrastructure is a super-system comprising all systems (buildings, lifelines, critical facilities, etc) and constitutes the physical layer supporting the functioning of a Society[2].

- Intra- and Inter-dependencies
  - Dependencies between components within (intra) the same system, or between (inter) different systems (see Fig. 1.1).
  - Dependencies can be of different types. Several classifications have been presented to categorize the types of dependencies. For instance, Rinaldi, Peerenboom, and Kelly (2001) describe dependencies in terms of four general categories: Physical: a physical reliance on material flow from one infrastructural system to another; Cyber: a reliance on information transfer between infrastructural systems; Geographic: a local environmental event affects components across multiple infrastructural systems due to physical proximity; Logical: a dependency that exists between infrastructural systems that does not fall into one of the above categories. In the slightly different classification proposed in Dudenhoeffer and Permann (2006) additional categories are introduced: Policy/Procedural Interdependency: An interdependency that exists due to policy or procedure that relates a state or event change in one infrastructure sector component to a subsequent effect on another component. Note hat the impact of this event may still exist given the recovery of an asset. Societal Interdependency: The interdependencies or influences that an infrastructure component event may have on societal factors such as public opinion, public confidence, fear, and cultural issues. Even if no physical linkage or relationship exists, consequences from events in one infrastructure may impact other infrastructures. This influence may also be time sensitive and decay over time from the original event grows.
- Loss (direct)
  - Loss incurred as a direct consequence of physical damage to systems' components. This category includes the economic value of damaged structural and non structural components (architectural, content, equipment, etc), the equivalent monetary value of lives lost.
- Loss (indirect)
  - Loss incurred as an indirect consequence of the physical damage and related to functional disruption in the systems. This category includes the monetary value of the increased travel times for people and goods on the damaged transportation system, the economic equivalent of the business interruption and industrial production, up to the complete halting of a whole economic sector in the affected region, the economic value of the social disruption.

[1] An adaptation of the definition of Infrastructure given in the 1997 report of the US President's Commission on Critical Infrastructure Protection.

[2] According to the Joint Committee on Structural Safety, Society is an entity of people for which common preferences may be identified, exogenous boundary conditions are the same and which share common resources.

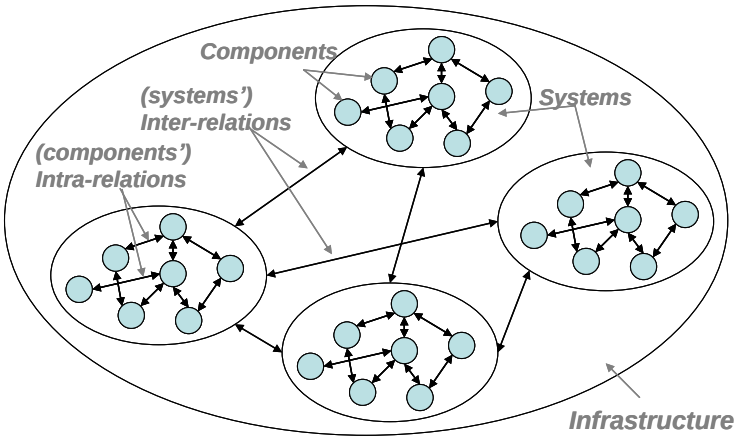

Fig. 1.1 Abstract representation of the Infrastructure

1.3 TIME, SPACE AND STAKEHOLDER DIMENSIONS IN A SYSTEMIC STUDY

The impact of the disaster caused by a natural hazard (the earthquake within SYNER-G) on a system evolves with *time* elapsed from the event and in *space*. Further, different *stakeholders* may have different stakes and play different roles in dealing with the various phases of the disaster, and are correspondingly interested in the assessment of the impact in different ways. These dimensions of the systemic study are represented in Fig. 1.2.

As far the time dimension is concerned, two aspects are of interest: the *time-frame* and the *observation point-in-time*. Typically, three frames are considered:

- **short-term**: in the aftermath of the event the damaged Infrastructure operates in a state of emergency;
- **mid-term**: the Infrastructure progressively returns to a new state of normal functionality;
- **long-term**: the Infrastructure is upgraded/retrofitted with available resources to mitigate the risk from the next event.

Correspondingly, the spatial extent of interest to the study of the Infrastructure response increases with time, initially (short-term) involving only the local struck area, then, an increasingly wide area covering adjacent regions up to the national scale in the economic recovery phase and long-term risk mitigation actions.

The position on the time axis of the observer with respect to the time-frame changes the goal of the systemic study:

- **before the time-frame**: the goal of the system analyst is forecasting the impact in order to set-up mitigation measures. It is important to underline how the information basis in this case can be considered as constant.
- **within the time-frame**: the goal of the system analyst is that of providing the managers with a real-time decision support system, which updates the Infrastructure state based on the continuously incoming flow of information.
- **after the time-frame**: the goal of the system analyst is to validate the models against occurred events.

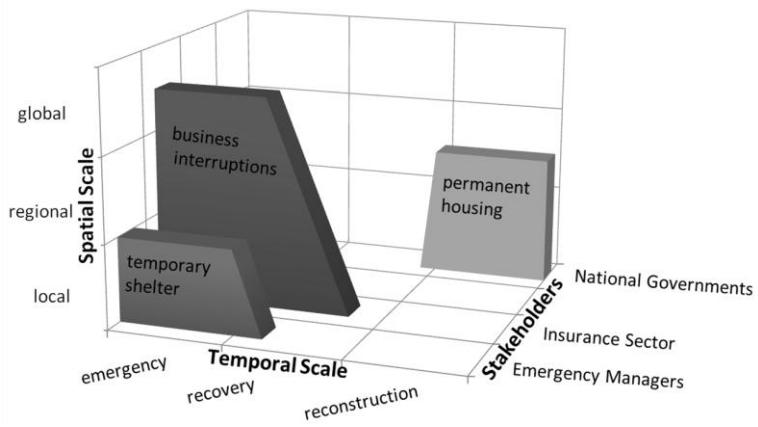

Fig. 1.2 The three dimensions in an Infrastructure vulnerability study

Systemic studies of different nature most commonly address the two phases:

1. Emergency phase: short-term (a few days/weeks) at the urban/regional scale
2. Economic recovery phase: medium to long-term, at the regional/national scale

The contribution of Engineering disciplines is obviously capital to the first phase. During the second phase their role becomes to some extent ancillary, due to the intervention of political and economic factors in the decision-making process.

The developed SYNER-G methodology focuses on the first phase only, with Emergency managers as the reference Stakeholders, and with the goal of forecasting before the event the expected impact for the purpose of planning and implementing risk mitigation measures.

1.4 SPATIAL CHARACTERISATION AND APPROACH LEVEL

The spatial characterization of the components (sub-systems) of the Infrastructure has a direct relation with the approaches to be used for the definition of both the corresponding hazard and vulnerability. From a *geometric* point of view three categories can be identified:

- **Point-like components (Critical facilities)**: single-site facilities whose importance for the functionality of the Infrastructure makes them critical, justifying a detailed description and analysis. Examples include hospitals, power-plants.
- **Line-like components (networks, lifelines)**: distributed systems comprising a number of vulnerable point-like sub-systems in their vertices, and strongly characterized by their *flow-transmission function*. Examples include Electric networks with vulnerable power plants, sub-stations, etc, or road networks with vulnerable bridges.
- **Area-like components**: this is a special category specifically intended to model large populations of residential, office and commercial buildings, which cannot be treated individually. These buildings make up the largest proportion of the built environment and generally give the predominant contribution to the total direct loss due to physical damage.

The approach for vulnerability study of the area-like components is not homogeneous with that of point-like and line-like sub-systems. As shown later on in Chapter 2, area-like

components for the purpose of a systemic study within SYNER-G have been modelled with geo-cells characterized in terms of physical (distribution of buildings amongst standardized typologies with associated fragilities) and socio-economic (population, income, etc) parameters. The above definitions are summarily illustrated in Fig. 1.3, where the area-like component is represented by a *census tract*.

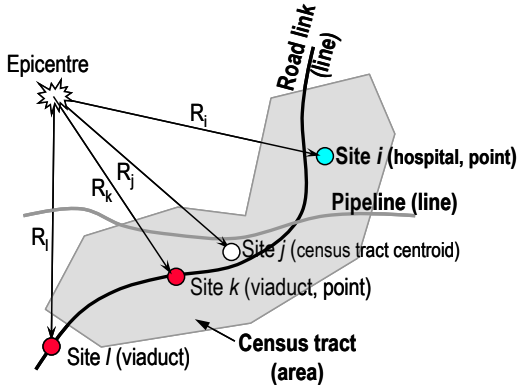

Fig. 1.3 Illustration of the different categories of components/sub-systems of the Infrastructure

1.5 THE SYNER-G TAXONOMY

In order to tackle the complexity of devising a model of the entire Infrastructure the first task undertaken within the project was the identification and description of a set of systems, sub-systems and components to focus on. This has resulted in what is called the SYNER-G taxonomy, described in this section (a more detailed version of this taxonomy can be found in the deliverable report D2.1, Appendix B, with description of each component type). All considered systems and their components have been assigned unique tags used consistently throughout the project. This taxonomy has been the guidance for the work carried out within work packages 3 and 5, within which for each component typology fragility models have been revised and/or developed, with a focus on European distinctive features, and systems have been modelled, respectively.

1.5.1 System 1 - Building aggregates (BDG)

Buildings are the basic point-like component of building aggregates/agglomerates/blocks (where buildings may or may not be in contact, with the ensuing interactions), which are delimited by roads. The description of the vulnerability of a urbanised area (e.g. a census tract, where several such building agglomerates are present) for the purpose of a system study requires fragility analysis of representative buildings for each typology, and statistical data on the incidence of each typology in the building population.

1.5.2 System 2 – Health-care system (HCS)

The health-care system is made up of health-care facilities (HCF), or hospitals. Hospitals are systems whose function is delivering medical services. From a social point of view, hospitals provide a fundamental assistance to citizens in every-day life; their function becomes of

paramount importance in the case of an earthquake event. This is the reason for including them among the critical facilities group.

Medical services, which consist of standardized procedures to guarantee an adequate treatment of patients, are delivered to patients by a joint contribution of the three “active” components of the system:

- The *operators* (human component): doctors, nurses and in general whoever plays an active role in providing medical care;
- The *facility* (physical component): where medical services are delivered;
- The *organisation* (organizational component): hospital management, responsible of setting up adequate conditions (standardized procedures for ordinary and emergency conditions) so that the medical services can be delivered.

The identified system components are:

- HCS01: Organisational component
- HCS02: Human component
- HCS03: Physical Component
  - HCS03-1: Structural elements (of the buildings within the complex/facility)
  - HCS03-2: Non-structural elements/Architectural
  - HCS03-3: Non-structural elements/Basic installations/Medical gases
  - HCS03-4: Non-structural elements/Basic installations/Power system
  - HCS03-5: Non-structural elements/Basic installations/Water system
  - HCS03-6: Non-structural elements/Basic installations/Conveying system
  - HCS03-7: Non-structural elements/Content-Equipment

1.5.3 System 3 – Harbour (HBRS)

A Harbour is a complex system comprising all the activities related to the transfer of goods/passengers between the maritime transportation and the earth-bound transportation systems. It is serviced by a number of other systems including: EPN, WSN, WWN, FFS, GAS, RDN, RWN. The identified system components are:

- HBR01: Waterfront components (wharves, breakwaters, etc)
- HBR02: Earthen embankments (hydraulic fills and native soil material)
- HBR03: Cargo handling and storage components (cranes, tanks, etc)
- HBR04: Buildings (sheds, warehouse, offices, etc)
- HBR05: Liquid fuel system (components as per the OIL system, see later)

1.5.4 System 4 – Road network (RDN)

The Road network is composed of a number of nodes and edges. It is a transportation network where edges can be directed (one-way) or undirected (two-way). All edges are in general vulnerable to seismic shaking or geotechnical hazards, with pavements that can

rupture due to surface ground deformation. Some types of edges or road segments, like those identified below, have specific types of response to seismic action and associated vulnerability.

The identified system components are:

- RDN01: Bridge
- RDN02: Tunnel
- RDN03: Embankment (road on)
- RDN04: Trench (road in a)
- RDN05: Unstable slope (road on, or running along)

1.5.5 System 5 – Railway network (RWN)

The Railway system as a whole is composed of a number of point-like critical facilities (Stations) and of the Railway network itself. The internal logic of the stations and their function in the traffic management of the whole system should be modelled explicitly. The network portion of the system has the same components as a Road network, plus a supervisory control and data acquisition – SCADA – sub-system. The difference is in the fragility models: the underlying limit-state relative to continued traffic over Railway bridges, embankments, etc. must consider the limitation associated with the tracks. This will lead in general to limitations to relative, maximum and residual, displacements stricter than for Roadway bridges.

The identified system components are:

- RWN01: Bridge, same as per RDN
- RWN02: Tunnel, same as per RDN
- RWN03: Embankment (road on) , same as per RDN
- RWN04: Trench (road in a) , same as per RDN
- RWN05: Unstable slope (road on, or running along) , same as per RDN
- RWN06: SCADA system
- RWN07: Station

1.5.6 System 6 – Water-supply network (WSN)

The Water-supply system as a whole is composed of a number of point-like critical facilities (Water sources, Treatment plants, Pumping stations, Storage tanks) and of the Water distribution network itself. The internal logic of the critical facilities and their function in the management of the whole system should be modelled explicitly. The network portion of the system is made of: pipelines, tunnels and canals and the supervisory control and data acquisition – SCADA – sub-system.

The identified system components are:

- WSN01: Water Source (Springs, shallow or deep wells, rivers, natural lakes, and impounding reservoirs)

- WSN02: Water Treatment Plant
- WSN03: Pumping station
- WSN04: Storage Tank
- WSN05: Pipe
- WSN06: Tunnel
- WSN07: Canal
- WSN08: SCADA system

1.5.7 System 7 – Waste-water network (WWN)

The Waste-water system as a whole is composed of a number of point-like critical facilities (Treatment plants, Pumping stations) and of the distribution network itself. The internal logic of the critical facilities and their function in the management of the whole system should be modelled explicitly. The network portion of the system is made of: pipelines, tunnels.

The identified system components are:

- WWN01: Waste-water treatment plant
- WWN02: Pumping station
- WWN03: same as per WSN
- WWN04: same as per WSN

1.5.8 System 8 – Fire-fighting system (HCS)

The Fire-fighting system as a whole can be a separate system or part of the WSS. In case it is a separate system, it is composed of a number of point-like facilities (Fire-fighters stations, Pumping stations, Storage tanks, Fire-hydrant) and of the distribution network itself. The internal logic of the critical facilities and their function in the management of the whole system should be modelled explicitly. The network portion of the system is made of: pipelines.

The identified system components are:

- FFS01: Fire-fighters station
- FFS02: Pumping station
- FFS03: Storage tank
- FFS04: Fire-hydrant
- FFS05: Pipe

1.5.9 System 9 – Electric power network (EPN)

The Electric-power system as a whole is composed of a number of point-like critical facilities (Power generation facilities, Transformation substations,) and of the Electric power transmission network itself. The internal logic of the critical facilities and their function in the management of the whole system should be modelled explicitly. The network portion of the

system is made of lines and of the supervisory control and data acquisition – SCADA – sub-system.

The identified system components are:

- EPN01: Power generation facility (Nuclear, hydro-electric, thermo-electric, geothermal, solar etc)
- EPN02: Sub-station (distribution, transformation-distribution)
- EPN03: Maintenance and technical support facilities
- EPN04: Line
- EPN05: SCADA system

1.5.10 System 10 – Natural gas system (GAS)

The Natural gas system as a whole is composed of a number of point-like critical facilities (Production and gathering facilities, Treatment plants, Storage facilities, Intermediate stations where gas is pressurized/depressurized or simply metered) and of the Gas transmission/distribution network itself. The internal logic of the critical facilities and their function in the management of the whole system should be modelled explicitly. The network portion of the system is made of lines and of the supervisory control and of data acquisition – SCADA – sub-system.

The identified system components are:

- GAS01: Production and gathering facility (Onshore, Offshore)
- GAS02: Treatment plant
- GAS03: Storage tank farm
- GAS04: Station (Compression, Metering Compression/metering, Regulator/metering)
- GAS05: Regasifier
- GAS06: Liquifier
- GAS07: Pipe
- GAS08: SCADA

1.5.11 System 11 – Oil system (OIL)

The Oil system as a whole is composed of a number of point-like critical facilities (Production and gathering facilities, Treatment plants, Storage facilities, Intermediate stations where gas is pressurized/depressurized or simply metered) and of the Gas transmission/distribution network itself. The internal logic of the critical facilities and their function in the management of the whole system should be modelled explicitly. The network portion of the system is made of lines and of the supervisory control and of data acquisition – SCADA – sub-system.

The identified system components are:

- OIL01: Production and gathering facility (Onshore, Offshore)
- OIL02: Refinery

- OIL03: Storage tank farm
- OIL04: Pumping Station
- OIL05: Pipe
- OIL06: SCADA

1.6 A SELECTED LITERATURE REVIEW

Amongst the vast amount of research on seismic risk analysis of single pieces of the Infrastructure, a few examples have been selected for a brief illustration, with the purpose of setting the premises of the methodological proposal presented in Chapter 2. The presentation of studies follows the SYNER-G Taxonomy of Infrastructural systems. Often, some studies present attempts to consider multiple systems (usually, at most two) and their interaction.

1.6.1 Buildings (BDG)

The very large number of buildings to be considered in a regional study, but even at an urban scale of analysis, can be treated according to two possible approaches:

- The first one is the single building analysis. Goda and Hong (2008) proposed a framework to investigate the sensitivity of the estimated seismic risk of sets of buildings to the degree of spatially correlated and simultaneously occurring seismic excitations. In particular, four correlation levels - no correlation, full correlation, and partial correlation with/without intra-event components - are considered. The authors compute the aggregate seismic loss for a set of buildings, subject to a number of earthquakes that occur in a given period of time. The analysis results highlight that underestimation or overestimation of correlation of seismic demand could lead to very different probabilistic characteristics of aggregate seismic loss although its mean is unaltered.
- The second approach, carried out in case a detailed individual analysis of all buildings is prevented, is to model buildings in ‘statistical terms’ as populations for which information is given at the level of the buildings group (group size depending on the refinement of the analysis and varying from a single block to a larger extent of the urban territory), in terms of percentage of each building typology within the group, with associated fragility models, population, income, education, and so on.

  In Bal et al. (2010) large groups of buildings are modelled with a uniform grid that covers the study region. The authors explored the influence of the geographical resolution of the exposure data (building groups) considering several different levels of spatial aggregation to estimate the losses due to a single earthquake scenario. In particular, for an idealized city four grids are used, subdivided into areas that are sequentially reduced by a factor of 4 each time, and in particular: four district levels, 16 postcode levels, 64 sub-district levels and 256 geo-cells. The results show that the total damage over an urban area, expressed as a mean damage ratio (MDR), is rather insensitive to the spatial resolution of the exposure data. However, a significant reduction in the variability of these estimates is achieved by moving to higher resolution grids.

In practice, while the vulnerability assessment of a single building of special interest is based on a detailed and specific structural analysis, the global evaluation of vulnerability (i.e. for several hundreds or thousands of buildings at an urban or regional scale) relies mostly on the use of statistical or probabilistic vulnerability functions. These functions represent the "typical" behaviour of a group of buildings characterized by a limited number of similar physical parameters. The vulnerability functions can be obtained from (Sedan et al., 2008):

- Data analysis from post-earthquake observations (empirical methods, calculation of a damage matrix or a vulnerability index for each building "type");
- Development of numerical models (mechanical methods, calculation of performance points for each building "type");

Whatever the procedure used, a vulnerability assessment study of common buildings at urban or regional scale is based on the following elements:

- A building typology and its census within the studied area: while the seismic behaviour of buildings cannot be specified one by one, it is required to define a building typology based on structural criteria (material used, height, bracing system…), that can be more or less accurate.
- A damage probability matrix or fragility curves that correspond to the chosen typology: for a given building typology, they represent the percentage of buildings that exceed a given damage state, for a given level of seismic intensity.

Empirical methods

The application of RISK-UE vulnerability indices can be done at different scales. One option is to work at the scale of homogeneous urban zones, within which we suppose a uniform distribution of building types (Bernardie et al. (2006) and Sedan et al. (2008)). Then, these different building types are related to RISK-UE building types.

In other cases, the assessment is directly adapted to the census data format, which sometimes has data about construction age and materials (Lantada et al. 2007).

Rossetto and Elnashai (2003) proposed a new approach in which data for different RC structural systems can be combined to produce a single set of 'homogenized' or 'general' curves applicable to all, through the use of a damage scale that accounts for the differences in the damage rate of disparate systems. Such damage scale, named the homogenized reinforced concrete damage scale (HRC scale), was used to generate vulnerability curves for reinforced concrete building populations, on the base of a data bank of 99 post-earthquake damage distributions observed in 19 earthquakes and concerning a total of 340,000 RC structures. The scale is subdivided into seven damage states, each of which is defined in terms of the typical structural and non-structural damage expected in the four main types of reinforced concrete structure found in Europe, namely ductile, non-ductile and infilled RC moment resisting frames and RC shear-wall structures.

It is important to note that the building-to-building variability for the same typology within each building group is implicitly although approximately captured when using empirically derived fragility functions, which are obtained from statistical elaboration of surveyed damage on buildings aggregated by typology and by construction account for this source of variability.

Mechanical methods

In the scope of large-scale vulnerability assessments, a dataset of capacity curves for various building typologies must first be developed and validated by a group of experts. These catalogues of capacity curves can contain the following information:

- Typology description (masonry bearing walls, reinforced-concrete with masonry infills, RC frames,… , number of stories, level of seismic code,…);
- The coordinates of the limit point between elastic and plastic domain (Dy and Ay);
- The coordinates of the ultimate displacement point (Du and Au).

These capacity curves can then be used to develop fragility curves for each typology, expressing the probability of damage for a given seismic intensity. These probabilities will finally be used as input in a GIS tool to perform the large scale vulnerability analysis.

Roads obstruction

Especially in urban context, serious damage to buildings may cause debris closing the roads. Thus, it is necessary to compare the road widths and debris deposits. The road width is an important parameter to estimate the effect of the area occupied by the generated debris for the road functionality. Additionally, the distance between the building face and the road is important: the longer is the distance, the lesser is the impact. This parameter is related to the type of urbanization in each area. Moreover, corner buildings are weakest as they are open on two sides.

The WP6 of RISK-UE project proposes two different approaches to assess these phenomena. In order to assess possible debris extensions, both empirical and analytical approaches are considered, respectively for reinforced concrete and masonry buildings.

The empirical approach proposed in the WP6 of RISK-UE is based on observations done after the Kocaeli 1999 earthquake for collapsed RC buildings. In this case, one may consider, as a first approximation, the following trend (with: *X*, debris obstruction in m):

$$X = \frac{2}{3} \times nb\ of\ floors \qquad (1.1)$$

The analytical approach, developed in the case of masonry buildings, considers that basic volume of debris depends on the following hypotheses:

- The pile of debris may be a simple volume, depending on the number and location of adjacent buildings;
- The debris volume is a ratio (kv, e.g. 30%) of the initial building volume.
- The slope of the pile of debris may be defined like a friction angle (ϕ, e.g. 45°).

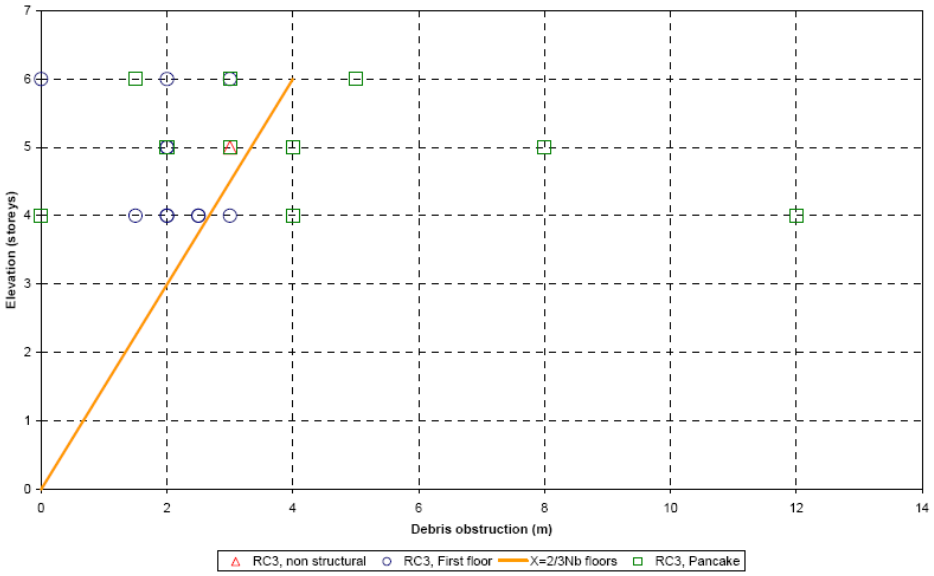

Fig. 1.4 Debris obstruction (collapsed RC buildings)

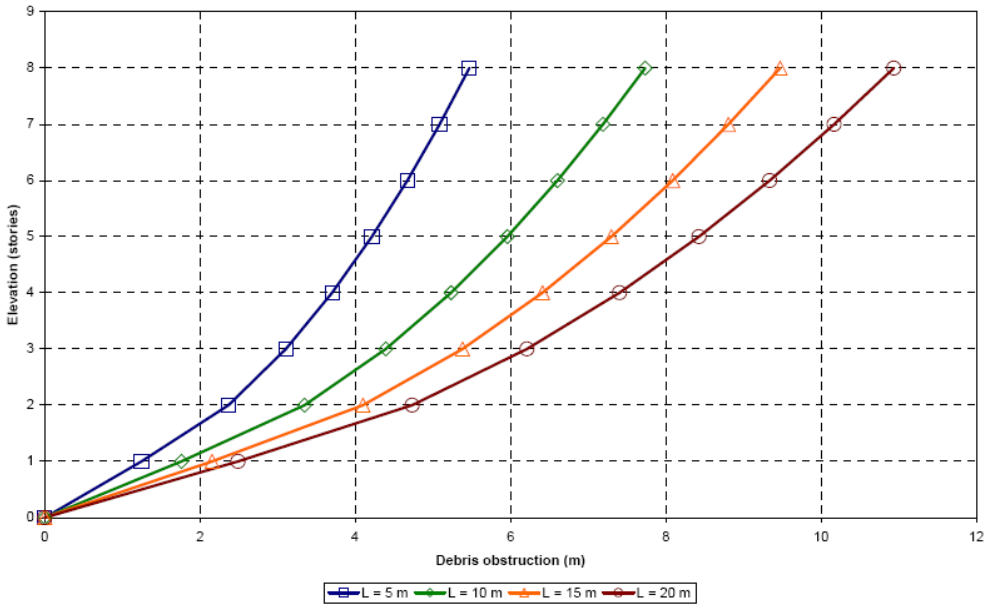

Fig. 1.5 Debris obstruction (collapsed buildings confined in two opposite sides, debris volume is 30% of initial volume, friction angle 45°)

In the project RISK Iran, which asses the seismic risk in 4 Iranian cities, the phenomena of streets obstruction was taken into account. The employed criterion was to evaluate the possibility that a collapsed building (D5 damage state) is close to one street with a width <= 2/3 * Nb of floors (WP6 RISK-UE). The assessment was done at district scale, because the number of collapsed buildings was only available at this scale.

The different input data was:

- Streets GIS and width.
- Estimation of collapsed buildings / by type / by district (result of seismic risk scenario in current buildings).

$$\frac{\text{Nb of collapsed buildings of N floors}}{\text{Total street length into district}} \cdot Length\_obstruct\_N \qquad (1.2)$$

where *Length_obstruct_N* is the total street length into a district with a width that could be obstructed by a collapsed building of N floors (width <= 4/3 * Nb of floors): it was considered here that a street is blocked in case half of the width is obstructed.

Finally the result was the number of probable obstructed streets into a district.

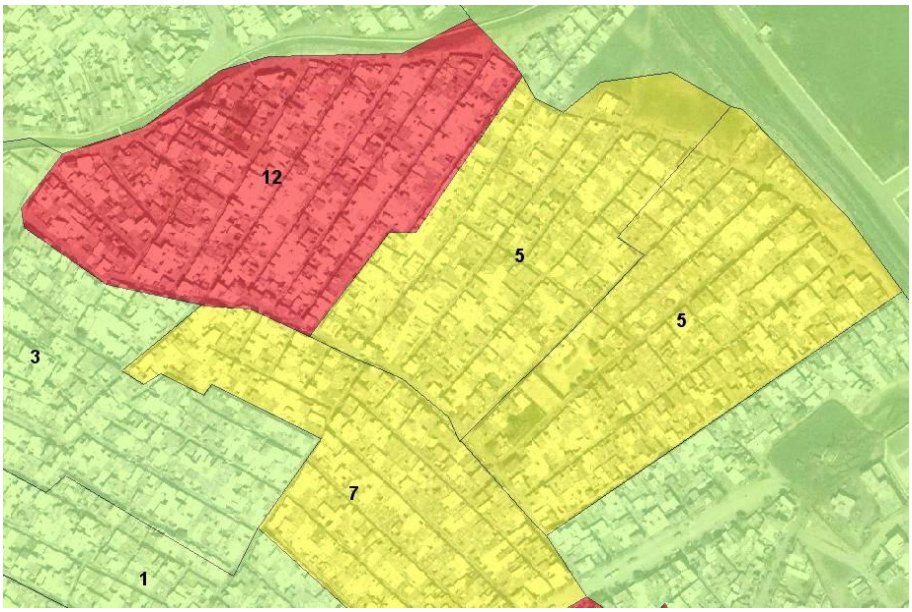

Fig. 1.6 Example of application, number of obstructed streets by district

1.6.2 Health-care system (HCS)

The health-care system is made up of health-care facilities, collectively serving a region and coping with the earthquake induced surge in treatment demand in the aftermath of an event. Notwithstanding the criticality of the function of the HCS, the technical literature on the matter is all but abundant. Few studies can be found, some with a focus on the assessment of the capacity of a single facility to remain operational, even if partially, under emergency conditions with possible damage to the facility structural and non-structural components. The remaining few studies deal with the entire system at the regional level and try to evaluate so-called community impact.

For instance, in (Monti *et al*, 1996)(Monti and Nuti, 1996) a reliability-based (FORM, SORM and bounds) procedure to evaluate the functional vulnerability of the surgical function of an hospital system is presented. In (Nuti and Vanzi, 1998) the regional system of hospitals is studied with the aim of setting up a model for their availability. Such a model is proposed to assess the best retrofit strategies from a systemic point of view, as well as emergency measures such as the use of camp hospitals. Another study which deals with the system as a collection of facilities is (Menoni *et al*, 2000), where the capacity of public facilities can continue providing their service under stressful conditions, even when a certain degree of physical damage has been suffered by structures or by medical equipment, is investigated.

Recent studies try to look at the resilience of the hospital system, as in (Cimellaro *et al*, 2010, 2011). The latter introduces an organizational model, a metamodel, describing the response of the Hospital Emergency Department (ED), able to estimate the hospital capacity and the dynamic response in real time and to incorporate the influence of the damage of structural and non-structural components on the organizational ones. The performance indicator chosen to assess the structure is the waiting time. The metamodel covers a large range of hospital configurations and takes into account hospital resources, in terms of staff and infrastructures, operational efficiency and existence of an emergency plan, maximum capacity and behaviour both in saturated and over-capacitated conditions.

Similarly, in (Lupoi *et al* 2008), a methodology is given to compare treatment demand and capacity for a facility under emergency conditions. Performance is measured in terms of the mean annual rate of demand exceeding a random treatment capacity:

$$\lambda\left(\frac{HTD}{HTC}>1\right)=\int_0^{\infty} P\left(\frac{HTD}{HTC}>1\middle| x\right) d\lambda_{PGA}(x) \tag{1.3}$$

Fig. 1.7 shows the mean and mean ± sigma bands of the HTD and HTC, as a function of seismic intensity at the site (measured in terms of PGA). The capacity is measured in terms of number of surgical operations that can be carried out per hour. The demand is evaluated starting from the total number of casualties and using severity classes to find the subset of those requiring surgical treatment.

The capacity term is the result of three contributions, coming from the three *macro-components* (m/c) making up the hospital system: the physical m/c (structural and non-structural element of the facility), the organizational m/c (the procedure in the emergency plans) and the human m/c (skill and training of the operators using the facilities and equipment according to the procedures):

$$HTC = \alpha\beta\gamma / t_m \tag{1.4}$$

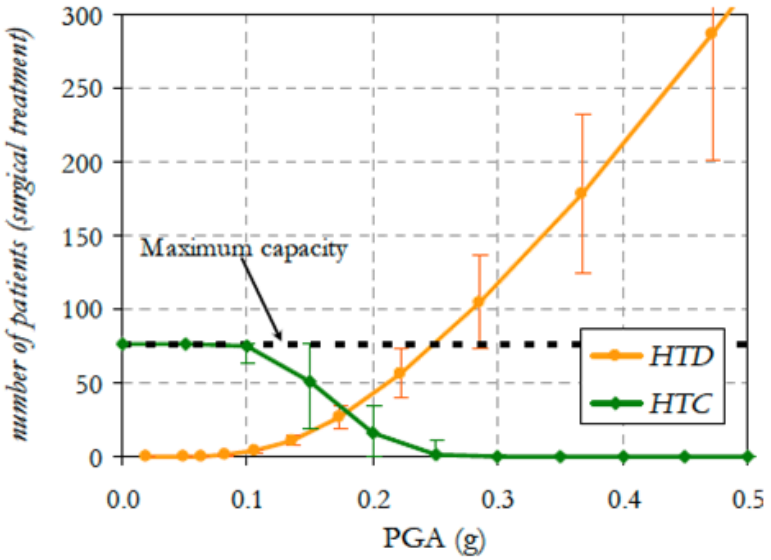

Fig. 1.7 Demand and capacity "distribution" as a function of peak ground acceleration

The three factors correspond to the three already mentioned m/c:

- $\alpha \rightarrow$ organisational m/c: measures the effectiveness of the emergency plan
- $\beta \rightarrow$ human m/c: measures quality/skill/training of the staff
- $\gamma = \gamma_1\gamma_2 \rightarrow$ physical m/c
  - γ_1 number of operating theatres still operational after the event
  - γ_2 system Boolean function: 1 if essential medical services (minimum subset of all the medical services required to support the operating theatres) are available, 0 otherwise

The quantitative assessment of the first two factors requires interaction with specialists from outside the Engineering disciplines, and direct contact (interview) of the local staff.

For the evaluation of the third factor, it is necessary to establish the conditions under which the hospital (system) can keep on providing its function (essential medical services). These are:

- Structural and non-structural damage are compatible with continued functioning
- Medical equipment and essential utilities (electric power, water, medical gases, etc.) are available

Establishing whether the above conditions are met requires checking that all necessary subsystems remain operational. This is done by describing the whole hospital system with a fault tree. The evaluation of the probability distribution of HTC is carried out by simulation. To limit the computational effort associated with the simulation this is split into two steps. In the first one a limited number of recorded ground motions is used to carry out nonlinear time-history analysis on a structural model of the building(s) housing the hospital and to collect samples of all the correlated response quantities (e.g. floor drifts, floor accelerations, columns shears, etc) needed to establish whether the structure stands after the earthquake and the non-structural elements and equipment are operational. The second step consists of a Monte Carlo simulation with structural responses sampled from a joint model fit to the responses collected in the first step, and structural and non-structural capacities sampled from their respective fragilities, to obtain the state of each component and that of the system as a whole (according to the logic spelled out in the fault tree).

1.6.3 Harbour (HBR)

Current engineering practice for seismic risk reduction for port facilities is typically based on design or retrofit criteria for individual physical components (e.g., wharf structures) expressed as prescribed levels of displacement, strain, etc. However, the resilience and continuity of shipping operations at a port after an earthquake depend not only on the performance of these individual components, but on their locations, redundancy, and physical and operational connectivity as well; that is, on the port system as a whole.

Several researchers have studied the seismic performance of systems such as highway, power supply, and water distribution networks, as described in the respective sections of the present report. On the contrary, available approaches for the seismic performance of port system are limited. In almost all past relevant studies, the evaluation of the post-earthquake performance of the port system is based on the simulation of the damage states of each component under given scenario earthquakes, i.e. without considering how damage and

downtime of these structures might disrupt the overall port system's ship handling operations and the regional, national, and even international economic impacts that could result from extended earthquake-induced disruption of a major port. These studies basically remain at the estimation of direct physical losses (structural damage and corresponding replacement and repair costs) (NIBS 2004). In few cases economic loss, such as business interruption and income loss (Pachakis and Kiremidjian 2003, 2004, Na et al. 2007, 2008) and economic impact that is driven by the damages in other sectors led by an earthquake (Rix et al. 2009) are assessed, but in general the interaction effects and the integrated response of the port system are not taken into consideration.

One of the most well-known and widely used risk assessment methodologies for analyzing potential losses from earthquakes (as well as other natural hazards such as floods and hurricane), including also the assessment of seismic risk for port facilities, is the one developed by FEMA (Federal Emergency Management Agency) and incorporated in the HAZUS software (NIBS 2004). It couples scientific and engineering knowledge with geographic information systems (GIS) technology to produce estimates of hazard-related damage before, or after, a disaster occurs. However, this methodology has been developed for application in the United States and its application in Europe may not be always appropriate given the specific feature of European elements at risk.

Seismic risk reduction decisions for a port depend on the particular operational, economic, and political framework within which the port operates. Werner et al. (1999) proposed a method for the reduction of seismic risk in port systems, which is based on the concept of "acceptable seismic risk" for evaluating various factors and deciding upon the final retrofit design approach. Different seismic scenarios are considered and Monte Carlo simulation is used, to assess the effect of the involved uncertainties.

Few years later Pachakis and Kiremidjian (2003, 2004) proposed a methodology to simulate the seismic response, planning and risk management of port facilities. A model for estimating physical losses is developed and a simulation model for evaluating revenue losses from wharf closure until repaired is described. The methodology is based on a set of data from a US port. Losses are classified as usual in the two categories: losses due to physical damage of port facilities (direct losses) and revenue losses due to reduction or loss of functionality for the time seismic damages are being repaired (indirect losses). The methodology is conditioned on specific seismic scenario events with known anticipated characteristics. For the estimation of revenue losses, two necessary interrelated components are needed: a methodology to predict the damage state of the port facilities after a seismic event (vulnerability model) and a methodology to relate the damage state with the monetary loss. The current methodology is based on the use of existing fragility curves proposed in HAZUS (NIBS 2004).

The analysis of seismic risk to the entire system of wharf structures at the Port of Oakland was performed by Werner and Taylor (2004), in order to assess the effectiveness of various seismic upgrade options in reducing potential economic losses from interruption of shipping operations and damage repair costs (which are typically much lower than losses due to shipping interruptions). Werner and Taylor (2004) have shown how deterministic or probabilistic estimates of economic losses may present important differences.

One of the most recent studies is the one developed by Na et al. (2007, 2008) and Na and Shinozuka (2009) aiming at the estimation of earthquake effects on the performance of the operation system of a container terminal in a seaport. In particular, the methodology focuses on indirect economic loss (revenue loss) of port operators, resulting from the reduced

throughput associated with downtime. To evaluate the economic loss of damaged system, an analytical framework is developed by integrating simulation models for terminal operation and fragility curves of port components in the context of seismic risk analysis. The simulation model is verified with actual terminal operation data obtained from 15 different container terminals. The assessment of the functionality of port components is performed using fragility functions proposed by the authors (for quay wall structures) incorporating uncertainties associated with a scenario earthquake. The critical components regarding port operations and earthquake recovery schedule are the quay walls and the container gantry cranes; therefore they considered only these two elements as the main components to represent the terminal operation system after an earthquake without taking into consideration functional and physical interdependencies between port facilities. The economic losses are described in terms of the reduced container throughput and increased ship waiting time. Based on the analytical procedure to assess the seismic performance of the terminal system, fragility curves for the entire system are also produced through Monte Carlo simulations. This approach can be used not only for estimating the seismically induced revenue loss but also serve as a decision-making tool to select specific seismic retrofit techniques on the basis of benefit–cost analysis.

A model to assess the seismic vulnerability of the port facility in the form of fragility curves, considering the associated uncertainties, has been developed by Shinozuka (2009). These fragility curves are derived from the seismic response analysis of wharf structures as a function of PGA, or any alternative measure of the base-rock ground motion intensity; different levels of damage and corresponding performance levels of the wharf allowing the ships to dock has been proposed. The seismic response analysis is performed through a Monte Carlo simulation of the facility response, and the response analysis is repeatedly carried out for each of a large number of probabilistic scenario earthquakes, consistent with the regional seismic hazard. The global fragility curves can be used to make probabilistic prediction of the expected damage states and associated direct losses of the port facilities under the seismic hazard in the form of a risk curve. The proposed methodology has been applied in the Port of Kobe.

Rix et al. (2009) describe an on-going research project for the seismic risk management and downtime of port systems. A probabilistic risk analysis framework is proposed through Monte Carlo analysis to estimate the system-wide economic consequences of a particular seismic risk management option. The port system fragility is expressed as business interruption losses due to reduced container throughput and ship delays or re-routing. In particular, the basic concepts and developed methods to address the analysis of seismic risks to a port-wide system of berths (with their particular wharf and crane structures) are presented. The way in which the results can guide port decision makers in making a better selection of design, retrofit, operational, and other seismic risk management options is also discussed. The framework is based on previous work to assess wharf seismic design criteria and upgrade strategies for major projects at the Ports of Los Angeles and Oakland (Taylor and Werner 1995, Werner 1998, Werner and Taylor 2004, Werner et al. 2002, Werner et al. 1999). Again, as in previous models, the port system is described only by its waterfront structures, and not by the whole system of components and facilities affecting the port functionality after the occurrence of an earthquake event.

1.6.4 Road network (RDN)

The selected works referenced in this section can be classified based on the importance of the role played by the transportation network itself. In a way of simplification available studies can be assigned to the following three levels:

- Level I: the attention is focused on the functioning of the network in terms of *pure connectivity*. This type of studies focuses on just one of the services provided by the network, e.g. most typically the rescue function immediately after the earthquake, and may be of interest in identifying portions of the network which are critical with respect to the continued connectivity of the network.
- Level II: the scope of the study is widened to include consideration of the network capacity to accommodate traffic flows. The damage to the network causes traffic congestion, resulting in increased travel time which is in turn translated into monetary terms. This indirect loss summed to direct loss incurred due to damage to the building stock results in a first partial estimate of the overall economic impact of an earthquake.
- Level III: The most general approach, which aims at obtaining a realistic estimate of total loss, inclusive of direct physical damage to the built environment (residential and industrial buildings as well as network components), loss due to reduced activity in the economic sectors (industry, services), and network-related loss (increased travel time). Economic interdependencies are accounted for, such as the reduction in demand and supply of commodities (due to damaged factories, etc.), hence in the demand for travel, and due to the increased travel costs. At this level the relevance and the complexity of the economic models become dominant over that of the transportation network. This is a full systemic study requiring important inputs from the economic disciplines.

Two similar examples of Level I studies can be found in (Franchin *et al* 2006), which is described in some detail in the next section, and in (Nuti and Vanzi, 1998). In the latter study the road network serves the purpose of connecting the hospitals in a regional health-care system. The mortality rate of casualties, in case of seismic event, is substantially reduced if they receive care in a short time. After a strong earthquake damage and/or congestion of hospitals, and of the transportation network, cause an increase in the distance to be covered, because casualties exceeding the hospitals capacity have to be moved to non-full ones and because of interrupted links which result in a decrease in the transportation speed. The study proposes the distance covered by each casualty, defined in probabilistic terms, as a meaningful system performance measure. Comparing the distance distribution after an earthquake (accounting for damage to hospitals and road network, as well as for casualties and congestion), under different seismic retrofit/upgrade scenarios with the baseline distribution gives useful indications for the allocation of resources.

A further example of Level I study is that in Kang *et al* (2008). This paper applies matrix-based system reliability (MSR) method to a transportation network consisting of bridge structures in order to evaluate the probability of disconnection between each city/county and a critical facility is estimated. Unlike existing system reliability methods whose complexity depends highly on that of the system event, the MSR method describes any general system event in a simple matrix form and therefore provides a more convenient way of handling the system event and estimating its probability. The probability mass function of the number of failed bridges is computed as well. In order to quantify the relative importance of bridges, the

MSR method is used to compute the conditional probabilities of bridge failures given that there is at least one city disconnected from the critical facility. The bounds on the probability of disconnection are also obtained for cases with incomplete information.

Examples of Level II studies are those in Shinozuka *et al* (2003) and Chang *et al* (2011). The approach in Shinozuka *et al.* (2003) aims at the determination of *direct* and *indirect* economic loss due to damage to a transportation network. Direct loss is related to physical damage to vulnerable components, while indirect loss is related to functionality of the system, whose degradation is measured in terms of a system-level performance index called *Driver's delay* (DD), i.e. the increase in total daily travel time for all travellers. Indirect loss is expressed as the DD times a unit cost of time. Traffic flows are evaluated by *equilibrium analysis* under a *static origin-destination matrix*. The vulnerable components are the bridges within the network, for which four states of increasing damage and corresponding fragilities are employed: minor, moderate, major and collapse. The state of each link, corresponding to a different residual traffic capacity, equals that of its most severely damaged bridge. Total DD is obtained by summing the values for all days over which the delay persists. However, the DD decreases over time due to repair activity taking place after the event, modelled in an admittedly over-simplified manner. This study is extended in Zhou *et al.* (2004), to consider the effect of retrofit strategies in improving the performance in future events.

The work by Chang *et al* (2011) advances a proposal for going beyond the use of the pre-earthquake (static) origin-destination matrix as an input for traffic flow analysis. The post-quake travel demand is complicated and the change of traffic pattern after the event is coupled with the damage of transportation infrastructures. To arrive at a new origin-destination matrix the paper modifies the trip generation and distribution stages of a traffic analysis to accommodate for earthquake-induced damage. Traffic analysis zones (TAZ) are classified into four types, depending on the presence of attractants (e.g., hospitals or emergency shelter) and repellents (e.g., HAZMAT release, fire following earthquake, or damaged facilities). Then the pre-earthquake travel demand of each TAZ is modified according to the classification. Several general assumptions are made on post-earthquake travel behaviour and emergency traffic management measures. The paper reports also an extensive literature review on attempts to model traffic pattern changes in the aftermath of an earthquake.

Finally, among the few available Level III studies, an example is the work by Karaca (2005). The work reports a regional earthquake loss methodology that emphasizes economic interdependencies at regional and ***national*** scales and the mediating role of the transportation network. In an application to the Central U.S. under threat from earthquakes from the New Madrid Seismic Zone, regional and national losses from scenario earthquakes are evaluated, together with a quantification of the corresponding uncertainty including contributions from seismicity, attenuation, fragilities, etc. The effectiveness of alternative mitigation strategies is also considered. The loss assessment methodology includes spatial interactions (through the transportation network) and business interaction (through an input-output model) and extends geographically to the entire conterminous U.S. The losses reflect damage to buildings and transportation components, reduced functionality, changes in the level of economic activity in different economic sectors and geographical regions, and the speed of the reconstruction/recovery process. Evaluation of losses for a number of scenario earthquakes indicates that losses from business interruption may be as significant as infrastructure repair costs.

1.6.5 Water-supply network (WSN)

Water is vital for human survival and for the continuity of all human activities. In general, water system may experience important damages during earthquakes, with significant impact on potable water uses and emergency activities such as fire suppression. This has been observed in almost all past strong earthquakes. *Reliability* assessment of water networks comprises a complex, yet essential process. Many issues should be taken into account, such as the variations in demands, the reliability of individual components and their locations, the fire fighting requirements, etc.

The seismic reliability of water networks is possible to be measured using different indices of physical nature or not, like *vulnerability, connectivity, serviceability, maximum flow, redundancy and economic loss* (ATC 25-1, 1992). Connectivity analyses measure post-earthquake integrity, the extent to which links and nodes in a network are connected or disconnected. *Serviceability* analyses estimate the remaining or residual capacity between selected nodes following an earthquake. Serviceability is a performance assessment measure that tends to focus more on the hydraulic perspective and less upon the underlying robustness of the network in terms of its layout.

Closely related to reliability is *redundancy*, a characteristic of the overall system performance that is often neglected. *Redundancy* in a water supply network indicates the existence of reserve capacity of the network and also the existence of alternative routing (supply paths to the demand nodes in case the supply links go out of service) (Awumah et al. 1991). The redundancy of water supply system under earthquake risk can be evaluated from three points of view; 1) along with reliability when assessing system performance, 2) in order to design a new network, 3) for efficient seismic mitigation of the existing network.

In several cases, *reliability* assessment is related with mitigation prioritization procedure. Multi-criteria analysis (MCA) is more efficient than traditionally benefit-cost analysis, as it copes with the uncertain judgment of experts. Moreover, the model should consider customers importance, pipeline properties and hazard factors. Hence, a fuzzy analytic hierarchy process (FAHP) to support the MCA for renewal prioritization of the lifeline systems can be developed. This optimized fuzzy prioritization method can be applied as an evaluation tool (Alexoudi et al., 2009), where uncertain and imprecise judgments of experts are translated into fuzzy numbers.

Seismic risk of water system has been investigated extensively (Ballantyne et al, 1990; Taylor 1991; Shinozuka et al, 1992; Hwang et al, 1998; Shi et al, 2006 and Wang, 2006). System reliability of San Francisco auxiliary water supply system and the effects of water supply performance on fire following earthquakes are described in Scawthorn et al. (2006) research for both 1906 San Francisco and 1989 Loma Prieta earthquakes. Seismic risk assessments have been reported for the water supply systems in Memphis Tennessee (Chang et al., 2002).

The methods presented in the selected references in this section can be classified in the following four levels:

- **Level I (Vulnerability Analysis)**: The scope is to estimate the percentage of the physical damages in a specific region based on the vulnerability analysis of water components. The latest can be estimated through appropriate fragility curves or/and Monte-Carlo technique.

- **Level II (Connectivity Analysis):** A vulnerability analysis is essential, as a first step, in order to estimate the physically damaged components (pipes, nodes). In a second stage, the damaged components should be removed from the network. Furthermore, some of the remaining nodes which can be completely isolated from all supply nodes must be removed from the original network. In a third stage, a connectivity analysis may be performed (simplified- Level IIa or advanced- Level IIb).
- **Level III (Flow Analysis)**: Firstly, water head, flow rate and amount of leakage at each demand node are calculated under intact (pre-earthquake) conditions as well as the quantity of flow and head loss in each pipe. After the evaluation of the physical vulnerability of the pipes (break, leak), a flow analysis is performed involving the newly formed network. It is assumed that, when a pipe is broken, a shutdown device will be automatically activated at the starting and terminating nodes of the pipe so that the water leakage is prevented. It is also postulated that capabilities of the supply nodes are not reduced by seismic damages.
- **Level IV (Serviceability Analysis)**: Vulnerability estimation of water system components beside with a flow analysis is repeated for different seismic intensities using Monte-Carlo simulations. When the task is completed, average values of the flow rate and water pressure are calculated at each node together with their ratio to the corresponding parameters under intact condition. The above procedure comprises a full serviceability analysis (Level IV.b). Moreover, a simplified serviceability analysis (Level IVa) can be accomplished connecting the pipeline break rate with a simple Serviceability Index.

The majority of the studies performed for water system can be categorized as **Level I** that means simple physical vulnerability studies of water system components (ATC-13, ATC-25, NIBS 2004). The performance index used in Level I studies is the *"Damage Ratio"* that describes the expected number of failures per unit length or per link or per node of the system. Moreover, the "Damage Ratio" can be considered as a percentage of the damaged nodes/ links.

A simple connectivity analysis (Level II) of the network can be accomplished using Graph Theory (clustering coefficient of a graph, Redundancy Ratio, Service Ratio Reachability Ratio) and Statistical Methods (Level IIa). Level IIb studies can be found in Shinozuka et al. (1977) and O'Rourke et al. (1985) that use minimal cut set paths in reliability evaluation of lifeline networks. Moreover, techniques available for tracing the minimal paths and minimal cut sets have mainly been presented in literatures as connectivity analysis of the network (Jasmon and Kai, 1985; Fotuhi-Firuzabad et al., 2004). Another example of Level II analysis is the study performed by Kawakami (1990), which uses the *"Damage Ratio"* and *"Service Ratio"* as performance indexes. Service Ratio indicates the ratio of normally supplied houses to the total number in the system. Dueñas-Osorio et al. (2007a) propose the concept of *"Connectivity Loss"* in order to quantify the average decrease of the ability of distribution vertices to receive flow from the generation vertices. Dueñas-Osorio et al. (2007b) introduce *"Redundancy Ratio"* as the appropriate parameter to measure the performance of water system. Moghtaderi-Zadeh et al. (1982) proposes *"Reachability"* of water as performance index, indicating the probability that a certain amount of water flow would reach key locations (nodes). Conclusively, *"Damage Ratio", "Service Ratio", "Connectivity Loss", "Redundancy Ratio" and "Reachability"* are the performance indicators used in such Level of Analysis (Level II).

Many researchers have contributed to the advancement of seismic reliability methods for water supply systems from the flow and serviceability analysis viewpoint (**Level III).** Examples of Level III studies are those of Shinozuka et al. (1981) that developed, for the first time, a methodology to assess seismic reliability of transmission pipeline system to the city of Los Angeles, in terms of the degree of serviceability. It was assumed that the system is considered serviceable when its fire-fighting capabilities remain intact in the aftermath of an earthquake. Monte Carlo simulation was carried out in order to estimate the probability of serviceability on the basis of simulated states of physical damage of the system under seismic condition. Furthermore, a Level III study is the one performed by Isoyama and Katayama (1981) that developed a Monte Carlo simulation method for evaluating the seismic reliability of Tokyo water supply system during the post-earthquake period using maximum possible flow method. The method was intended for relatively large water supply systems, considering network topology, supply and distribution station capacities, and system operating strategies. Moreover, O'Rourke et al. (1985) simulated the serviceability of seismically damaged water supply system for the city of San Francisco through a flow analysis. Performance of the system was defined explicitly as the ratio of available to required water flow at a standard operating pressure of 14 m near the location of the predicted fire outbreak (Level III). The performance indexes used in Level III analyses accounts the probability distribution of the percentage of customers who would lose their service after a specific earthquake.

Level IV approaches necessities complex hydraulic analyses, which are time consuming and require expertise and availability of several data. For this reasons, a number of researches have developed simplified models to assess the *serviceability* of pipeline networks under various amounts of pipe damages. A diagram correlating the *Serviceability Index (SI)* to average break rate is proposed in HAZUS (NIBS, 2004 – Level IVa). If SI is over 90%, the capability of water system for fire suppression is high, compared to SI below 20%. Generally, the performance indexes of Level VI studies involve the system *ability to meet hydraulic requirements including existing and future water needs (i.e. fire flow, maximum day or MD and maximum hour or MH domestic needs, storage needs, etc.) and to properly size future facilities*.

The works of Markov et al. (1994), Hwang et al. (1998), Javanbarg et al. (2006) and Shi (2006) can be classified as Level IVb analyses. In particular Markov et al. (1994) developed a special algorithm for the hydraulic analysis of the seismically damaged network and calculated serviceability measures for the auxiliary water supply system in San Francisco. Hwang et al. (1998) performed a hydraulic simulation analysis to assess the serviceability of the water supply system in the city of Memphis. The serviceability of a system was determined based on the connectivity and flow analysis of a seismically damaged network, which was established through a Monte Carlo simulation. Javanbarg et al. (2006) evaluated the performance of water supply in Osaka City considering hydraulic analysis and modelling both breakage and leakage as the damage states of pipeline systems. Two *performance parameters* were considered; *availability index,* which is the ratio between the output available water pressure in damaged network and the required pressure at each demand node within the undamaged network, and *serviceability index*, which is the ratio between the output available water flow in damaged network and the required water flow volume at each demand node within the undamaged network. Shi (2006) developed a hydraulic network model for earthquake simulation of water network operated by the Los Angeles Department of Water and Power. The model accounted for flows and pressures in a heavily damaged system and provided a method for simulating pipeline leakage and breakage.

Besides models classified in the above four categories (Level I to IV), other models have been also proposed, such as r*edundancy* approaches (Awumah et al., 1991; Kalungi and Tanyimboh, 2003; Hoshiya and Yamamoto, 2002; Hoshiya et al., 2004) and studies for the identification of critical links of water supply systems under earthquakes (Yu Wang et al. 2008). Yu Wang et al. (2008) describe a process for seismic risk assessment and identification of critical links of water supply systems under earthquakes. Probabilistic performance of water supply systems is reflected by the *System Serviceability Index (SSI)*- a ratio of sum of the satisfied customer demands after an earthquake, and two other performance indices like *Damage Consequence Index (DCI)* and *Upgrade Benefit Index (UBI).* With the aid of Monte- Carlo simulations in conjunction with a special hydraulic analysis computer program (GIRAFEE), the seismic risk of the system is evaluated for a hypothetical seismic damage scenario. The concept of efficient frontier is then employed to identify critical links of the system.

Awumah et al. (1991) and Kalungi and Tanyimboh (2003) have been extensively studied *the redundancy* for water networks. They developed an entropy-based measure of redundancy and examined through a series of network simulations a range of network layouts when a link goes out of service. However, one or two damaged components are taken into account for redundancy estimations, therefore these methods cannot be applied to a heavily damaged system. Hoshiya and Yamamoto (2002) and Hoshiya et al. (2004) proposed a redundancy index for the lifeline systems under seismic risk based on the entropy of an event of damage modes conditioned on system damage. In particular Hoshiya and Yamamoto (2002), consider the physical probability of connectivity between nodes within a network as a remarkable parameter in redundancy analysis. However, the leakage state of damage of pipelines may not be considered in simulations.

1.6.6 Waste-water network (WWN)

Over the last twenty years, waste-water systems have been heavily damaged by natural disasters as earthquakes, worldwide. The societal and economic disruption caused by waste-water network damages is important, as for example, the impact on public health and environment due to the discharge of raw/inadequately treated sewage.

There is limited real data specifically referring to the vulnerability of waste-water system components and furthermore to the post-earthquake functionality of waste-water networks. However, relevant damage databases have been assembled for buildings associated to the waste water systems and of course for certain waste water components (pipes, tunnels, reservoirs and treatment plants). In general almost all available methodologies use “water” damage databases for waste-water systems. Moreover, the vulnerability analysis for waste-water system components is performed using the same fragility curves with the components of the water supply system (ATC-13, ATC-25, NIBS, 2004).

Nevertheless, there are some differences between water and waste water systems that should be mentioned and emphasized:

- Waste- water facilities are, in general, located in low-level areas to take advantage of transporting sewage via gravity. As a result, waste-water treatment and pumping facilities typically have larger exposure to earthquakes, because they are more likely to be located in soft and loose alluvial soils exposed to large ground deformations and probably to liquefaction.
- Gravity sewers differ from water pipelines because:

- They are generally buried deeper.
- The pipe body/materials and joints are typically weaker as they are not designed for pressure.
- They are more buoyant as they are partially filled with sewage. This makes them more vulnerable to flotation in areas with high groundwater tables or liquefaction. Similarly, manholes are vulnerable to displacement under surcharged conditions.
- Sewer pipelines can generally withstand more damage and remain functional (even partially) compared to pressurized water pipelines. Damaged sewers often continue to operate, transporting sewage until the sewer pipe is offset (shear) and/or separated to the point that sewage flow is blocked. By comparison, pressurized pipelines (such as water pipelines) will discharge far greater amounts of water than gravity pipelines given the same physical leak size.

o Furthermore, waste-water lift stations differ from water booster stations. They are designed with a deep wet well (typically over 5m deep and in extreme cases approaching 30m deep) where sewage is collected by gravity. Water booster stations are usually located on grade or in shallow vaults. Therefore, lift stations can be vulnerable to liquefaction or excessive buoyant forces in areas with high groundwater tables.

The required effort to assess the performance of waste-water systems varies with the level of analysis and the complexity of the system. Most of the available methodologies used for waste-water systems, stop their analysis in the estimation of the vulnerability, the estimation of the replacement cost and the restoration time (ATC-13, ATC-25, NIBS, 2004). No specific care is given to the performance of the waste-water network.

ALA (2004) propose as performance indicators for waste-water system, *capacity measures* (e.g. flow of waste-water at selected points); *measures of reliability* (such as frequency and magnitude of sanitary or combined sewer overflows (SSOs, CSOs), and the frequency and magnitude of discharge of inadequately treated sewage, percentage treated, etc.); *measures of safety and health* (backup of any raw sewage into buildings-not acceptable, overflow of raw sewage into streets-acceptable in localized areas for less than 24 hrs); *and financial measures*. The Environmental Protection Agency National Pollution Discharge Elimination System (EPA NPDES) permit requirements incorporate relevant performance measures such as *discharge volume and water quality*.

Potential metrics recommended for the performance of waste-water system according to ALA (2004), are:

1. *Public health/backup of raw sewage*: This accounts the probability of achieving performance objective (e.g. – 90% probability of achieving), the probabilities of occurrence (e.g. 50% in 50 years) and different criteria as a function of method of contact (backup into buildings, overflow onto city streets).
2. *Discharge of raw/inadequately treated sewage*: Metrics commonly used quantify the impact on public health and the environment (e.g. flow associated with biochemical oxygen demand, dissolved oxygen of the receiving water).
3. *Direct damage/financial impact*: Direct damage to waste-water system components can include cleanup and repair costs associated with flood inundation of a treatment plant or repair cost of the collection system (pipelines, tunnels etc) while secondary

damage (economical cost) can be occurred to commercial or industrial facilities (e.g., factories shut down) due to loss of waste-water service.

4. *Security system performance*: The performance objective is stated in terms of probability of limiting raw sewage discharge when subjected to a design basis threat.

Moreover, performance indexes for waste-water system can account *"Societal Factors"* (ALA, 2004):

- Fines and/or jail time - resulting from illegal discharges.
- Loss of public confidence – resulting from release of raw sewage, backup of raw sewage into households, or discharging partially treated sewage into the receiving body.
- Political – resulting from peer pressure from other regional waste-water organizations, or local politicians concerned about discharge of raw or partially treated sewage in their area.
- Public health and safety – injury or death to utility staff or the public due to exposure to raw or partially treated sewage, chemical release or building collapse

According to ALA (2004), the performance of waste-water systems can be assessed in three levels: Simplified, Intermediate and Advanced.

- **Simplified Assessment: It** can be a deterministic one, where the result is calculated directly (no uncertainty taken into account), using scenario events without using the probability of the event in the calculations. A normal probabilistic risk assessment is also possible, using approximations (e.g., high, medium, and low) for the three risk components (hazard, vulnerability, consequence).
- **Intermediate Assessment: It** is a probabilistic risk assessment using a mean or median value for each of the three risk parameters, with minimal consideration of the variability of each term.
- **Advanced Assessment: It** is again a probabilistic risk assessment incorporating the variability of one or more of the risk parameters to capture their randomness and uncertainty.

The three levels of assessment are summarized below:

Level I: Simplified Assessment

- *Step 1:* This is a screening assessment for either the collection system or the treatment plant(s). The risk of loss of function is calculated for each component and for each relevant hazard, using the risk equation.

$$\text{Relative Risk} = \text{Hazard} \times \text{Vulnerability} \times \text{Consequence} \quad (1.5)$$

- *Step 2:* The "system" is considered by the consequence term, but no system method is prepared.
- *Step 3:* A "feel" for the variability of the result can be estimated by using the extremes of the ranges for each of the parameters in the risk equation
- *Step 4:* The correlation factor is incorporated to the risk equation.

- *Step 5:* After proper review and validation the highest risk components and hazards are selected for an Intermediate or Advanced Assessment.
- *Step 6:* There is no repair cost or outage time evaluation.

Level II: Intermediate Assessment

- *Step 1*: The quantitative hazard intensity and vulnerability is defined using ranges (i.e. high, medium, low).
- *Step 2:* The results for each sewer branch and flow train in the treatment plant are properly reviewed and combined; the probability of loss of function is estimated for each one.
- *Step 3:* The outage time can be calculated by combining the total number of pipeline failures or man-hours for the treatment plant and lift station restoration. The results can be divided by the available manpower to estimate the system restoration time.
- *Step 4:* The repair cost can be calculated by applying a repair cost-damage relationship to each component, and summing the results. Repair cost-damage relationships are typically developed in terms of percentage of replacement cost, so replacement costs of each component must be developed.

It must be mentioned that probabilistic assessments to address uncertainties are not required for this level of assessment

Level III: Advanced Assessment

- *Step 1:* A spread sheet method is in general developed incorporating the connectivity of the system. For each component (including pipeline segments), the specific seismic scenario probability of loss of function is calculated by multiplying the hazard probability of occurrence by the probability of loss of function. The probabilities of loss of function for each component along the pipeline branch or treatment plant train are then combined, and the sub-system or system probability of loss of function is calculated. A method is designed to show where loss of function occurs and where sewage overflows take place. Then each branch and flow train through the plant is analysed, and the results are combined. Depending on the complexity of the system, as for example in the case of the treatment plant, the method can take the form of a fault tree.
- *Step 2:* The outage time is calculated by developing restoration rates for pipelines and other system components. The repair rates are applied to the various components until they are all repaired. This is performed in incremental steps and the method can be run at each step, showing the status of the system in progressive time increments.
- *Step 3:* The same procedure can be used to calculate repair costs, except if the connectivity module is not required. Damage relationships for repair costs are applied rather than loss of functionality estimates. The total repair cost for the specific scenario is estimated as the sum of the repair cost of the individual components.
- *Step 4:* A probabilistic estimate is made taking into account the variability of the risk parameters and quantification of the uncertainty of the results. Both the hazard

intensities and the vulnerability relationships cover a range with a distribution of probabilities.

- Step 5: At the end the functionality assessment is the probability of collecting (or treating) the sewage flow through the selected portions of the system. This result is updated in time steps until the system is totally restored.

1.6.7 Fire-fighting system (FFS)

Fire is a common consequence of large earthquakes in urban and industrial areas. Fire fighting activities can be prevented due to damages in the water or other (e.g. roadway) networks after large earthquakes, resulting to serious loss of life and property. Losses from such fires can vary from insignificant (e.g. Izmit earthquake 1999, Turkey; ChiChi earthquake 1999, Taiwan) to disastrous (e.g. San Francisco 1906, USA; Tokyo 1923, Japan, Kobe 1995). In the other hand, fire following earthquake is an extremely variable phenomenon, characterized by a high level of variability in the number of ignitions and in the extent of fire-spread from each ignition.

The fire fighting system is characterized by strong interactions with other lifelines such as the water supply, gas, electric power and communication-transportation networks. However, the supply of water and the functionality of fire hydrants employ the major role for the functionality of the fire fighting system. It is possible that the water pressure will be reduced after an earthquake due to pipe breaks/leaks or/and tank failures, aggravating the fire effects in case of lack or inadequacy of alternative water supplies. Fire-station buildings and tanks are also important components, as they house the fire fighting vehicles, they provide the necessary water quantities and they constitute administrative and management centers in cases of crisis. Consequently, the vulnerability of fire fighting system is strongly related to water system. The literature review of available approaches for the seismic risk analysis of water system was previously described (section 1.6.5). A short review of available methods for the estimation of fire ignitions and fire spreading is presented in the following.

Cousins et al. (1991) developed a methodology for the assessment of areas susceptible to fire conflagrations and estimation of induced losses due to post-earthquake fires in central New Zealand. The fire losses are estimated in comparison to losses due to ground shaking based on empirical earthquake data from North America. More recently, a model for post-earthquake fires spreading was elaborated for Wellington City, by Cousins et al. (2002). The life-safety risk against post-earthquake fires from the perspective of gas and electricity distribution systems was investigated by Williamson and Groner (2000), based on data from 11 earthquake events.

A study by Robertson and Mehaffey (2000) recommends that performance based building codes should contain a framework to prevent undue reliance on sprinkler and other life safety systems that are dependent on seismically vulnerable water and electrical services. A two-level design procedure is proposed to be applied to the fire safety design of buildings located in areas of high seismicity. The first level assumes normal operational conditions for detection and suppression systems as well as fire service response, while the second level is based on impaired lifelines services and fire service response following a major earthquake.

At the individual building level, Chen et al. (2004) proposed a performance-based seismic analysis procedure considering earthquake and subsequent fires. It consists of four major

steps: hazard analysis, structural and/or non-structural analyses, damage analysis and loss analysis. Further details are provided in the next section.

Scawthorn (1986, 1987, 1991, 1997, NDC, 1992; ICLR 2001) developed different models for the simulation of post-earthquake fire spread in urban areas. The annual expected loss is estimated considering the building density, the wind speed, the adequacy of fire fighting response and the seismic intensity. Himoto and Tanaka (2002) have been focused on fire spread based on the physics of fire, assuming building- to- building fire spread due to thermal radiation and fire-induced plume.

Several computer codes were developed for the estimation of Burnt Area, such as HAZUS, URAMP, SERA and RiskLink. HAZUS (NIBS 2004) proposed a relationship for the estimation of ignition rate per square meter of built area as a function of PGA, based on the study of Eidinger et al. (1995). HAZUS except of the prediction of the fire ignitions, estimates the potential dollar loss caused by fires assuming wind speed, fire engine response time etc. URAMP estimates losses and incorporates avoid losses as benefits in a benefit – cost framework to determine the most effective seismic risk reduction program for water utility. URAMP incorporates the functionality of EPANET, a hydraulic modelling software package. URAMP analysis modules include modern hazard models to facilitate regional network analysis and consider both deterministic and probabilistic seismic risk assessment. Moreover, it calculates potential damage and economic losses due to fire-following earthquake and other economic impacts on the provider utility and community such as lost revenue, business impacts of fire and cost of sewage clean up. In a simplified way, the procedure provided includes an identification of the neighbourhoods as high, medium or low density residential, commercial or industrial occupancies. Final, the burnt areas are determined using Monte-Carlo simulation (see Fig. 1.3).

A recent monograph (Scawthorn et al. 2005) details the current state of the art in modelling fire following earthquake. Post – earthquake ignitions for a particular locality can be calculated as a random Poisson process with mean probability determined as a function of MMI or PGA and building inventory (i.e. millions of building floor area).

All previous post-earthquake fire spread models are based on the use of empirical approaches. Recent efforts combine physical laws and empirical data, attempting to simulate separately the different modes of fire spread (Lee et al. 2008).

In several studies a detailed examination of the causes of ignitions is also illustrated based on the building contents, type of use, usage hours, structural types and time of day. Tokyo Fire Department (1997) has developed a set of curves (six) considering the building occupancies (residential, commercial, industrial) and materials (wood and non-wood). These curves have been calibrated against recent US earthquakes such as San Fernando (1971), Morgan Hill (1984), Whittier (1987), Loma Prieta (1989) and Northridge (1994). Moreover, four ignition curves were produced considering the effect of time and season based on fuzzy approach. In addition, Tokyo Fire Department developed the TOSHO model that determines the fire spreading speed in four directions as a function of time. It requires a specific description of the exposure at risk and is therefore location independent.

1.6.8 Electric power network (EPN)

Damage scenarios following recent earthquakes showed that electric power delivering, one of the most important services that need to be guaranteed after an earthquake is maybe the least reliable function supplied by a civil infrastructure. Examples suggesting this include

earthquakes in many countries. After the earthquake of Kocaeli, Turkey, in 1999, a half of the region hospitals were not fed; about the same happened in Kobe, Japan, 1995, when the whole area was isolated for a period from three to five days; in Northridge, U.S.A., 1994, the electric isolation lasted a day; further earthquakes, even of moderate intensity, caused severe damage either to the whole network, preventing power flow, or to single stations, isolating single nodes.

There are many reasons for carrying out a seismic vulnerability analysis of an EPN. First, the construction of electric networks, in industrialized countries, dates back to a period when earthquake engineering was not at an advanced stage: priority was naturally given to electrical issues when designing components, and thus the equipment currently in place within the stations is not designed for horizontal forces. Further, for many pieces of equipment, the most effective electrical configuration (a slender vertical beam, with steel below, ceramic above and heavy equipment on top) happened to be the least effective structural configuration. Moreover, short-circuits may spread from one station to another, thus isolating large parts of the network.

It should be noted, however, that for a widely distributed and redundant network, damage to a few of the network components will not necessarily lead to a widespread power black-out as a result of alternative paths within the system. Also, as a result of its redundancy, the seismic performance and reliability of an electric power transmission system may be enhanced by upgrading just a few of the network components (Matsuda et al. 1991, Shumuta 2007). Quantitative (probabilistic) information on the likelihood of different levels of damage and extent of affected areas under different earthquake intensities would, therefore, be worthwhile for determining the necessary upgrading of an existing system and for emergency planning and disaster reduction preparedness, including restoration of power.

Monetary losses arising from direct and indirect losses due to seismic failures are huge, since post-emergency civil protection operations, hospitals, telecommunications, factories are all affected.

Seismic behaviour of electric power network thus appears a rewarding field of research; however, it has been the object of little effort, as compared to other topics. This is probably due to the fact that electric networks more naturally fall within the expertise of electrical engineers, and also to intrinsic complexity in modelling, requiring advanced mathematical tools and interdisciplinary knowledge.

The analysis of an EPN in a seismically active environment can be carried out, as for other lifeline systems, at two different levels.

- The first one focuses on connectivity only, hence does not involve the computation of power flows in the network. Connectivity-based methods focus on finding enough connected components within the network so that supply and demand can be balanced. In their basic form, the methods only lead to a binary statement on whether any given node is connected with another node, specifically a source node, through the network. This approach is particularly inadequate for a system such as an EPN since the tolerance on the amount and quality, in terms of voltage, of the power fed to any demand node for maintaining serviceability is very low. Actually, these methods are unable to capture flow dynamics within the network. In the recent years, a number of works dealt with seismic vulnerability analysis of an EPN based on complex system theory, which uses indicators such as betweenness, centrality and degree distribution to detect the system's vulnerabilities.

Dueñas-Osorio and Vemuru (2009) included in their reliability assessment study the analysis of flow dynamics, thus allowing to capture the possibility that the system undergoes large-scale cascading failures, the latter being caused by flow redistribution after the occurrence of disruptive events.

Li and He (2002), Lim and Song (2011) and Kim and Kang (2013) used a non-simulation-based network reliability method, the Recursive Decomposition Algorithm (RDA), for risk assessment of generic networks whose operation is defined by the connections of multiple initial and terminal node pairs. Kang et al. (2008) proposed another non-simulation-based method, the Matrix-based System Reliability (MSR) method, which is able to compute the probability of general system events (at the connectivity level) with correlated system components based on efficient matrix manipulations and minimal set identification.

Given the large computational effort required by simulation techniques for network reliability and the current availability of analytical approaches which apply mainly to simple network topologies and are limited to providing average values, low order moments, or confidence bounds of reliability metrics, Dueñas-Osorio and Rojo (2011) introduced a closed form technique to obtain the entire probability distribution of a reliability metric of customer service availability (CSA) for generic radial lifeline systems.

Further works falling within the framework of complex system theory are those by Arianos et al. (2009) and Bompard et al. (2011). The network efficiency, defined in previous works in terms of the inverse of geodesic distance between all pairs of nodes, is now replaced by the network net-ability, involving the concept of *electrical distance*, a function of line impedance and power transmission distribution factors. The work by Buritica et al. (2012) also relies on a hierarchical representation of networks, the Markov Clustering Algorithm (Gomez et al. 2011), which uses the affinity matrix and random walks to simulate flow through the network and identify communities.

- The second level of analysis, the capacitive one, is based on the power flow analysis and the point that the actual electrical quantities (voltages, currents, powers) in the network nodes and lines must be determined to make any meaningful statement on the satisfaction of the power demand at the node, not just its state of continued connectivity. The latter is an intrinsically systemic problem since it depends on the determination of the flows on the entire (damaged) network. Further, before being able to evaluate flows it is necessary to determine which is the EPN portion still up and running after an event.

  Pires et al. (1996) presented a simulation-based model to evaluate the seismic reliability of electric power transmission systems, allowing to estimate the probability of disconnection of substations from supply nodes, as well as the probability of abnormal power flow in substations. These latter facilities are considered as series systems of a number of electrical components, characterized each by a fragility function.

  Some authors (Vanzi 1995, 1996, 2000, Giannini et al. 1999, Nuti et al. 2007) did not simply consider the network nodes (buses) as points characterized by a unique fragility function; rather, they modelled the substations' internal logic. In this model, seismically-induced damage to the components of a substation can have non-local

consequences, leading to a short-circuit that may or may not propagate within the substation and eventually further away from that substation to adjacent others, generating in extreme cases very large black-outs. In the analysis of short-circuit propagation, circuit breakers are the only active components playing a key role in arresting the short-circuit spreading. This model allows for intermediate non-binary states to be captured.

Among the "probability-based" vulnerability assessment methods, Ma et al. (2010) proposed a method to evaluate the power system vulnerability in terms of voltage magnitudes and transmission lines passing their limits; a probabilistic technique is applied to obtain the PDF and CDF of the voltage magnitude and transmission line power flows. Xingbin and Singh (2004) employed the power flow computation within an integrated scheme to study the power system vulnerability considering protection system failures.

1.6.9 Natural Gas system (GAS)

The selected works referenced in this section can be classified based on the different goals that the network is expected to meet and the approach used for the network analysis.

- The reliability of an utility network such as a gas network can be measured in three perspectives: a) structural component reliability where the main goal is related to the performance of a single component of the network (e.g. for a gas system it could involve the number of breaks per kilometre for the pipeline system). In particular, regarding the pipeline system, the commonly used approaches express pipeline damage in terms of number of repairs occurring per unit of length of pipeline; meanwhile various quantitative approaches to estimate seismic performance are developed in order to account for structural parameters and to identify specific location of damage (Wijewickreme et al. 2005); b) connectivity reliability between node pairs where the main goal is related to determine the probability of the existence of a path connecting the source and the demand node when the links and the nodes are subjected to random failure events (Ching and Hsu 2007) or in terms of serviceability defined by the aggregate functionality of facilities (nodes) composing the system, i.e. the number of distribution nodes which remain accessible from at least on supply node following the earthquake (Adachi and Ellingwood 2006, Poljanšek et al. 2012); c) flow-performance reliability includes consideration of the network capacity, e.g. maintaining minimum head pressure related to leakages from two particular points of the network or related to a demand node (Li et al. 2006, Helseth and Holen 2006) or determining flow discharge of the network that quantifies the undelivered flow related to *i*-th distribution demand node related to leakages.
- Methodologies used in the evaluation of risk of natural gas networks usually rely on sampling methods, i.e. repeated simulation runs on network connectivity or flow, each one being based on random samples of seismic intensities and corresponding components' status. These methods suffer for the huge computational effort due to the large number of simulation runs needed to achieve an acceptable level of convergence. However, novel computationally-efficient simulation methods (e.g. Jayaram and Baker 2010) based on importance sampling and K-means clustering have been developed to solve this issue. In fact, the importance sampling technique can be used to preferentially sample important hazard maps and the K-means

clustering technique can be used to identify and combine redundant maps. Meanwhile various non-simulation-based approaches have been also developed such as the Matrix-based System Reliability (MSR) method (Kang et al. 2008) and usually those methods dealing with network connectivity. The basic idea of analytic network reliability analysis is to convert a complex network to the combination of simple sub-networks computing the system reliability from the probabilities of the sub-systems. In addition, the MSR method allows to account for the statistical dependence between demands and capacities of network components through efficient matrix-calculations (Chang and Song 2007). Using also efficient decomposition algorithms it is possible to handle large-scale networks; multi-scale methods (Song and Ok 2009) allow to reduce the level of computational effort and to identify the relative importance of components and sub-systems at multiple scale. In Song an Ok (2009), gas networks are decomposed into super-components representing line elements (pipelines) and node elements (stations) and each link is decomposed in a series of discretized segments whose number is related to the strength of spatial correlation. The failure probabilities of the links are computed by lower-scale MSR analyses based on the failure probabilities of the links segments and the probability that a service area is disconnected from the sources is computed by higher-scale MSR analysis based on the results of the lower-scale analyses.

1.6.10 Oil system (OIL)

The methodology for dealing with the vulnerability assessment of natural gas systems can be also applied to oil systems. The above mentioned classification can be used considering that the performance of a single component of the oil system can be different for the structural component reliability perspective (e.g. the structural damage state potentially related to loss of content of a storage tank farm [Fabbrocino et al., 2005])

2 The SYNER-G methodology

2.1 INTRODUCTION

The goal of the general methodology developed within the SYNER-G project is to *assess the seismic vulnerability of an Infrastructure of urban/regional extension*, accounting for inter- and intra-dependencies among infrastructural components, as well as for the uncertainties characterizing the problem. The goal has been achieved setting up a *model* of the Infrastructure and of the hazard acting upon it, and then *enhancing* it with the introduction of the *uncertainty* and of the analysis methods that can evaluate the system performance accounting for such uncertainty.

The Infrastructure *model* actually consists of two sets of models: the first set consists of the *physical models* of the systems making up the Infrastructure. These models take as an input the hazards and provide as an output the state of physical/functional damage of the Infrastructure. The second set of models consists of the *socio-economic models* that take among their input the output of the physical models and provide the socio-economic consequences of the event[3]. The SYNER-G methodology integrates these models in a unified analysis procedure. In its final form the entire procedure is based on a sequence of three models: a) seismic hazard model, b) components' physical vulnerability model, and c) system (functional and socio-economic) model.

For illustration purposes, with reference to the two socio-economic models identified and studied within Work Package 4 (the SHELTER and HEALTH-CARE models), Fig. 2.1 shows in qualitative terms the *integrated procedure* that leads from the evaluation of the hazard to that of the demands on the shelter and health-care system in terms of **Displaced Population** and **Casualties**, down to the assessment of social indexes like the **Health Impact** and the **Shelter Needs**.

The **Environment** acts upon the Infrastructure through the **Hazards**. These induce in the components of the Infrastructural systems a certain level of **physical damage**. In the figure, this is represented in terms of damage to **buildings**, to lifelines (**Utility loss**), to **critical facilities** and to the **transportation system**. The stack symbol in the figure employed for quantities such as damage to critical facilities and utility/transportation networks indicates that several other models, components and quantities enter into their evaluation. Taking for instance buildings as an example, the level of induced damage depends not only on the hazard but also on the fragility, a function of **Building Typology**. To compute both casualties and displaced population the occupancy level of the buildings (**Building occupancy**) is used as a first input. Building occupancy also depends on the typology, and moreover on the total **built-up area**, the **Population**, the building usage (**Use type**) and the **Time** of the day. The population at risk of being displaced is computed from the building occupancy and habitability at the time of the event (**Building habitability**). Building habitability in turn depends upon the state of **Building usability**, i.e. whether the buildings

[3] Within the SYNER-G project physical models have been developed in WP3 and WP5, while socio-economic models were developed in WP4.

are still served by fundamental utilities, and also on the **Weather** conditions. Casualties are obtained as the number of deaths and injured by combining building occupancy, building damage and building typology.

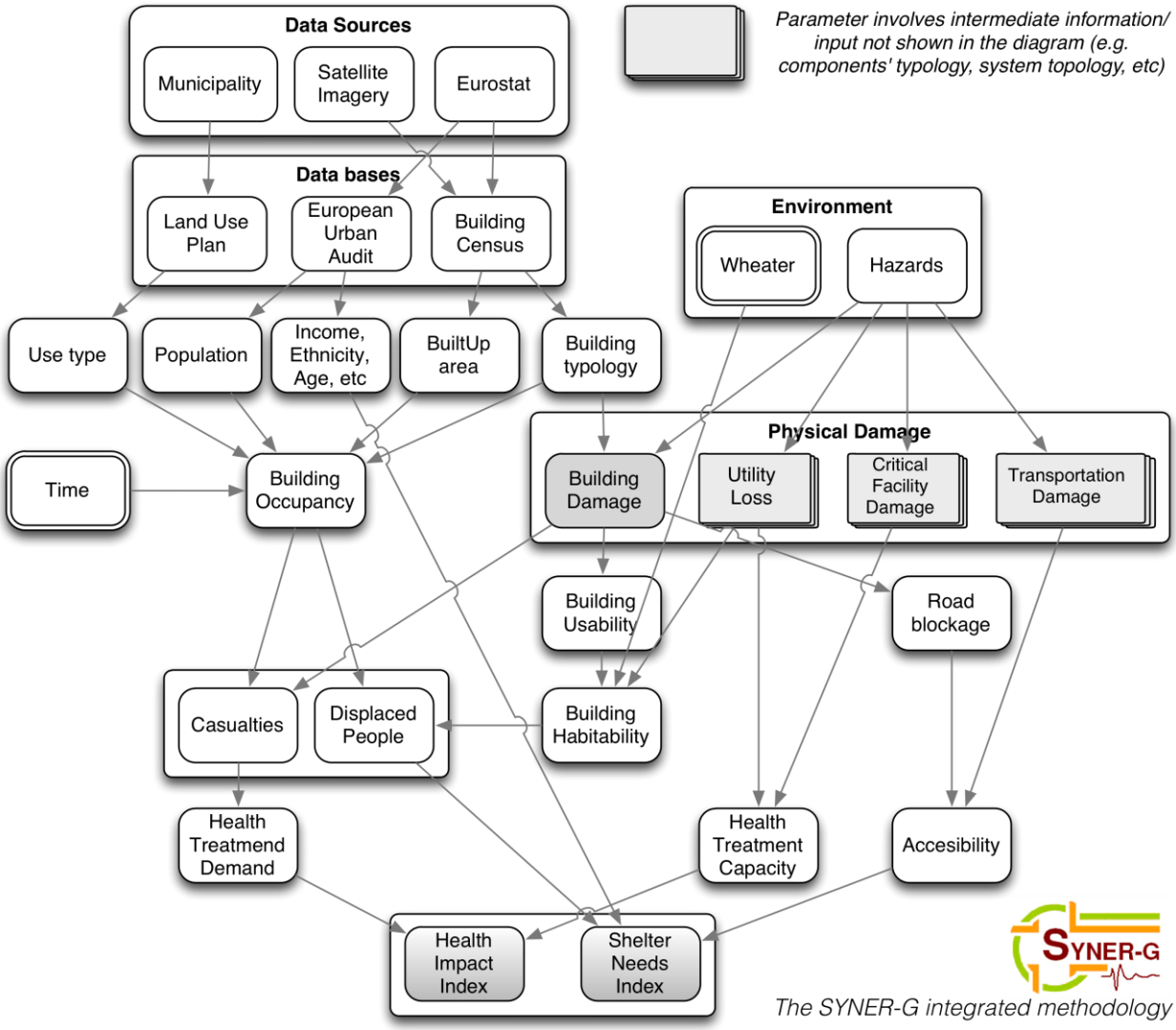

Fig. 2.1 Integrated evaluation of physical and socio-economic performance indicators

The number of casualties and displaced persons are inputs into a multi-criteria utility model to determine health impacts and shelter needs. A *Shelter Needs Index* (**SNI**) is determined by simulating a households' decision-making process and considers the *Resistance to Evacuate* (**RE**) as a multi-criteria function of the individual's vulnerabilities and coping capacities (e.g., age, housing type, housing tenure and household type), as well as external spatial and temporal factors in the community. Furthermore, not all persons who leave their homes will seek public shelter, and some may find alternative shelter accommodations (rent motel rooms or apartments), stay with family and friends, or leave the affected area. Thus, the SNI also accounts for a *Shelter Seeking factors* (**SSF**) by combining major factors contributing to demand for public shelters.

The post-disaster *Health Impacts Index* (**HII**) combines the estimated casualty numbers with three additional inputs in a multi-criteria utility model: *Health-care Treatment Capacity* (**HTC**), hospital **accessibility**, and a health impact vulnerability model which accounts for *Health Vulnerability Factors* (**HVF**) pre-disposing the exposed population to aggravated health impacts following the earthquake disaster.

Fig. 2.1 shows also how the required input information is usually contained in three distinct data bases maintained by different sources. In Europe a harmonized source for physical data on the buildings and for socio-economic data on urban areas, in the form of the **Building Census** and **European Urban Audit**, respectively, is **EUROSTAT**. The information on usage is usually provided in the form of a **Land Use Plan**, maintained from a local source (the **Municipality**)

The conceptual sketch in Fig. 2.1 can be practically implemented by developing:

- A model for the spatially distributed seismic hazard
- A physical model of the Infrastructure
- Socio-economic models

Development of the hazard model has the goal of providing a tool for: a) sampling events in terms of location (epicentre) and possibly extension, magnitude and faulting style according to the seismicity of the study region b) predicting maps of seismic intensities at the sites of the vulnerable components in the Infrastructure. These maps, conditional on M, epicentre, etc. should correctly describe the variability and spatial correlation of intensities at different sites. Further, when more vulnerable components exist at the same location and are sensitive to different intensities (e.g. acceleration and displacement), the model should predict intensities that are consistent at the same site.

Development of the physical model starts from the SYNER-G Taxonomy presented in the previous chapter and requires: a) for each system within the Taxonomy, a description of the functioning of the system under both *undisturbed* and *disturbed* conditions (i.e. in the damaged state following an earthquake); b) a model for the physical and functional (seismic) damageability of each component within each system; c) identification of all dependencies between the systems; d) definition of adequate performance indicators for components and systems, and the Infrastructure as a whole.

Development of the socio-economic model starts with an interface to outputs from the physical model in each of the four domains of SYNER-G (i.e., buildings, transportation systems, utility systems and critical facilities). Thus, four main performance indicators - Building Usability, Transportation Accessibility, Utility Functionality and Healthcare Treatment Capacity – are used to determine both direct and indirect impacts on society. Direct social losses are computed in terms of casualties and displaced populations. Indirect social losses are considered in two models – Shelter Needs and Health Impact – which employ the multi-criteria decision analysis (MCDA) theory for combining performance indicators from the physical and social vulnerability models.

In order to tackle the complexity of the described problem the object-oriented paradigm (OOP) has been adopted. In abstract terms, within such a paradigm, the problem is described as a set of *objects*, characterized in terms of *attributes* and *methods*, interacting with each other (see 2.2.1). Objects are *instances* (concrete realizations) of *classes* (abstract models, or *templates* for all objects with the same set of properties and methods).

The developed model of the problem (*domain*, in the OO setting described in the following) is described in the next sections as follows:

- Section 2.2 has an introductory character and, without entering into the details of their attributes and methods, provides an outline description of the classes, focussing on their mutual relations. This is done by means of so-called *class-diagrams*. The section gives also examples of actual sets of objects corresponding to sample physical systems, through so-called *object-diagrams*.
- Section 2.3 illustrates the Infrastructure portion of the model. In particular, a detailed description is given of the functioning (governing flow equations for networks, demand models, seismic damageability of components, physical and socio-economic performance indicators, inter-dependencies) of a sub-set of the systems in the Taxonomy (specification of the methodology for all other systems is the task of WP5 and the interested reader can found this material in the reports from that work package).
- Section 2.4 illustrates the Hazard portion of the model. In particular, the method used to simulate spatially correlated fields of vector intensities at the sites of the vulnerable components is described.
- Section 2.5 describes the Uncertainty model and the Analysis methods for the probabilistic evaluation of Infrastructure performance.

2.2 OBJECT-ORIENTED MODEL: GENERAL

2.2.1 A brief overview of basic concepts in OO modelling

As anticipated, an important choice in the development of the SYNER-G methodology has been to adopt the paradigm of object-oriented modelling. This approach to modelling has emerged in the computer science community starting from the ‘60s (introduction of classes and data abstraction in programming languages such as e.g. Pascal) but has seen a real boom in the ‘80s and a widespread adoption only since the ‘90s.

Object-oriented technology is built on a sound engineering foundation, whose elements are collectively called the *object model of development* or, simply, the **object model**, which is the conceptual framework for all things *object-oriented*. The object model encompasses the seven principles or elements of **abstraction**, **encapsulation**, **modularity**, **hierarchy**, **typing**, **concurrency**, and **persistence**. By themselves, none of these principles are new. What is important about the object model is that these elements are brought together in a synergistic way.

The *first four elements* or principles of the model play a *major* role (i.e. a model without any one of these elements is not object- oriented):

1. **Abstraction**: An abstraction denotes the essential characteristics of an object that distinguish it from all other kinds of objects and thus provide crisply defined conceptual boundaries, relative to the perspective of the viewer. Abstraction is at the very core of object-oriented model, without it the idea of class of objects could not exist. Deciding on the right set of abstractions for a given domain is the central problem in object-oriented design. Amongst various types of abstraction, **entity abstractions** are very appealing since they represent a useful model of a problem

domain or solution domain entity. One usually strives to build entity abstractions because they directly parallel the vocabulary of a given problem domain (e.g. the classes Infrastructure, and sub-classes, or Hazard, and sub-classes).

2. **Encapsulation**: Encapsulation is the process of compartmentalizing the elements of an abstraction that constitute its structure and behaviour; encapsulation serves to separate the contractual interface of an abstraction and its implementation. Abstraction and encapsulation are complementary concepts: Abstraction focuses on the observable behaviour of an object, whereas encapsulation focuses on the implementation that gives rise to this behaviour. Encapsulation is most often achieved through information hiding (not just data hiding), which is the process of hiding all the secrets of an object that do not contribute to its essential characteristics; typically, the structure of an object is hidden, as well as the implementation of its methods. *"No part of a complex system should depend on the internal details of any other part"*. Whereas abstraction "helps people to think about what they are doing," encapsulation "allows program changes to be reliably made with limited effort".
3. **Modularity**: Modularity is the property of a system that has been decomposed into a set of cohesive and loosely coupled modules. Modularization consists of dividing a program into modules which can be compiled separately, but which have connections with other modules. Most languages that support the module as a separate concept also distinguish between the interface of a module and its implementation. Thus, it is fair to say that modularity and encapsulation go hand in hand. Deciding on the right set of modules for a given problem is almost as hard a problem as deciding on the right set of abstractions. Modules serve as the physical containers in which we declare the classes and objects of our logical design. The overall goal of the decomposition into modules is the reduction of software cost by allowing modules to be designed and revised independently. Each module's structure should be simple enough that it can be understood fully; it should be possible to change the implementation of other modules without knowledge of the implementation of other modules and without affecting the behaviour of other modules (e.g. in the seismic vulnerability problem at hand, three possible modules are the seismic hazard, the physical vulnerability and the systemic behaviour models).
4. **Hierarchy**: Hierarchy is a ranking or ordering of abstractions. The two most important hierarchies in a complex system are its class structure (the "is a" hierarchy) and its object structure (the "part of" hierarchy). Abstraction is a good thing, but in all except the most trivial applications, one may find many more different abstractions than can comprehend at one time. Encapsulation helps manage this complexity by hiding the inside view of our abstractions. Modularity helps also, by giving us a way to cluster logically related abstractions. Still, this is not enough. A set of abstractions often forms a hierarchy, and by identifying these hierarchies in our design, we greatly simplify our understanding of the problem (e.g. Infrastructure, above critical facilities/networks/inhabited areas, each above its component sub-classes, etc etc).

Finally, the *last three elements/principles* of the object model play a *minor* role (i.e. each of these elements is a useful, but not essential, part of the object model), and the reader is referred again to (Booch et al, 2007) for their meaning.

The importance of abstraction in mastering complexity cannot be understated: *"The nature of abstractions that may be achieved through the use of procedures is well suited to the description of abstract operations, but is not particularly well suited to the description of abstract objects. This is a serious drawback, for in many applications, the complexity of the data objects to be manipulated contributes substantially to the overall complexity of the problem"* (Booch *et al* 2007). This is exactly the nature of the application considered within the SYNER-G project: the analysis of a large complex system of interconnected systems. There are limits to the amount of complexity we can handle using only algorithmic decomposition; thus we must turn to object-oriented decomposition. This is the reason why for the seismic vulnerability problem at hand, the OO paradigm has been adopted to produce the problem model.

2.2.2 Fundamentals of the Unified Modelling Language (UML)

Having a well-defined and expressive notation is important to the process of software development, and more generally to the design of any model. The *Unified Modelling Language* (UML) is the primary modelling language used to analyze, specify, and design software systems. Following the growth of object-oriented programming languages, object-oriented methodologies began to arise and be subsequently modified and refined. Only in 1997 the standard modelling language was approved by the *Object Management Group* (OMG), a consortium that creates and maintains standards for the computer industry.

It should be apparent how it is impossible to capture all the subtle details of a complex system, and of the software that models it, in just one large diagram. Thus, the UML has numerous types of diagrams, each providing a certain view of your system. One must understand both the structure and the function of the objects involved. One must understand the taxonomic structure of the class objects, the inheritance mechanisms used, the individual behaviours of objects, and the dynamic behaviour of the system as a whole. Amongst various available types of diagrams only two are used within this report: the *class* and the *object* diagrams.

A class diagram is used to show the existence of classes and their relationships in the logical view of a system. A single class diagram represents a view of the class structure of a system. The two essential elements of a class diagram are *classes* and *their basic relationships*.

The *class* icon (used to represent a class in a class diagram, see Fig. 2.2 left) consists of three compartments, with the first occupied by the class *name*, the second by the *properties* (or *attributes*), and the third by the *methods* (or *functions/operations*). A name is required for each class and must be unique to its enclosing namespace. By convention, the name begins in capital letters, and the space between multiple words is omitted. Again by convention, the first letter of the property and method names is lowercase, with subsequent words starting in uppercase, and spaces are omitted just as in the class name.

An *abstract class* is one for which no instances may be created. Because such classes are so important to engineering good class *inheritance trees*, there is a special way to designate an abstract class, as shown in Fig. 2.2 right (class *FoodItem*). Specifically, the class name is italicized to show that one can have only instances of its subclasses (that is Tomatoes, in the figure). Similarly, to denote that an operation is abstract, we simply italicize the operation name; this means that this operation may be implemented differently by all instances of its subclasses.

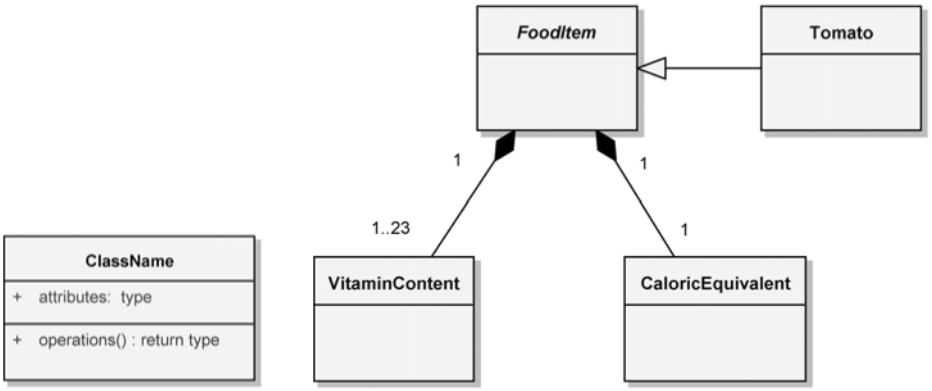

Fig. 2.2 The class icon (left) and abstract classes (right)

Classes rarely stand alone; instead, they collaborate with other classes in a variety of ways. The essential connections among classes include **association**, **generalization**, **aggregation**, and **composition**, whose icons are summarized in Fig. 2.3. Each such relationship may include a textual label that documents the name of the relationship or suggests its purpose, or the association ends may have names—but typically both are not used at the same time.

The *association* icon connects two classes and *denotes a semantic connection*. Associations are often labelled with noun phrases, such as Analyzes in the figure, denoting the nature of the relationship. A class may have an association to itself (called a *reflexive association*), such as the collaboration among instances of the PlanAnalyst class. Note here the use of both the association end names and the association name to provide clarity. It is also possible to have more than one association between the same pair of classes. Associations may be further adorned with their **multiplicity**, using the syntax in the following examples:

- 1 Exactly one
- * Unlimited number (zero or more)
- 0..* Zero or more
- 1..* One or more
- 0..1 Zero or one
- 3..7 Specified range (from three through seven, inclusive)

The multiplicity adornment is applied to the target end of an association and denotes the number of links between each instance of the source class and instances of the target class. Unless explicitly adorned, the multiplicity of a relationship should be considered unspecified.

The remaining three essential class relationships are drawn as refinements of the more general association icon. Indeed, during development, this is exactly how relationships tend to evolve. We first assert the existence of a semantic connection between two classes and then, as we make tactical decisions about the exact nature of their relationship, often refine them into generalization, aggregation, or composition relationships.

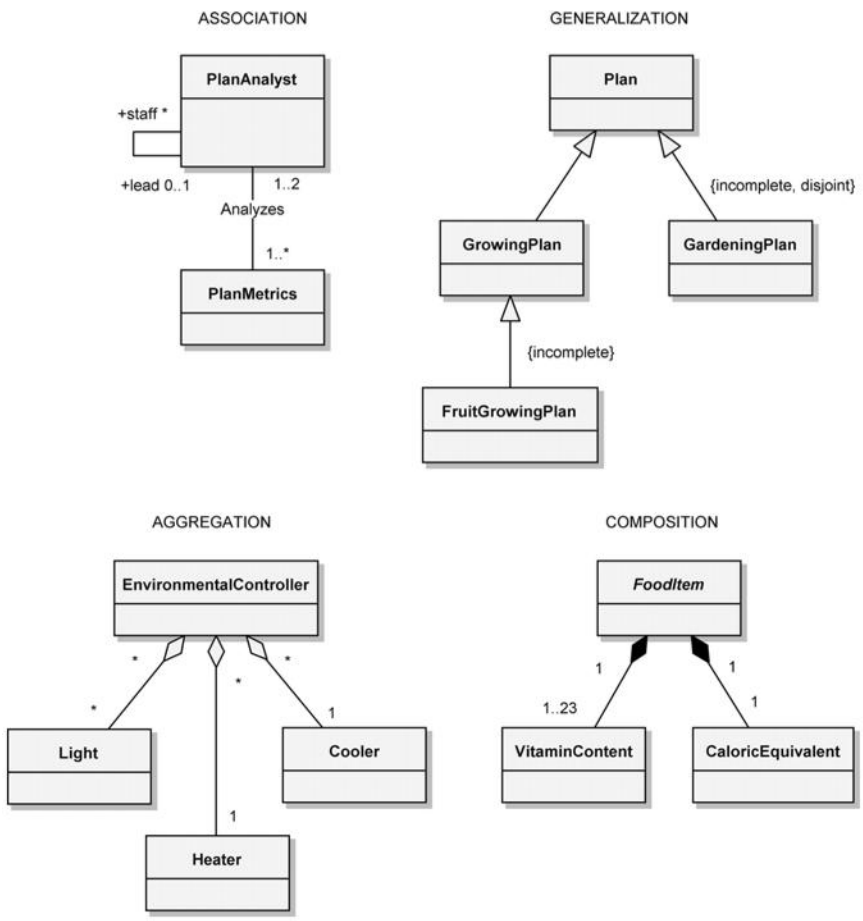

Fig. 2.3 Relationships between classes

The **generalization** icon denotes a generalization/specialization relationship (the “is a” relationship) and appears as an association with a closed arrowhead. The arrowhead points to the *superclass*, and the opposite end of the association designates the *subclass*. The GrowingPlan class in the figure is the superclass and its subclass is the FruitGrowingPlan. According to the rules of the chosen implementation language, the subclass inherits the structure and behaviour of its superclass. Also according to these rules, a class may have one (single inheritance) or more (multiple inheritance) superclasses; name clashes among the superclasses are also resolved according to the rules of the chosen language. Also, generalization relationships may not have multiplicity adornments.

Aggregation, as manifested in the “part of ” relationship, is a constrained form of the more general association relationship. The aggregation icon *denotes a whole/part hierarchy* and also implies the ability to navigate from the aggregate to its parts. It appears as an association with an unfilled diamond at the end denoting the aggregate (the whole). The class at the other end denotes the class whose instances are part of the aggregate object. Reflexive and cyclic aggregation is possible. This whole/part hierarchy *does not mean physical containment*: A professional society has a number of members, but by no means does the society own its members. In the figure, we see that an individual EnvironmentalController class has the Light, Heater, and Cooler classes as its parts. The multiplicity of * (zero or more) at the aggregate end of the relationship further highlights this lack of physical containment.

The choice of aggregation is usually an analysis or architectural design decision; the choice of **composition** (physical containment) is usually a detailed, tactical issue. Distinguishing physical containment is important because it has semantics that play a role in the construction and destruction of an aggregate's parts. The composition icon denoting a containment relationship appears as an association with a filled diamond at the end denoting the aggregate. The multiplicity at this end is 1 because the parts are defined as having no meaning outside the whole, which owns the parts; their lifetime is tied to that of the whole. The FoodItem class in the figure physically contains the VitaminContent and CaloricEquivalent classes.

2.2.3 Class diagrams of the SYNER-G model

A high-level representation of the object-oriented model of the Infrastructural vulnerability assessment problem is shown in Fig. 2.4. The first class in the scheme is the *Analysis* one. This class is an abstract one with two generalizations: *simulationMethod* and *nonSimulationMethod*. As explained later, these are the two large groups of methods that can be used to perform a probabilistic analysis of the system, and even though only simulation methods have been implemented so far (see Section 2.5.2),, the object-oriented model has been set up in a general manner. The figure shows that also the *simulationMethod* class is abstract, though it contains both abstract and concrete methods, and that two concrete classes are provided so far: the plain Monte Carlo simulation method (class *MCS*) and the importance sampling simulation method (*ISS*), which may be enhanced with the K-means clustering procedure (see Section 2.5.2).

The object of the analysis is the *Environment* which is *composed* of three classes, the *Infrastructure*, the *Hazard* and the *Weather*.

The Environment is the portion of physical space, inclusive of the Earth crust and the atmosphere, which needs to be considered in evaluating the impact of the hazard on the Infrastructure. Within this general scheme, ideally, one could evaluate the impact of a chain of events such as an earthquake occurring on a fault, inducing physical damage in the Infrastructure, triggering e.g. fires and the dispersion of pollutants, as affected by *weather* conditions, in the atmosphere. Within the SYNER-G project the scope is the evaluation of the direct physical damage due to an earthquake and of its direct and indirect socio-economic consequences, but an attempt has been made to set up a model that is general and leaves room for later extensions to multi-hazard contexts.

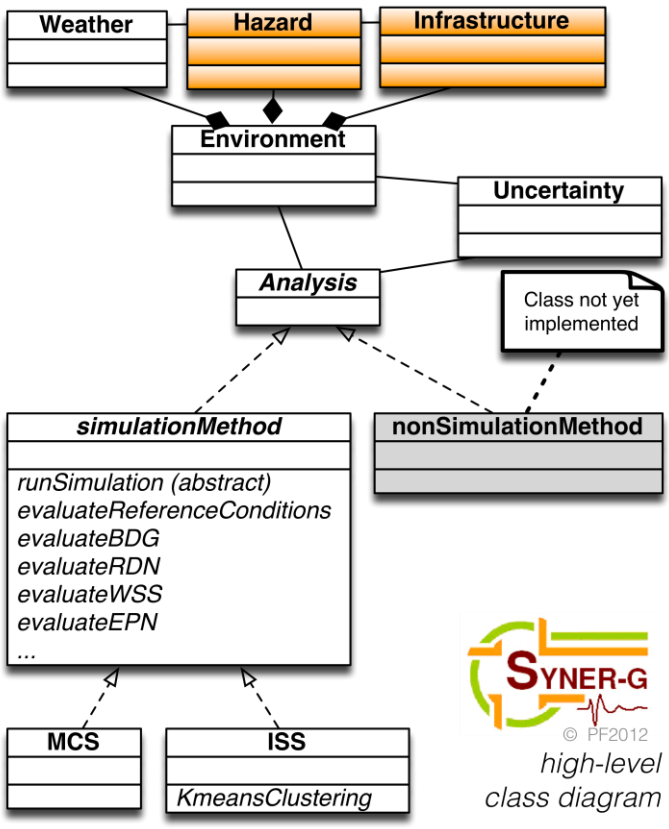

Fig. 2.4 Highest level class diagram for the Infrastructural vulnerability assessment problem (the grey hatch, as indicated, denotes classes that have been included at the conceptual level but have not yet been implemented; the orange hatch indicates classes that are detailed in the following)

Fig. 2.5 shows the *Hazard* class in more detail. This class is the *composition* of two *abstract* classes: *man-made* and *natural* hazards. The class Natural contains environmental hazards such as the seismic one, volcano eruption, floods, etc. The Seismic hazard, in turn, is modelled as the composition of three classes: one class for seismo-genetic sources, one for events and the third one for the local intensity at each site.

Objects from the SeismicSource class are, as the name says, sources that can generate earthquakes. So far two subclasses have been designed to account for fault models of different complexity. In any given problem a set of objects from this class will described the regional seismicity. The class SeismicEvent is the class from which earthquakes in terms of localization and magnitude are instantiated. The passage from macro-seismic parameters to intensity values at each site of interest is performed by objects instantiated from the third class LocalIntensity. The class is further detailed in a sub-hierarchy, as shown in Fig. 2.6.

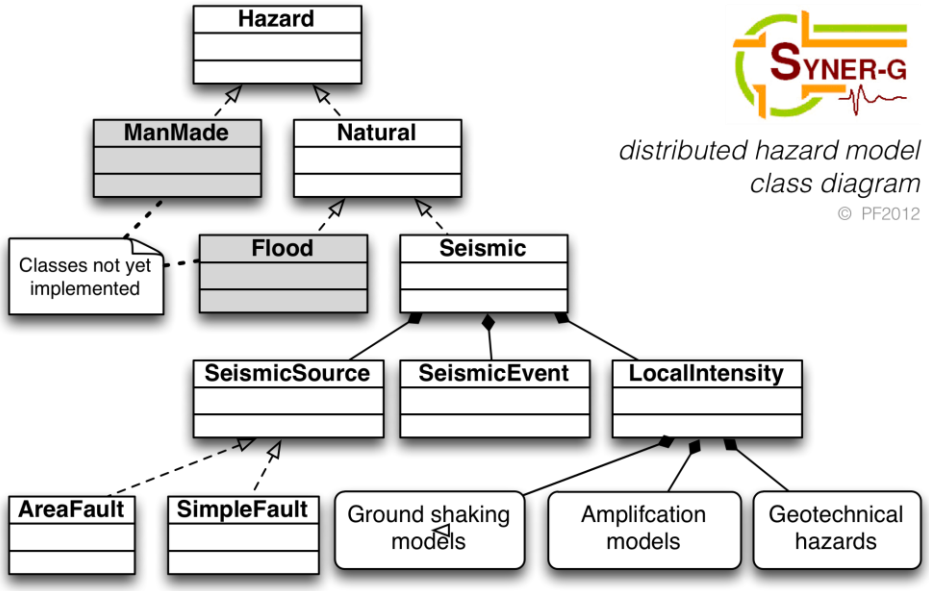

Fig. 2.5 Class diagram for the Hazard class (the grey hatch, as indicated, denotes classes that have been included at the conceptual level but have not yet been implemented)

Local intensity of ground motion at a site at distance R from the epicentre/fault surface, during an event of magnitude M, can be predicted both in terms of a ground shaking parameter by means of ground motion prediction equations (GMPE), or in terms of a so-called geotechnical hazard, that is a displacement measure such as permanent ground deformation. The exact measure of the local intensity, commonly denoted as Intensity Measure (IM), depends on the components at the site of interest, and in particular on the required input to their fragility models. Furthermore, local intensity strongly depends on the site response, which is a function of the soil profile in the upper layers. As a result the LocalIntensity class is the composition of the GMPE, Amplification and GeotechnicalHazard classes.

The GMPE class is an abstract one, with concrete realizations providing alternative GMPEs. Currently only one model has been implemented, based on the GMPE by Akkar and Bommer (2010), which is fit for use in the European, Mediterranean and Middle-East regions. In the already mentioned strive for generality, it was foreseen that local shaking could be described by more than just one scalar or vector IM, i.e. in terms of an entire ground motion time series. Models that take as an input the same parameters as a GMPE, but produce such time-series matching mean and variance of natural motions have appeared recently and could be easily implemented and integrated into the SYNER-G OO-model. In this respect, the SYNER-G model can be seen as versatile container framework where existing models and new ones can be easily integrated for the purpose of systemic vulnerability analysis.

The Amplification class is abstract. Amplification can be treated, based on the amount of available information, either in simple deterministic manner (which includes even basic code-type scalar amplification factors), or in mode refined probabilistic manner (see next Section 2.4.4).

Finally, the GeotechHazard class is also an abstract class, with three concrete subclasses corresponding to the physical counterparts of co-seismic rupture, landslide and liquefaction, all of which produce permanent ground deformations (see next Section).

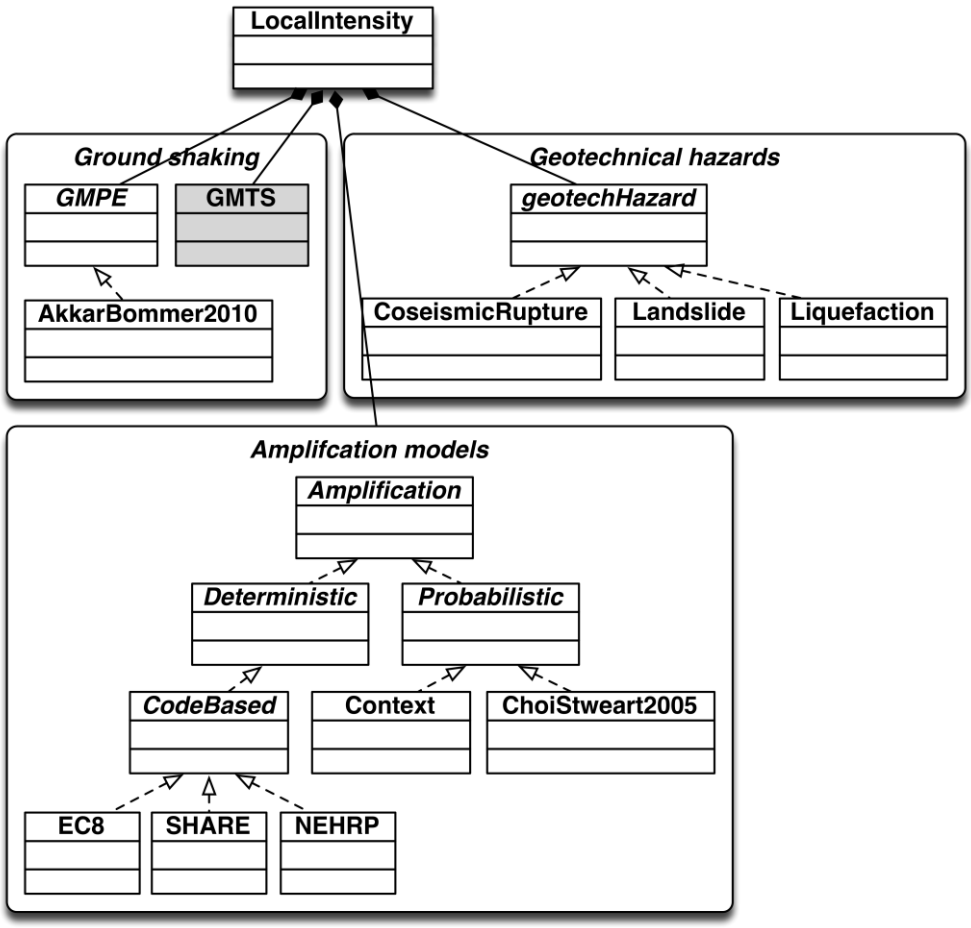

Fig. 2.6 Class diagram for the LocalIntensity class (the grey hatch denotes classes that have been included at the conceptual level but have not yet been implemented)

Fig. 2.7 shows the Infrastructure class and sub-classes. As already stated in Section 1.4, the physical portion of the Infrastructure is made up of a number of systems that can be subdivided into three groups from a geometric point of view: point-like, line-like and area-like systems. Correspondingly, the *Physical* class is the composition of three classes: the *Critical facility* class (point-like), the *Network* class (line-like) and the *Region* class (area-like). The Network and Critical facility classes are abstract ones, and are the generalizations of all types of networks and of critical facilities.

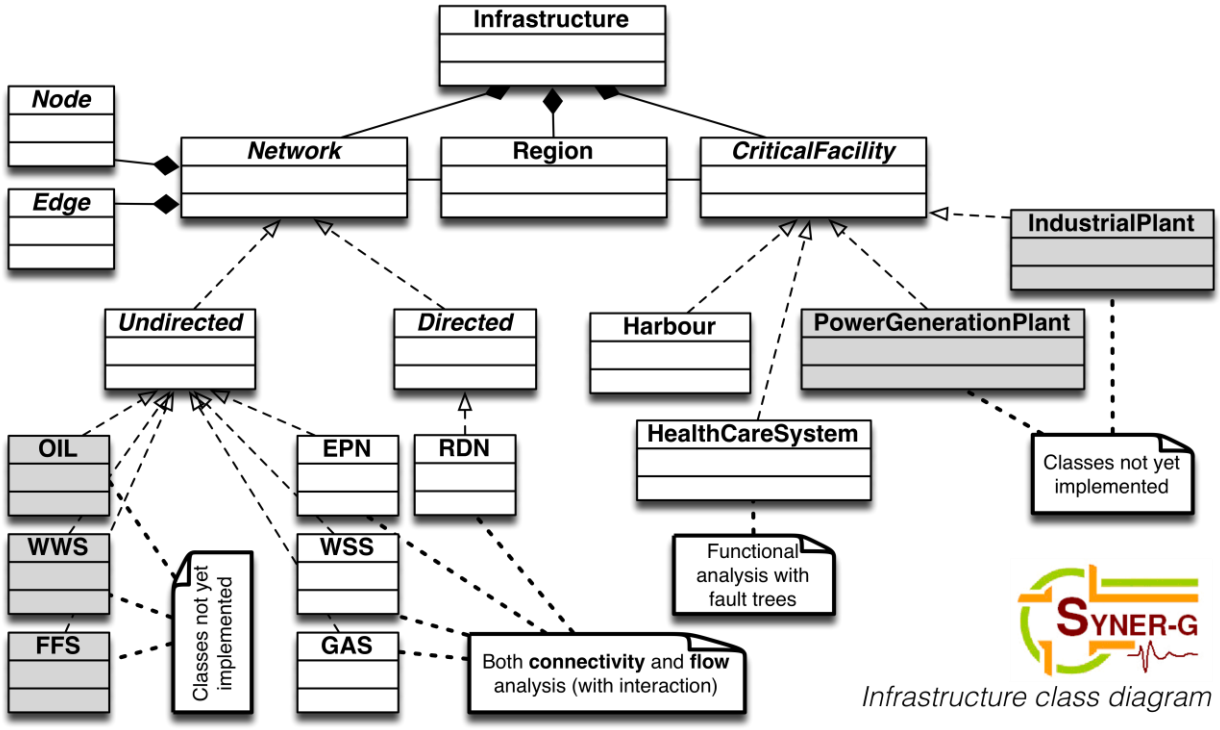

Fig. 2.7 Class diagram for the Infrastructure portion of the model (the grey hatch denotes classes included at the conceptual level but not yet implemented)

The indicated association relationships between Network, Region and CriticalFacility extend to their subclasses. This means that an object from one of these classes can call the methods from another class. This is used, for instance, in a way that the object describing the set of buildings in a neighbourhood (an object from the class Region) can “ask” to the object electric power network (from the corresponding class) whether there is still electric power fed to the neighbourhood after the seismic event, or, for example, in a way that a pumping station object within the water supply system object (from Network/WSS), can make the same query to the distribution station object within the electric power network object.

As shown in the figure, the Network class is the generalization of all the networks in the Taxonomy: the road and railway networks (transportation networks), the electric power networks, the oil and gas distribution networks, the water and waste-water networks and the fire-fighting network (utility/lifeline networks). At the very basic level of analysis, which is the connectivity one, all networks are described as graphs and a host of graph theoretic results can be exploited for their analysis. For this reason a deep level of abstraction has been used in Network and its subclasses. In particular, the class is abstract and composed of two abstract classes for *Nodes* and *Edges*, the basic components of all graphs. Further, *Network* is defined as the generalization/abstraction of two intermediate abstractions: they correspond to the two groups of *Directed* (in the considered domain this is transportation networks) and *Undirected* (lifelines/utilities) graphs. This abstraction allows together with the principle of inheritance, to design the lower level sub-classes with a much lower effort, since the appropriate basic network structure is already set up for all networks at a higher level. Two concrete classes are described in the following in more detail for illustration purposes:

the water supply system and the electric power network. Their class-diagrams are shown together in Fig. 2.8.

Both the WSS and EPN classes are composition of the corresponding node and link classes. The latter, in general, are abstract classes, since there can be several types of links and nodes within a network, differentiated in terms of properties and functions. For instance, for the water-supply system, links can either be pipes or tunnels, while nodes can be end-user demand nodes, water sources or pumping stations. The *Water source* class is an abstract one, since there can be both variable head (like tanks) and constant head (like large reservoirs) water sources.

As far as the electric-power network is concerned, links can be either overhead or buried lines, and there three node types: end-user demand nodes (load bus), electric power sources (generator) and a balance node, called the SlackBus, which is usually chosen as one of the power sources and is used, as explained later, as a mathematical expedient to solve the nonlinear alternate current (AC) equations (it provides the balance of flows during iterations in the solution). Load buses can be either distribution (D) or transformation/distribution sub-stations (TD). These nodes are assemblies of several micro-components, each one with its electrical function. A more detailed description of this internal logic of the sub-stations in an EPN is given in the later Section 2.3.7.

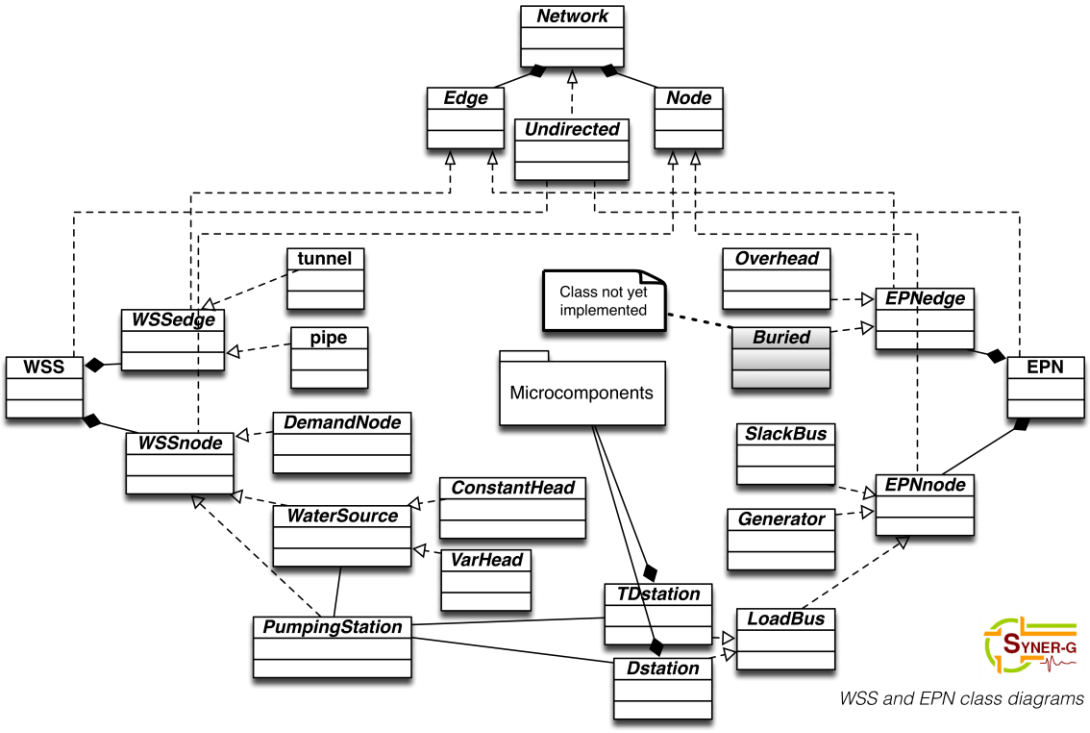

Fig. 2.8 Class diagram for the WSS and EPN classes (the grey hatch denotes classes included at the conceptual level but not yet implemented)

The two networks are shown in the same figure to highlight the association between the pumping station class in the WSS and the distribution and transformation/distribution classes in the EPN. This is an example of the way inter-dependencies of the *physical* type (see Section 1.2 and the later Section 2.3.2) are modelled within the SYNER-G methodology. The

association means that a pumping station object can query the reference EPN station to know its state and the actual power fed at any time, so that operational level f the pumps can be established. At the same time, a variable head water source (a tank, a well-field) can be out-of-service if the corresponding pumping station is not fed with power, and the connection between these objects is shown with another association in the figure.

The specification of the full set of class-diagrams down to the basic component level for all systems in the SYNER-G Taxonomy is the output of WP5 and the interested reader can refer to the corresponding reports.

2.2.4 Sample object diagrams

While classes are useful to represent all the systems with their high-level relationships, the actual models on which the vulnerability analysis is carried out are not made of them, but, rather, as already explained in the Section 2.1, they are collection of objects. For the purpose of illustration Fig. 2.9 and Fig. 2.10 show a sample WSS and a sample EPN (top), respectively, with the corresponding set of objects (bottom). For example, the elementary WSS has two sources, a tank and a well (with the associated pump), four demand nodes (two end-users with non-zero demands, and two junctions, which are modelled as demand nodes with zero assigned demand) and a number of connecting elements (five pipe segments and a tunnel). Correspondingly, there are five objects (*pipe1* to *pipe5*) of the class Pipe, one object *tunnel* of class Tunnel, etc. In the UML notation objects are labelled with their name and the corresponding class, separated by a colon.x\

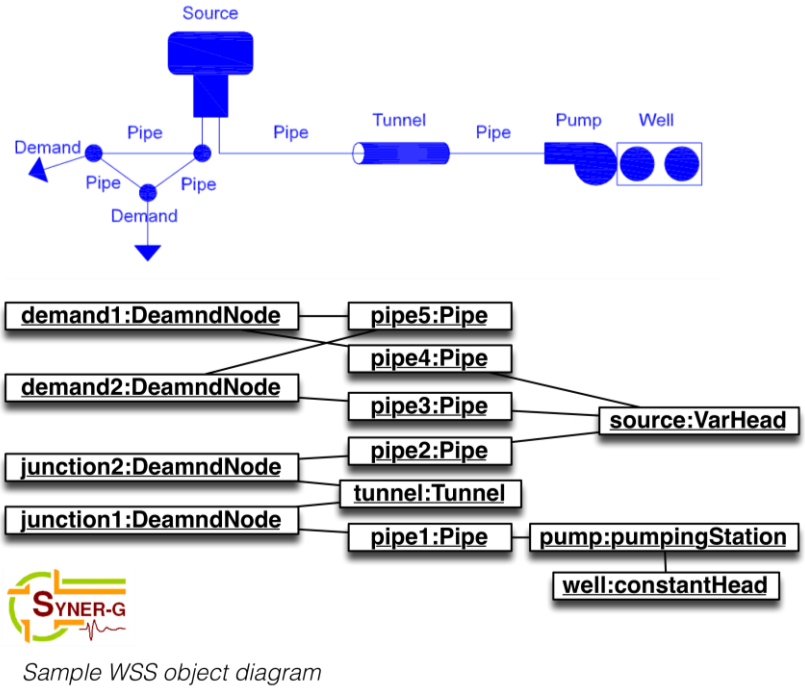

Fig. 2.9 Sample WSS (top) and corresponding object-diagram (bottom)

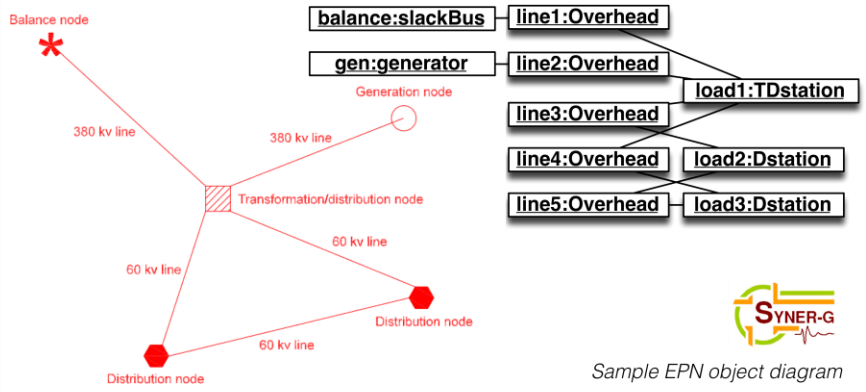

Fig. 2.10 Sample EPN (top) and corresponding object-diagram (bottom)

2.3 INFRASTRUCTURE MODEL

2.3.1 Introduction

This section provides details on the modelling of the physical behaviour of a sub-set of the systems from the SYNER-G Taxonomy: buildings and two utilities, the water supply system and the electric power network. In particular, with reference to the WSS and EPN systems, the description consists of an explanation of the *governing flow equations*, on information on the *fragility models for their components*, as well as on the *models to evaluate demands on these networks*, both in reference pre-earthquake conditions and in the damaged post-earthquake state. The selected systems constitute a minimum set in which interdependencies can already be illustrated, as shown in Section 2.3.2.

A central role is played by the area-like system made up of all residential/commercial/ industrial buildings and in general of buildings that are not included among critical facilities. These buildings are where people live, work and consume goods and services. For this reason this system is the source of demands on all other systems (e.g. electric power and water supply demands, but also casualties to be transported through the road network to health-care facilities, displaced households seeking public shelter, etc.). Further, in terms of economic loss estimation, the largest proportion of direct loss due to physical damage and a considerable one of the indirect (e.g. business interruption) come from damage to these buildings. The corresponding class (Region, in Fig. 2.7) is thus described first and in more detail in Section 2.3.4, followed by WSS (Section 2.3.6) and EPN (Section 2.3.7).

2.3.2 Interdependencies

Interaction within and between systems have been classified in Section 1.2, as Physical, Cyber, Geographic, Logical, Societal, Policy-related. Not all of them have been modelled within the methodology.

Geographic interactions (physical proximity) are modelled in the seismic case by correctly incorporating within the seismic hazard model the statistical dependence structure between intensities at the same or close sites.

Societal interactions are accounted for, e.g. in passing from a potential number of shelter-seeking population to the actual figure, incorporating factors such as anxiety, neighbourhood effects, income, etc. as shown in Fig. 2.1.

In this Section and the remainder of the chapter, the focus is on Physical (functional) interactions which are those related to the physical modelling of the Infrastructure.

Table 2.1 reports the interdependencies between some of the systems in the Taxonomy: the i-th row presents the influences of the i-th system on the other systems, while the j-th column collects the influences from other systems on the j-th system. The letter codes stand for: Physical (P), Demand (D) and Geographical (G) interactions. Numbers refer to the following descriptions of the interdependency type:

1. Fires in buildings can be triggered by earthquake induced damage thus raising the water-supply demand on the WSS (when this is not independent of the FFS);
2. In a urban setting, structural damage to buildings produces debris that can cause road blockages;
3. Structural and non-structural damage to buildings may result in casualties that need to be treated in a health-care facility and hence determine the demand on this system;
4. Damage to the EPN can lower the service level in the struck area, possibly below tolerance thresholds thus leading to population displacement and demand on the Shelter model;
5. Damage to the EPN can prevent functioning of pumping stations in the WSS;
6. Damage to the EPN can prevent functioning of re-gasification and regulation/metering stations in the GAS system;
7. Damage to the EPN can prevent functioning of stations in the OIL system;
8. Damage to the EPN can prevent functioning of critical components in the HBR system;
9. Damage to the EPN can prevent power to be fed to the health-care facilities hindering emergency response in case a joint failure of backup power sources occur.
10. Damage to the WSS can lower the service level in the struck area, possibly below tolerance thresholds thus leading to population displacement and demand on the Shelter model;
11. Damage to the WSS can prevent water to be delivered to the health-care facilities hindering emergency response over time in case backup reservoirs are depleted;
12. Damage to the GAS system lower the service level in the struck area, possibly below tolerance thresholds, especially in adverse weather conditions, thus leading to population displacement and demand on the Shelter model;
13. Damage to the GAS system can stop production in generators within the EPN inducing power shortages;
14. Damage to the GAS system can prevent natural gas to be fed to the health-care facilities hindering emergency response in case backup power sources depend on gas fuel.

15. Damage to the OIL system can stop production in generators within the EPN inducing power shortages;
16. Damage to the transportation network can block access to damaged buildings hindering emergency response;
17. Damage to the transportation network can block access to the HBR preventing goods to be dispatched and causing large economic loss;
18. Damage to the transportation network can block access to health-care facilities hindering emergency response;
19. Demand for transportation (which concur to the determination of the origin-destination matrix that drives traffic flows) of goods is generated in HBR (HBR is an origin)
20. Demand for transportation is generated in HCS (as a destination)

Table 2.1 Interdependencies for sample system from the Taxonomy

	BDG	EPN	WSS	GAS	OIL	RDN	HBR	HCS
BDG		D	D_1	D		D G_2		D_3
EPN	P_4		P_5	P_6	P_7		P_8	P_9
WSS	P_{10}							P_{11}
GAS	P_{12}	P_{13}						P_{14}
OIL		P_{15}						
RDN	P_{16}						P_{17}	P_{18}
HBR						D_{19}		
HCS						D_{20}		

The evaluation of the above interactions requires establishing a sequence of actions and messages between the objects making up the model. This sequence establishes an order in the evaluation of states of the objects, something that is described within UML with a so-called *state diagram*. Fig. 2.11 presents such a diagram. In any given overall system-of-systems evaluation an inizialization phase is performed first, with the BDG object settingp the region discretization into cells and passing their centroids to the other systems, which in turn compile a list of tributary cells for each of their demand node and assign this demand node as a reference node to the cells. Demand for goods and services is then evaluated and an analysis of all systems in the pre-earthquake undisturbed conditions is carried out. Then, for all considered events, generation of shake field (local intensities at all relevant locations, i.e. the systems' components sites and cell centroids) is followed by evaluation of: 1) the EPN; 2) all other utilities, with direct damage and possible power losses from the EPN; 3) the BDG, with direct damage and utility loss; 4) the RDN, with demand from the BDG and closures due to direct damage to its elements as well as from road blockages; 5) the HCS

with demand from the BDG system, service level from all utilities and accessibility from the RDN.

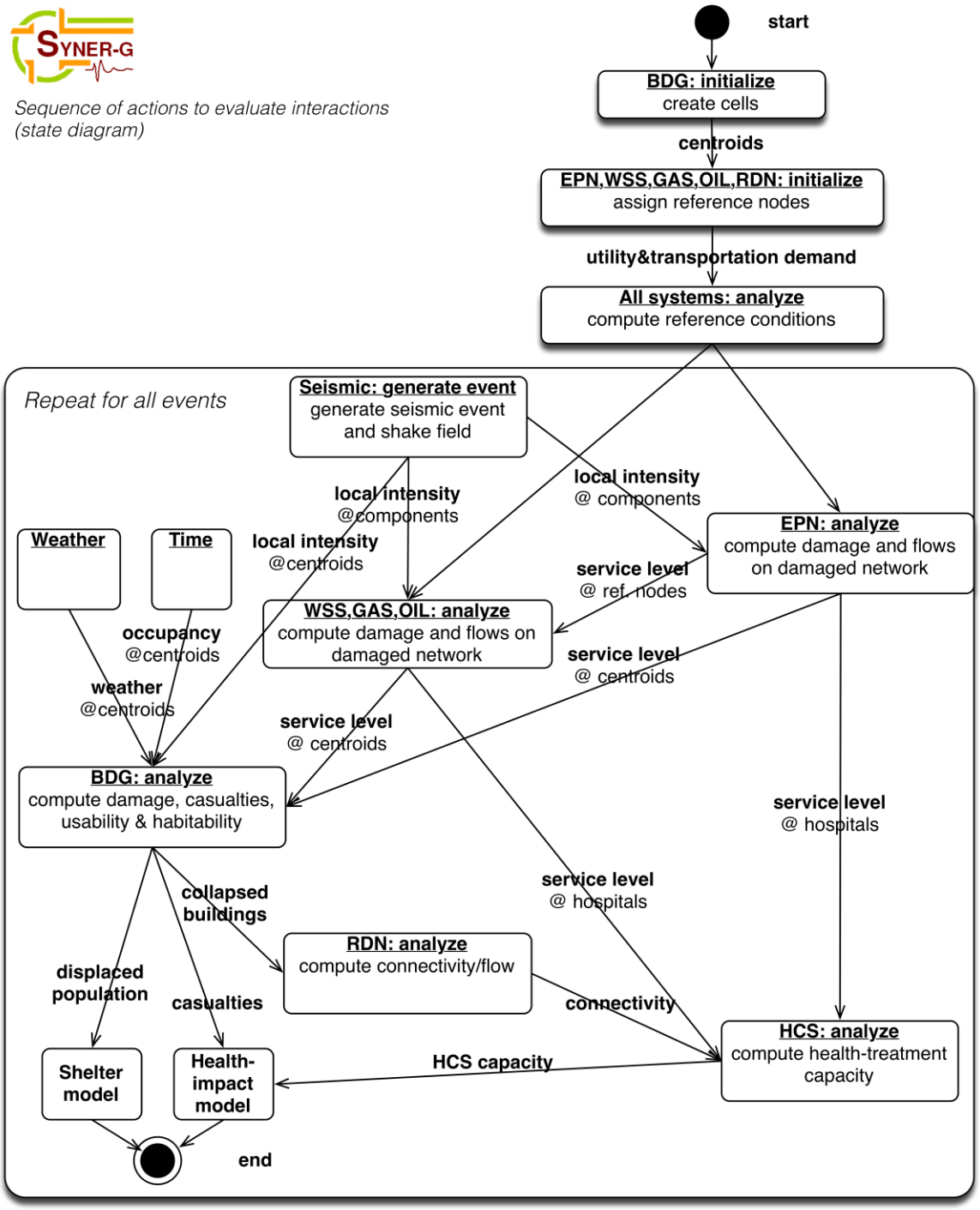

Fig. 2.11 State diagram to model the inter-dependencies: sequence in the evaluation of states of the objects and messages (quantities) transmitted between objects

2.3.3 Deterministic link vs. non-deterministic links

To preserve generality of the developed methodology it is paramount to devise a scheme which can accommodate information from the very detailed to the less accurate. In many practical applications there will not be enough data to adopt a modelling approach whereby all physical components are characterized and their functional links are described deterministically.

A distinction is thus made between:

- **Deterministic (hard) links**: direct physical/functional link between components that allow for deterministic evaluation of a system state from a known components' states vector. This is the case, e.g. when one knows the exact topology of an electric power network with enough details on the lines and loads that the system behaviour can be modelled through the governing power flow equations.
- **Non-deterministic (soft) links**: links of "statistical" nature, which describe the probability of a given system state, given the state of its components, or of another system. This links are an additional source of uncertainty that needs to be accounted for in the vulnerability estimation and one that ideally should be removed by improving on the data gathering phase. A typical example of a situation in which such a link is unavoidable, since the required resolution is not compatible with a realistic study, is that of road blockage due to debris.

2.3.4 Selected systems: Buildings (the Region class)

Functional modelling

Three dimensions have been identified for the regional seismic vulnerability assessment problem: the time, space and stakeholder dimensions (see Fig. 2.1). Each stakeholder is interested in different outcomes from such an analysis. For instance, the insurance industry as well as, in view of reconstruction, government agencies, are interested in an estimate of the economic loss, while in the emergency phase, civil protection and emergency managers are more interested in the number of casualties and displaced people. Evaluation of all these quantities starts from the assessment of damage to buildings, which can be safely said to make up the largest proportion of the built environment.

The very large number of buildings to be considered in a study at the regional or urban scale, prevents in most cases a detailed individual analysis of all buildings. The approach taken within SYNER-G as well as in similar large-scale projects is to model buildings in "statistical terms" as populations where information is given at the level of the **buildings group** (the group size depends on the refinement of the analysis and can vary from a single block to a larger extent of the urban territory), in terms of percentage of each building typologies within the group, with associated physical and socio-economic data such as the fragility models, the population, income, education, etc.

As already mentioned in Section 2.1 and depicted in Fig. 2.1, the above information is usually available in a fragmented form through several data bases. These are e.g. the Building Census data base or the European Urban Audit, maintained by EUROSTAT, or the Land Use Plan.

A first problem to be solved in modelling buildings for the purpose of a regional study is that of “mesh compatibility”. Each of the above sources adopts a different meshing of the urban territory, according to its own criteria. For example, the urban territory is subdivided in the EAU into sub-city districts (SCD) which are areas sufficiently homogeneous in terms of some socio-economic indicators (e.g. income). The Land Use Plan by its very nature, on the other hand, subdivides the territory in areas that are homogenous per use type (green, industrial, commercial, residential).

Two approaches can be adopted to arrive at a set of mutually exclusive and collectively exhaustive cells that cover the study region. One is the so-called *vector* approach. It consists in taking the intersections of all the polygons describing meshing in different data bases to define the cells and their content. The second one, illustrated in Fig. 2.12, is more convenient from a numerical point of view, and is called the *raster* approach. In this approach, adopted within SYNER-G, cells are defined in a regular grid and the intersections between these predefined cells and the polygons from the data bases are used only to project the data to the grid cells using an area ratio. As a result, as shown in Fig. 2.12, in the physical model of the Infrastructure all buildings/structures that are not modelled as Critical facilities, nor belong to one of the Networks, are modelled as a set of Cells on a regular grid that covers the entire study region. The grid has a variable mesh-size, being finer in urban areas, and coarser outside.

By construction, the cells are not internally homogeneous neither in terms of buildings, nor in terms of socio-economic indicators, since in general they receive contributions from different SCD’s, different BC areas, etc. Hence all cells are characterized in terms of physical and socio-economic parameters that describe the total number of buildings, as well as its distribution among different types, together with fragility, the total population, and its distribution in income and education classes, etc.

Further, in order to model inter-dependencies, each cell maintains a link with a number of nodes in the other systems of the Infrastructure. In particular each cell “knows” its reference node in each of the lifelines, i.e. the EPN substation feeding power to it or the WSS node supplying water, the RDN junction where incoming and outgoing traffic transits into the transportation system, etc. Conversely, nodes in the networks maintain a list of links to all tributary cells.

This is an important feature of the adopted modelling strategy, since it makes the meshing refinement of each system within the Infrastructure independent of each other. For example, if a model of the RDN is set up, that is coarse with respect to the building cells, this translates into a larger number of cells per RDN node. The accuracy of the analysis results will of course be affected by large differences in the meshing refinement. The approach, however, has the advantage of allowing for different meshing, which may be the only possibility in some cases, due to the inhomogeneous quality of available data, and it is of course convergent upon mesh refinement.

According to the OOP adopted for the model, the Region class has no sub-classes, and each object istantiated from this class describes a single cell of the grid.

The following section presents a list of the *attributes/properties* of the class, followed by a list of its *methods*, only the more significant of which are described in some detail. This applies also to the classes described in the following for other systems.

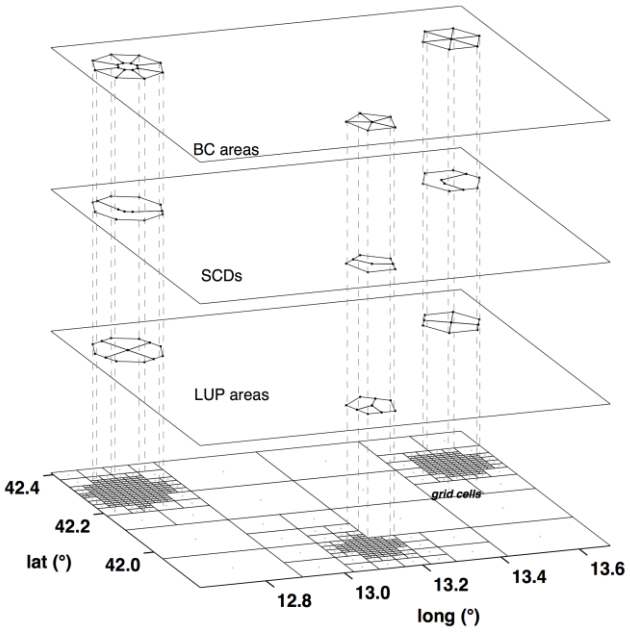

Fig. 2.12 Raster approach to the discretization of the study region (the region is that of the illustrative example presented in Chapter 3)

List of class attributes and methods

The following is the list of attributes of the Region class (multi-word names have no blank spaces in between words; the latter are separated by capitalizing the initial letter of each word). Some properties have sub-properties. The list is split into four parts:

Geometry

- **parentInfrastructure**: this is a pointer to the parent object which is in this case the Infrastructure (the object from the Infrastructure class)
- **vertices**: the coordinates of two vertices on a diagonal of the square cell
- **centroid**: average of the vertices, used to evaluate the IMs from the seismic hazard model to be used for damage evaluation
- **adjacentCells**: pointers to the grid cells that share a border with the current cell

Physical and Socio-economic data (projected from relevant data bases)

- **buildingTypologies**: a n_T×1 vector with the percentages of buildings in each of the n_T typologies (see Deliverable 3.1 and 3.2) (from BC)
- **fragilitySets**: a n_T×n_{DS}×3 matrix with n_T fragility curves for each of the n_{DS} damage states, specified in terms of IM, median and logarithmic standard deviation (from SYNER-G/WP3)
- **demographic**: collection of demographic properties (from EAU):
  - **population**: total population in the cell
  - **households**:
- **economic**: collection of demographic indicators (from EAU):
  - **income**

    - **unemployment**
- **social** (from EAU):
    - **socialHousing**
- **bldgUsage**: a 4×1 vector of percentages of usage of the cell area in the use types Green, Residential, Commercial, Industrial
- **builtUpArea:**

Connection with other systems in the Infrastructure

- **refNodes**: pointers to reference nodes in each of the other systems
    - **WSS**
    - **EPN**
    - **RDN**
    - **GAS**
    - **OIL**

Properties that record the state of the cell for each event

- **states**: n_E×1 collection of properties that describe the current state for each of the n_E events
    - **buildingDamage:**
    - **utilityLoss**
        - **WSS**
        - **EPN**
        - **…**
    - **buildingUsability**
    - **DP**
    - **Casualties**
    - **supplyRequirements**

The following is the list of the methods of the class:

- evaluateBuildingDamage
- readUtilityLoss
- evaluateBuildingUsability
- evaluateBuildingOccupancy
- evaluateCasualties
- evaluateResistanceEvacuation
- evaluateDisplacedPopulation
- evaluateSupplyRequirements

The method evaluateBuildingDamage and the damageability model

The *evaluateBuildingDamage* method is illustrated qualitatively in Fig. 2.13. In a rather standard way, the damage state is determined for all buildings within each typology by sampling a standard uniform variable. The value between 0 and 1 falls within one and only one of the intervals defined, at the intensity value obtained for the cell centroid from the seismic hazard model, by the set of fragility curves for increasing damage states stored for the typology in the property *fragilitySets* of the cell. This is the damage state of the buildings of this type within this cell for the event.

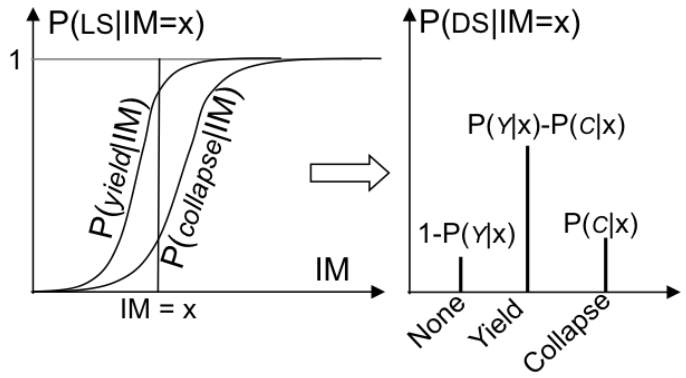

Fig. 2.13 The evaluateBuildingDamage method of the Region class

Assigning the same damage state to all buildings within the same cell is an approximation whose relevance on the accuracy of the results depends on a number of factors. Obviously the first one is the cell-size. In practical application this will be as small as computationally possible given the region size and computational resources available. Other factors, as pointed out in Bal et al (2010), is the type of hazard model considered. Errors in the description of buildings damage state become of secondary importance when the full seismic hazard is considered, rather than a single scenario event. This is exactly what is done within SYNER-G. Of course caution should be used in employing the SYNER-G model for a single scenario earthquake. It is also necessary to point out how the cell size adopted for damage prediction is independent of the spatial resolution o f available data: if data are available at the district of postal code level they can always be projected to smaller cells (see Fig. 2.12) for the only purpose of better damage discretization.

The set of fragility functions for each building typology constitute its *damageability*. The review of the existing fragility functions, the categorization of building typologies into a number of classes, the attribution of each reviewed study into a class and the harmonization of fragilities to the same IM (PGA), has been the object of WP3, Task 3.1. All assumptions and detailed results of this work are reported in reports D3.1 (RC and steel buildings) and D3.2 (Masonry buildings), respectively. One main choice made within this WP is to limit the number of limit states to two: yield and collapse. This results in the three possible damage states already shown in Fig. 2.13. This is motivated on one hand by the fact that several sources of fragility functions have been collected and harmonized and that the number of considered performance levels is the minimum available in all studies, and on the other hand by the fact that casualty and displaced people models that take damage as an input have this level of resolution of damage states.

As expected, fragility functions within each class show a significant amount of dispersion, mainly due to two sources: the differences in buildings lumped into the same class (within-class variability), and the difference in the methods employed to produce the fragilities (consider, for example, the conventional character of the definition of yielding for masonry buildings). Hence, for each class, all curves have been fitted with a lognormal function. The sets of values of log-mean and log-standard deviation have been used to estimate mean and cov of both parameters. This allows for explicit consideration in the probabilistic analysis of the uncertainty in the damageability model (see Section 2.5.1, Fig. 2.22).

For illustration purposes the curves and corresponding parameters for the two typologies considered in the example application (see Section 3.1.2) are reported below.

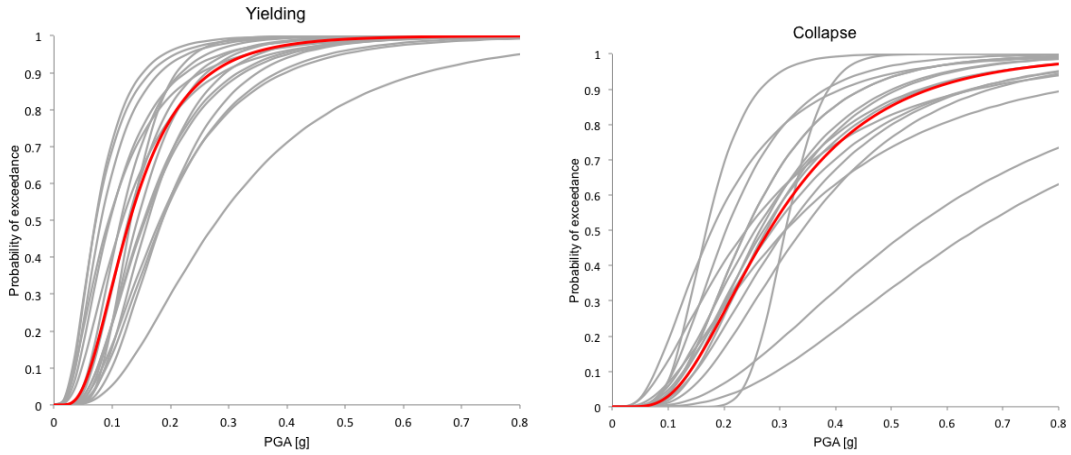

Fig. 2.14 Mean and individual curves for the (a) yielding and (b) collapse limit states, for low rise bearing wall un-reinforced masonry buildings

For *low-rise un-reinforced bearing wall masonry buildings*, 29 sets with two limit states (yielding and collapse) and the same intensity measure type of reference (PGA) have been collected after harmonization. Some sets have then been removed from the comparison for a number of reasons. Thus, 17 sets have finally been used in the comparison. Fig. 2.14 shows the individual and the mean fragility curves, while Table 2.2 reports the mean and coefficient of variation (CoV) of the parameters of the fragility functions (i.e. logarithmic mean and logarithmic standard deviation).

For *RC moment-resisting frame buildings, mid rise, seismically designed, bare, non ductile*, 9 sets with two limit states (yielding and collapse) and the same intensity measure type of reference (PGA) have been collected after harmonization. Fig. 2.14 shows the individual and the mean fragility curves, while Table 2.4 reports the mean and coefficient of variation (CoV) of the parameters of the fragility functions (i.e. logarithmic mean and logarithmic standard deviation).

Table 2.2 Mean and CoV of the lognormal fragility parameters for low rise bearing wall un-reinforced masonry buildings

	Yielding		Collapse	
	Log-Mean	Log-Standard Deviation	Log-Mean	Log-Standard Deviation
Mean	-2.041	0.574	-1.269	0.550
CoV (%)	18	17	27	26

Table 2.3 Correlation coefficient matrix for low rise bearing wall masonry

	λ_{yield}	ζ_{yield}	$\lambda_{collapse}$	$\zeta_{collapse}$
λ_{yield}	1	-0.302	**0.642**	-0.098
ζ_{yield}	-0.302	1	0.053	**0.710**
$\lambda_{collapse}$	**0.642**	0.053	1	0.209
$\zeta_{collapse}$	-0.098	**0.710**	0.209	1

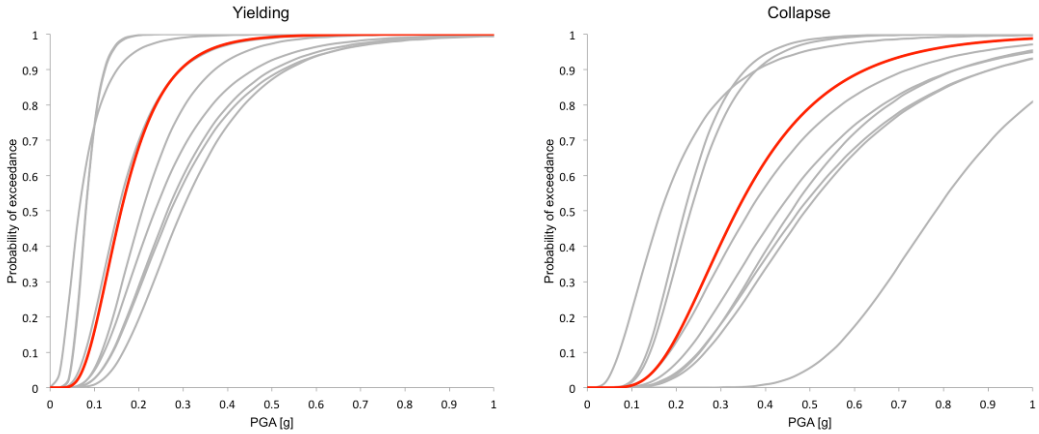

Fig. 2.15 Mean and individual curves for the (a) yielding and (b) collapse limit states, for RC moment-resisting frame, mid rise, seismically designed, bare, non ductile buildings

Table 2.4 Mean and CoV of the lognormal fragility parameters for low rise bearing wall un-reinforced masonry buildings

	Yielding		Collapse	
	Log-Mean	Log-Standard Deviation	Log-Mean	Log-Standard Deviation
Mean	-1.832	0.474	-1.091	0.485
CoV (%)	33	21	48	24

Table 2.5 Correlation coefficient matrix for reinforced concrete with moment resisting frame buildings, mid rise, seismically designed, bare non ductile model building type

	λ_{yield}	ζ_{yield}	$\lambda_{collapse}$	$\zeta_{collapse}$
λ_{yield}	1	0.158	**0.783**	0.033
ζ_{yield}	0.158	1	0.118	**0.614**
$\lambda_{collapse}$	**0.783**	0.118	1	-0.453
$\zeta_{collapse}$	0.033	**0.614**	-0.453	1

The method evaluateBuildingUsability

The *evaluateBuildingUsability* method is based on a simplified semi-empirical approach by which building usability is derived from estimates of building damage rates for three building usability classes. Buildings can be either immediately non usable (NU), partially usable (PU) or fully usable (FU) as a function of the severity of damage and an empirically-derived Usability Ratio (UR).

The method evaluateBuildingHabitability

The *evaluateBuildingHabitability* method is illustrated in Fig. 2.16. Habitability of a building is different from its usability. If a building is fully or partially usable, depending on the level of residual service in the utilities and weather conditions, the buildings can be habitable or inhabitable. Non-usable buildings are assumed to also be uninhabitable. As shown before in Fig. 2.1, building habitability is a function of BuildingUsability, UtilityLoss, and Weather conditions. For each utility, the level of residual service is satisfactory when the utility loss (defined as one minus the ratio of satisfied to required demand) is lower than a threshold value ($UL_i<UL_{Ti}$). The total Utility loss is a weighted average of UL_i/UL_{Ti} on each of the utilities (with weights w_i). The threshold values depend on Weather conditions and BuildingUsability.

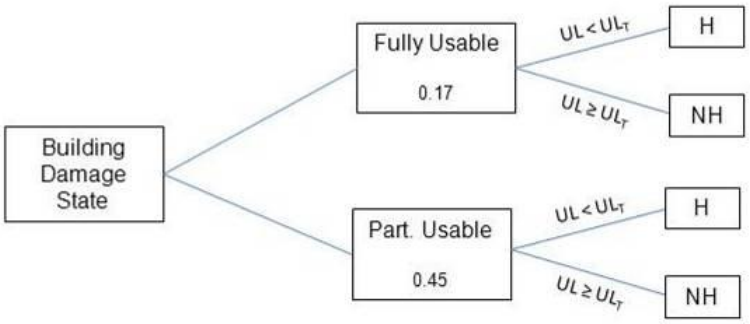

Fig. 2.16 The evaluateBuildingHabitability method of the Region class

The method evaluateCasualties and the Casualty Model

The casualty model is derived from an original idea developed by Coburn and Spence (1992). The model computes casualties directly caused by building damage for each class of buildings using a “Lethality Ratio” (LR). LR is defined as the ratio of the number of people killed to the number of occupants present in collapsed buildings of that class. Multiplying LR

by the number of collapsed buildings of each class, the number of deaths for that building type can be estimated. Lethality Ratios used in Coburn and Spence (2002), Spence and So (2010), ELER (Erdik et al, 2008), and ATC-13 (HAZUS) were evaluated. As Lethality Ratios are very specific to the building typologies and vulnerability classes in each region, a Global or Pan-European casualty model is not feasible. The aim is to produce a semi-empirical approach by which Lethality Ratios would be derived from empirical data on building damage classes and Super classes of building typologies. In the current approach Lethality Ratios for an Italian Model are obtained by optimization with casualty and damage data for 3 Italian earthquakes (1976 Friuli, 1980 Irpinia, 2008 L'Aquila). The approach can be described in terms of three components:

- The building stock of any region is grouped in terms of its distribution in 3 (vulnerability-to-lethality) building classes (Classes A to C).
- Using assumed occupancy rates for each of the building classes, lethality rates are computed by optimizing their values so that a best-fit is achieved between simulated and surveyed casualty numbers. The optimization algorithms used constraints and restrictions derived from common assumptions in Coburn and Spence (2002), Spence and So (2010) and ATC 13.
- Using the optimized Lethality Ratios for the region, the number of deaths are determined for that region, using the mean inhabitants by building type, and occupancy rate by day and night

As the lethality ratio computations have not yet been finalized, the lethality ratios from Zuccaro and Cacace (2011) which are based on an application to the L'Aquila event are used. Accordingly, the number of deaths (N_d) and injured (N_i) are determined using the following expressions:

$$N_d = \sum_{t=1}^{n} \sum_{i=1}^{3} N_{t,i} NO_t QD_{t,i} \tag{2.1}$$

$$N_i = \sum_{t=1}^{n} \sum_{i=1}^{3} N_{t,i} NO_t QI_{t,i} \tag{2.2}$$

where:

- t = building type (t = 1, … n)
- i = damage level (i = 1, … 3), none, yeild and collapse
- $N_{t,i}$= number of buildings of type *t* having damage level *j*
- NO_t = number of occupants (at the time of the event) by building type
- $QD_{t,i}$ = proportion of deaths by building type and damage level
- $QI_{t,i}$ = proportion of injured by building type and damage level

Table 2.6 Lethality Ratios by damage level and building type, adapted from (Zuccaro and Cacace, 2011) where five damage states were used

Lethality Ratios	D1	D2	D3	Vertical Structure	Vulnerability Class
QD	0	0.04	0.15	Masonry	A or B or C
QD	0	0.08	0.3	R.C	C or D
QI	0	0.14	0.7	Masonry	A or B or C
QI	0	0.12	0.5	R.C	C or D

The method evaluateDisplacedPopulation and the Displaced Persons Model

The methodology for the evaluation of the number of homeless persons considers all persons located in buildings that are estimated to be **uninhabitable** at risk of being displaced. The *buildingHabitability* method uses the *buildingUsability*, *UtilityLoss* and *WeatherConditions* attributes to compute the portion of buildings that are uninhabitable.

It has been observed that buildings experiencing the same damage levels can be physically non-usable, partially usable or usable depending on the building typology and building use. To compute buildingUsability, for each building usability class, empirical data from the L'Aquila event was used (preliminary results) to estimate the Usability Ratio (UR) for buildings in each of the three usability classes as a function of damage state in Table 2.7.

Table 2.7 Usability percentages by damage level

Usability Ratio	D1	D2	D3
FU – Fully Usable	0,87	0,22	0,00
PU – Partially Usable	0,13	0,25	0,02
NU – Non Usable	0,00	0,53	0,98

Using the Usability Ratios in Table 2.7, the number of persons in each of the three building usability classes can be obtained using the following expressions:

$$N_{FU} = \sum_{i=1}^{3} N_i NO_i UR_{FU,i} \tag{2.3}$$

$$N_{PU} = \sum_{i=1}^{3} N_i NO_i UR_{PU,i} \tag{2.4}$$

$$N_{NU} = \sum_{i=1}^{3} N_i NO_i UR_{NU,i} \tag{2.5}$$

where:

- i = damage level (i = 1, … 3)
- N_i = number of buildings having damage level *i*

- NO_i = number of occupants (at the time of the event) in each building for damage level i
- $UR_{j,i}$ = usability ratio for damage level *i* for the j-th usability class

The number of uninhabitable buildings is derived as a proportion of partially usable and usable buildings where the total Utility loss is greater or equal to the threshold level of the tolerated utility levels (Figure 2.16). The threshold utility loss values depend on Weather conditions and BuildingUsability for which default values are proposed in Table 2.8. The total Utility loss for each building (UL) is a weighted average utility loss for each of the three utility systems (EPN, GAS and WSS), with proposed default weights w_i provided in Table 2.9. Due to the subjective nature of perceptions, users may want to change proposed values provided in Table 4-8 and Table 4-9. Thus, the total Utility loss for each building (UL) is computed according to the following expression:

$$UL = \sum_{j=1}^{3} UL_j w_j \tag{2.6}$$

where:

- j = utility system (j = 1, …3)
- UL_j = Utility Loss in system *j* defined as one minus the ratio of satisfied to required demand
- w_j = weight associated with the importance of loss of utility system *j* in making the building uninhabitable

Table 2.8 Default values proposed for Utility Loss Tolerance Thresholds

Utility Loss Tolerance Thresholds UL_T	Weather Conditions	
	Good	Bad
FU – Fully Usable	1.0	0.0
PU – Partially Usable	0.9	0.0

Table 2.9 Defaults weights proposed for each utility system

Weight Factor	Default Value
W_{EPN}	0.5
W_{GAS}	0.3
W_{WSS}	0.2

The total number of displaced persons (DP) is thus calculated as the portion of occupants of buildings that are uninhabitable according to the following relationship:

$$DP = N_{FU} NH_{FU} + N_{PU} NH_{PU} + N_{NU} - N_d \tag{2.7}$$

where:

- N_{FU} = number of occupants in buildings that are fully usable
- N_{PU} = number of occupants in buildings that are partially usable
- N_{NU} = number of occupants in buildings that are non-usable
- N_{FU} = number of occupants in buildings that are fully usable
- NH_{FU} = percent fully usable buildings that are non-habitable, where $UL \geq UL_T$
- NH_{PU} = percent partially usable buildings that are non-habitable, where $UL \geq UL_T$
- N_d = number of dead persons estimated in casualty model

2.3.5 Selected systems: The Network, Node and Edge abstract classes

The two systems illustrated in the following are both utility networks. As such, these are described within the OO model as subclasses of the *Network* abstract class (actually, of its *Undirected* subclass). Through the inheritance mechanism of the OOP, the WSS and EPN classes share a number of properties and methods that are defined only once at the highest network level. These properties and methods common to all network-type systems are listed and briefly described below.

The *Network* class

Network pointers

- **parent:** this is a pointer to the parent object which, in this case, is the Infrastructure (the object from the Infrastructure class)
- **nodesPointers:** list of pointers to all network nodes
- **edgesPointers:** list of pointers to all network edges

Network global properties

- **nEdges**: number of edges in the network
- **nNodes**: number of nodes in the network
- **edges**: connectivity matrix listing the start and end nodes of each edge
- **adjacencyMatrix**
- **incidenceMatrix**
- **incidenceList**
- **deadEnds**: list of network dead ends
- **articPTS**: list of network articulation points (a graph-theoretic notion: nodes whose removal increases the number of connected sub-networks)
- **bridges**: list of network bridges (a graph-theoretic notion: edges whose removal increases the number of connected sub-networks)
- **vulnSites**: list of vulnerable sites of the network, containing their location and IM type(s)
- **ULweight**: influence of the considered network (only for utilities) in the computation of utility loss (UL) in buildings (if present); the sum of ULweight values of the utility

networks present in the Infrastructure must be 1. This is an important parameter in the model for the evaluation of the buildings habitability and hence the demand on the shelter model

- **states**
- **MAF**

Edge properties stored at network level. Many of the following properties have counterparts in the Edge class: in this class the properties are vectors collecting values that are also stored individually within each edge object

- **edgeVs30**: Vs30 value at the edges' centroid
- **edgeType**: typology (e.g. pipe or tunnel for WSS, overhead or buried for EPN) of edges
- **edgeLength**
- **edgeIsVulnerable**: flag indicating if the generic edge is considered vulnerable or not
- **edgeIMType**: intensity measure used in the fragility of the edge
- **edgeCentroidPosition**
- **edgeSiteClass**: site class at the edge centroid according to the amplification method to be used (valid for all *a posteriori* amplification methods, see Section 2.4.4)
- **edgeDepth2GW**: depth of the groundwater at the edge centroid site
- **edgeLiqSusClass**: liquefaction susceptibility of the edge centroid site
- **edgeLandSusClass**: landsliding susceptibility of the edge centroid site
- **edgeYieldAcc**: yielding or critical acceleration for landsliding at the edge centroid site

Node properties stored at network level. Many of the following properties have counterparts in the Node class: in this class the properties are vectors collecting values that are also stored individually within each node object

- **nodePosition**
- **nodeAltitude**
- **nodeType**: typology (e.g. sink, source or junction, etc) of nodes
- **nodeVs30**
- **nodeIsVulnerable**: flag indicating if the generic node is considered vulnerable or not
- **nodeIMType**
- **nodeSiteClass**: site class at the node sites according to the site amplification method to be used (valid for all *a posteriori* amplification methods, see Section 2.4.4)

Methods (names of abstract methods, whose implementation is different in each network class, are italicized); some of them are specific for undirected networks and thus are included in the Undirected subclass)

- **anySDFS**: performs the Depth First Search algorithm, to know which vertices can be reached by a path starting from any source

- **connectedNodes**: lists of nodes belonging to the different (eventually present) connected components in the network; a connected component of an undirected graph is a subgraph in which any two vertices are connected to each other by paths, and which is connected to no additional vertices in the supergraph
- detectArticulationPoints
- **detectBridges**
- **edges2Adjacency**: perform corresponding transformation
- **edges2IncidenceList**: perform corresponding transformation
- **edges2IncidenceMatrix**: perform corresponding transformation
- **findDeadEnds**
- **isConnected**: determines whether a path exists between any two nodes in an undirected graph
- **minPath**: finds the minimum path between a pair of nodes
- **subnetwork**: returns the list of edges connecting a subset of network nodes
- **retrieveLandSusEdges**: assigns the landsliding susceptibility class to edges, in case it is not assigned in the input file and a landsliding susceptibility map (in the form of a shape file) is available
- **retrieveLiqSusEdges**: assigns the liquefaction susceptibility class to edges, in case it is not assigned in the input file and a liquefaction susceptibility map (in the form of a shape file) is available
- **retrieveSiteClassEdges**: assigns the site class to edges (if an *a posteriori* amplification method is to be used), in case it is not assigned in the input file and a geological map (in the form of a shape file) is available
- **retrieveSiteClassNodes**: assigns the site class to nodes (if an *a posteriori* amplification method is to be used), in case it is not assigned in the input file and a geological map (in the form of a shape file) is available
- **retrieveVs30edges**
- **retrieveVs30nodes**
- **retrieveYieldAccEdges**
- **discretizeEdges**: all the edges with a length larger than a specified threshold are subdivided into smaller segments, so as to allow a higher spatial resolution in the evaluation of damage
- ***updateConnectivity***: updates the connectivity matrix for the damaged network
- ***computeDemand***
- ***computeFlow***: performs the computation of flows
- ***computePerformanceIndicator***
- ***computeCovMean***
- ***saveResults***

The *Node* class

Similarly, nodes and edges in the WSS and EPN systems are concrete counterparts of the *Node* and *Edge* abstract classes from which they inherit a number of properties and methods.

Properties:

- **parent:** this is a pointer to the parent object, which is a Network type object from a concrete class (WSS, EPN, etc)
- **position**
- **altitude**
- **Vs30:** Vs30 at edge centroid
- **type**
- **isVulnerable**
- **IMType**
- **siteClass**
- **depth2GW**
- **liqSusClass**
- **landSusClass**
- **yieldAcc**
- **states**

The *Edge* class

Properties:

- **parent:** this is a pointer to the parent object, which is a Network type object from a concrete class (WSS, EPN, etc)
- **connectivity:** start and end node of the edge
- **centroid:** edge centroid location
- **L:** edge length
- **Vs30:** Vs30 at edge centroid
- **isVulnerable**
- **IMType**
- **siteClass**
- **depth2GW**
- **liqSusClass**
- **landSusClass**
- **yieldAcc**
- **states**

2.3.6 Selected systems: Water supply system (the WSS class)

The next sections describe briefly water supply systems, their function and analytical modelling, their representation within the presented object-oriented framework, the fragility models for representative components and the demand models under both reference non-seismic and seismic conditions. The illustration does not cover all details which can be found in the specific deliverable from WP5, report D5.4.

Description of the system

Water supply systems are networks whose links and nodes are pressure pipes and either pipe junctions, water sources or end-users, respectively. The function of a WSS is to provide end-users with water with a sufficient pressure level.

For obvious reasons pipes usually follow the plan layout of the road network. From a topological point of view, WSS can be either *tree-like* networks or *grid-like* networks, as shown in Fig. 2.17. In tree-like networks whenever an interruption (due to failure or maintenance) occurs in a point of the network, the whole downward portion of the network is out-of-service. This undesirable behaviour is avoided with grid-like networks, which are more reliable since water can flow through pipes in different directions upon changed boundary conditions reaching otherwise unserviced end-users.

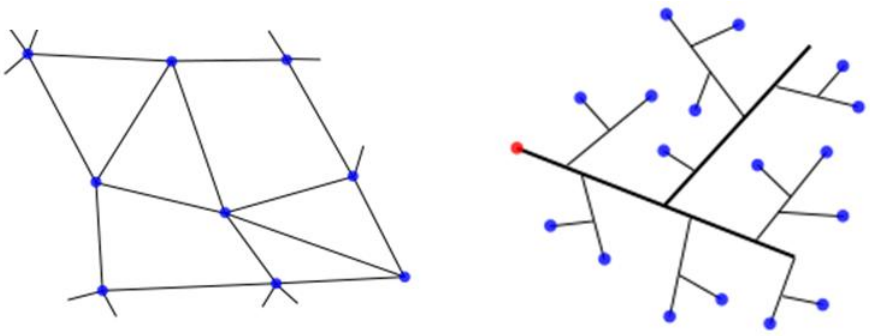

Fig. 2.17 Typical topological structures, grid-like (on the left) and tree-like (on the right)

The network can be decomposed into hierarchically arranged levels or *orders*. The *first order* collects all pipes in the main distribution, which follows the main roads in the area and through which the largest water volumes flow. This is usually designed as a grid-like network in order to reliably reach the *second* and *third order networks*. The latter follow the lower-order roads and have the task of reaching as close as possible to the end-users. Mainly for economic reasons these portions of the networks are most often of the tree-type. This represents only a limited inconvenience since, on one hand, each of these sub-networks serves a smaller demand, thus limiting the impact of service interruption, and on the other is made up of smaller diameter pipes which can be repaired with ease.

In terms of components the WSS is comprised mainly of pipes and junctions, which depend on the pipes' typology. Then there are tanks, pumps, water meters and other pieces of equipment.

Pipes currently in use are of three types:

- Metallic pipes
  - Cast iron pipes: diameter usually in the 60mm to 700mm range, with custom diameters easily arranged by producers; junctions are commonly of the spigot-and-socket joint, which is realized by means of compression of an O-ring positioned on the pipe entering the junction (this junction has the advantages of having some flexibility to accommodate relative movements of the pipes thus reducing seismic vulnerability and being pressure-tight in both directions).
  - Steel pipes: diameters as above; junctions usually welded, with the conic type allowing some flexibility and being used mostly for larger diameters; they usually have lower thickness for the same diameter with respect to cast-iron pipes; they are more flexible and resistant to seismically induced ground deformations.
- Concrete pipes
  - Reinforced (possibly prestressed) concrete pipes: diameters in the range 400mm to 1000mm;
  - Asbestos cement pipes: older pipes, not produced for health reasons since the early '90s and in the process of being replaced, they are still in use, however, and may be part of older portions of the WSS; the asbestos fibers are used to provide tensile strength to the concrete matrix. Junctions of the Simplex and Gibault types. Main advantage was the reduced cost.
- Plastic pipes (*PVC*, *PEad, PRFV*): these pipes have reduced roughness which is convenient from a hydraulic point of view; they are highly resistant to corrosion and are light and flexible, thus being easily installed and able to accommodate ground displacements; they have, however, reduced mechanical properties with respect to metallic pipes; PVC pipes have diameters up to 630mm and can be jointed mechanically or by chemical welding; PEad pipes up to 1200mm, and can be jointed either mechanically or by welding (polifusion or electrofusion); PRFV pipes have high strength due to the glass fibers and can be produced in diameters up to 2000mm.

Finally, pipe-work requires a number of *special pieces* and pieces of *equipment* beyond pipes. The most common special pieces are curves (denominated 1/4, 1/8, 1/16, 1/32, 1/64), T-junctions and H-junctions, connections, sleeve joints, filters. The main equipment typologies are gate valves, air valves, pressure valves, devices for water delivery (public drinking fountains and hydrants); water meters and all domestic distribution equipment.

Functional modelling

The functioning of a WSS is described analytically by a set of *N+L* nonlinear equations in *N+L* unknowns, written in matrix form as:

$$\begin{cases} \mathbf{A}_N^T \mathbf{q} - \mathbf{Q}\left(\mathbf{h}_N\right) = \mathbf{0} \\ \mathbf{R}\left|\mathbf{q}\right|\mathbf{q} + \left(\mathbf{A}_N \mathbf{h}_N + \mathbf{A}_S \mathbf{h}_S\right) = \mathbf{0} \end{cases} \tag{2.8}$$

where *N, L* and *S* are the number of internal (non-source) nodes, the number of links and the number of water sources, respectively. The first *N* equations are balance equations and express flow balance at the internal nodes (sum of incoming and outgoing flows equal to zero or the end-user demands $\mathbf{Q}\left(\mathbf{h}_N\right)$ in end-user nodes), while the second *L* equations

express resistance in the links. The $L \times N$ and $L \times S$ matrices $\mathbf{A}_N$ and $\mathbf{A}_S$ are sub-matrices of the $L \times (N+S)$ matrix $\mathbf{A}$ which contains 0, 1 and -1 terms as a function of the network connectivity. The Nx1 and Sx1 vectors $\mathbf{h}_N$ and $\mathbf{h}_S$ are the corresponding partition of the $(N+S)$x1 vector $\mathbf{h}$ collecting the N unknown heads in the internal nodes and the S known heads in the water-source nodes. The $L \times 1$ vector $\mathbf{q}$ collects the unknown flows in the L links and $\mathbf{R}$ is the LxL diagonal matrix of resistances, with terms $r_i = u_i L_i$, where $u_i = \beta D^{-5}$ (according to Darcy's law) and L_i the i-th link length.

It is customary in the analysis of WSS for the purpose of design to treat the end-user demands $\mathbf{Q}$ as fixed boundary conditions (the system must be proportioned in order to satisfy them). The solution of the system with $\mathbf{Q}$ independent of $\mathbf{h}_N$ is called "demand-driven". In the above set of equations, on the contrary, the end-user demands are written as $\mathbf{Q}(\mathbf{h}_N)$, i.e. as functions of the unknown heads in the internal nodes. The solution of the system in this form is called "head-driven", and is employed here since in the perturbed seismic conditions satisfaction of prescribed demands is not guaranteed.

The set of nonlinear equations holds in so-called stationary conditions, i.e. it assumes constant end-user demands. This is a simplification, which is valid as long as the boundary conditions vary smoothly with time, in which case one speaks of quasi-stationary conditions. In seismic conditions this is not the case but the abrupt variation due to ruptures and leakages is soon replaced by a new stationary state.

Solution of the above set of equations by a numerical algorithm allows verification of the serviceability level in each end-user node. The performance indicators to express satisfaction of performance requirements are reported later in Section2.3.8. In general, however, what is required is that heads are always positive and larger than minima within accepted ranges depending on the typology of the end-users. Heads should never fall below 5m above the highest tap in the building which is "hydraulically" farthest away from the water sources, nor they should be more than 70m above the lowest floors taps in order to avoid excessive pressure and damage to equipment. Further requirements and range modifications can follow from Fire-fighting needs when the systems are not separated.

Description of the classes

As shown in the left part of Fig. 2.8, the water supply system is made up of nodes and links connecting them. As a consequence, the WSS class is the composition of *WSSlink* and *WSSnode* abstract classes, of which the first is the generalization of the Pipe and Tunnel classes, while the second is the generalization of the DemandNode, *WaterSource* and PumpingStation classes. In particular, the *WaterSource* abstract class is the generalization of the VariableHead and ConstantHead water source classes.

The following is the list of properties of the WSS class, with the names following the usual naming convention. The list is split into four parts:

List of pointers

- **pipe:** pointers to all the pipes in the system, objects from the Pipe class
- **demand:** pointers to all end-user nodes, objects from the DemandNode class

- **source:** pointers to all sources in the system, in general objects from the ConstantHeadWaterSource and VariableHeadWaterSource classes (at present, though, the prototype software includes only the ConstantHeadWaterSource class)
- **pump:** pointers to objects from the PumpingStation class

Water supply system global properties

- **edgeDiameterNumber:** number of diameter sizes present in the WSS
- **refEPNnode:** node(s) of the EPN which feeds power to the pumping station(s)
- **sourceHead:** water head at the source nodes
- **endUserDemand:** water flows at demand nodes
- **hydricEquipment:** water daily equipment of the region of interest
- **interdependentEPN:** flag indicating if the WSS and the eventually present EPN are to be considered interdependent or not

Edge and node properties (many of these properties have counterparts in the WSSedge and WSSnode classes. Those in this class are vectors collecting values that are also stored individually within each node and edge object)

- **edgeMaterial**
- **edgeDiameter**
- **edgeRoughness**
- **edgeDepth:** laying depth of edges
- **nodeDepth**: laying depth of nodes
- **nodeMinimalHead**: minimal head required at nodes for delivery of the assigned demand water flow; this property is a function of the average building elevation in the region of interest

Properties that record the state of the WSS for each event

- **states:** n_E×1 collection of properties that describe the current state for each of the n_E events
  - **AHR:** Average Head Ratio, system-level performance indicator (see Section 2.3.8)
  - **SSI:** System Serviceability Index, system-level performance indicator (see Section 2.3.8)
  - **covAHR:** coefficient of variation of AHR
  - **covSSI:** coefficient of variation of SSI
  - **covTot:** maximum value among covAHR and covSSI; this value is monitored during simulation, so to stop the simulation itself in case its threshold is reached
  - **mean_AHR:** moving average of AHR (until the current event)
  - **mean_SSI:** moving average of SSI (until the current event)
  - **mean_HR:** moving average (until the current event) of HR (component-level performance indicator, see Section 2.3.8) for all nodes

- **mean_DCI:** moving average (until the current event) of DCI (component-level performance indicator, see Section 2.3.8) for all nodes
- **mean_UBI:** moving average (until the current event) of UBI (component-level performance indicator, see Section 2.3.8) for all nodes
- **std_AHR:** moving std of AHR (until the current event)
- **std_SSI:** moving std of SSI (until the current event)

The following is the list of the methods of the WSS class (some of these are briefly explained):

- **computeDemand:** determines the water demand for all demand nodes in which the flow is set to 0 in the textual input. The computation for the generic demand node is based on the user-specified water daily equipment and the population of its reference cells, if any, i.e. the cells fed by the node itself. In both reference, non-seismic conditions and in damaged seismic conditions the water demand is assigned to each demand node based on the reference cells population and a value of water daily equipment, 250 l/(inhab.*day), which is common for Italian cities
- **computeFlow:** performs the computation of flows in all pipes and heads in all demand nodes, in both seismic and non-seismic conditions

The *WSSedge* class and sub-classes

The following is the list of properties of the *WSSedge* abstract class. These properties are inherited by all subclasses (Pipe and Tunnel):

- **D:** edge diameter
- **Roughness:** edge roughness
- **material:** edge material; it can be set to one of the following: 'castIron', 'weldedSteel', 'asbestosCement', 'concreteW/StlCyl', 'pvc', 'ductileIron'
- **states:** n_E×1 collection of properties that describe the current state for each of the n_E events
  - **flow:** edge flow
  - **distance:** distance of edge centroid to epicenter
  - **primaryIM:** primary intensity measure at edge centroid, as interpolated from the regular grid points
  - **localIMs:** secondary or local intensity measures, correlated to the primary IM
  - **leaksNumber:** number of edge leaks, caused by earthquake shaking
  - **leakageArea:** edge leakage area, sum over all leaks in the edge
  - **DCI:** Damage Consequence Index, component-level performance indicator (see Section 2.3.8)
  - **UBI:** Upgrade Benefit Index, component-level performance indicator (see Section 2.3.8)
  - **broken:** flag indicating if the edge is broken or not

The subclass Pipe has one further property, i.e. **Depth**, that objects of this class do not share with those of class Tunnel.

The *WSSedge a*bstract class has no methods. The subclass Pipe has the following methods:

- **isBreakAndLeaksNumber**
- **computeLeakageArea**

Damageability model and the isBreakAndLeaksNumber and computeLeakageArea methods

Within a seismic reliability analysis of water supply systems, buried pipelines are usually considered the only vulnerable components. Separate pipeline fragility relations exist for permanent ground deformation and ground shaking effects. Referring the reader interested in fragility models for permanent ground deformation to the relevant reports from WP5 on the WSS, herein only damage induced by ground shaking is discussed. Typical pipeline fragility functions for ground shaking damage, are formulated in terms of PGV and PGA. The number of pipe breaks or leaks per unit length is denominated interchangeably as *repair rate (RR)*, *damage rate*, *damage ratio* or *failure rate*.

Some of the available fragility models employ a linear model of the type $RR = a \cdot IM$, whereas others employ a power model of type $RR = b \cdot IM^c$. Parameter *a*, for instance, is the median slope of the data set, while parameters *b* and *c* are retrieved by applying the least squares method. As an example reference, two pipeline fragility relations that have been included within the SYNER-G toolbox are given here.

The first is proposed in HAZUS (FEMA 1999) to estimate the regional damage induced by an earthquake over the US water pipelines. The relation is derived from those of O'Rourke & Ayala (1993) and Barenberg (1988), who took into account mostly US earthquakes. Its expression is:

$$RR = 0.0001 \cdot PGV^{2.25} \tag{2.9}$$

where PGV is input in cm/s and the repair rate *RR* is returned in km^{-1}.

The second relation was proposed by the American Lifelines Alliance (ALA, 2001), based on a data set of pipeline damage rates induced by 18 earthquakes from 1923 to 1995 and provided by different authors, such as Katayama *et al.* (1975), O'Rourke & Ayala (1993), Eidinger *et al.* (1995), Shirozu *et al.* (1996) and Toprak (1998). The linear relation is:

$$RR = K_{1ALA} \cdot 0.002416 \cdot PGV \tag{2.10}$$

where again PGV is input in cm/s and repair rate *RR* is returned in km^{-1}. K_{1ALA} is a tabulated corrective factor, accounting for material, joint type, soil type and pipe diameter.

The **isBreakAndLeaksNumber** method, in case the pipe is not broken, estimates the number of leaks, based on the selected damageability model and the assumption that the leaks number along a water edge is Poisson distributed. The **computeLeakageArea** method computes the total outflow area, e.g. assuming an area for each leak along the pipe equal to 3% of the whole pipe section.

The WSSnode class and sub-classes

The following is the list of properties of the *WSSNode* abstract class. These properties are common to all subclasses (DemandNode, *WaterSource* and PumpingStation) of this class.

- **states:** n_E×1 collection of properties that describe the current state for each of the n_E events
  - **demandFlow:** demand water flow at the node
  - **head:** water head at the node
  - **outFlow:** water flow outgoing from the node, simulating half the flows outgoing from all links converging in the node
  - **HR:** Head Ratio, component-level performance indicator

The subclass DemandNode has two further properties, i.e. **minimalHead** and **refCells** (cells fed by the demand node), that objects of this subclass do not share with those of the other subclasses. Only the subclass *WaterSource* has one further property, i.e. **head**. Only the subclass PumpingStation has two further properties, i.e. **refSource** and **refEPNStation**, indicating respectively the source node served by the pumping station and the EPN node which feeds power to the pumping station.

The *WSSNode a*bstract class and its subclasses do not have any methods (only the object constructor for the concrete subclasses).

2.3.7 Selected systems: Electric power network (the EPN class)

Description of an EPN

A modern Electric Power Network (EPN) is a complex interconnected system that can be subdivided into four major parts:

- Generation
- Transformation
- Transmission and Distribution
- Loads

These are described in some detail in reference report 2, and the interested reader can also see Saadat (2002).

A major components of a power network is the transformer (Fig. 2.18), which transfers power with very high efficiency from one level of voltage to another level. The power transferred to the secondary winding is almost the same as the primary, except for losses in the transformer. Therefore, using a *step-up* transformer of voltage ratio *a* will reduce the secondary current of a ratio 1/*a*, reducing losses in the line, which are inversely proportional to voltage and directly proportional to distance. This makes the transmission of power over long distances possible. At the receiving end of the transmission lines *step-down* transformers are used to reduce the voltage to suitable values for distribution or utilization.

The purpose of a *power delivery system* (simple sketch in Fig. 2.19), also known as *transmission and distribution (T&D) system*, is to transfer electric energy from generating units at various locations to the customers demanding the loads.

Fig. 2.18 High voltage transformer

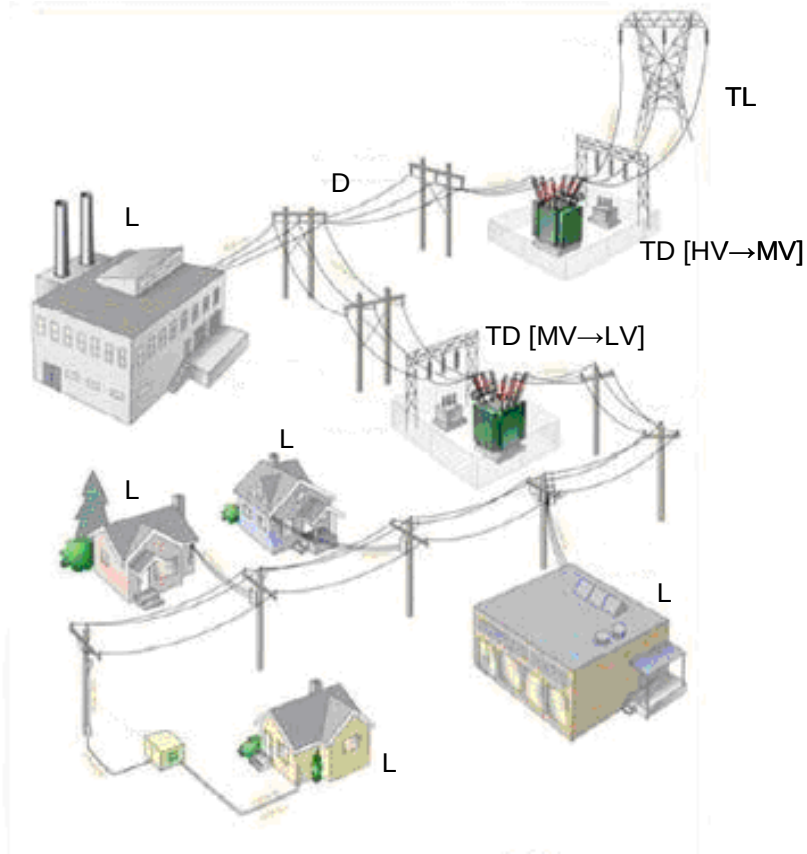

Fig. 2.19 Sketch of a T&D system for an EPN (TL = Transmission Lines, D = Distribution lines, TD [HV→MV] = Transformation (from high to medium voltage) and Distribution station, TD [MV→LV] = Transformation (from medium to low voltage) and Distribution station, L = Load)

A T&D system is divided into two general tiers: a *transmission system* that spans long distances at high voltages on the order of hundred of kilovolts (kV), usually between 60 and 750 kV, and a more local *distribution system* at intermediate voltages. The latter is further divided into a medium voltage distribution system, at voltages in the low tens of kV, and a low voltage distribution system, which consists of the wires that directly connect most domestic and small commercial customers, at voltages in the 220-240 V range for Europe. The distribution system can be both overhead and underground.

The transmission and distribution systems are generally characterized by two different topological structures (Fig. 2.17): the transmission system is an interconnected redundant grid, composed of stations as nodes and transmission lines as edges, while the distribution system is a tree-like network, following the main streets in a city and reaching the end users.

The lines at different voltages are terminated in *substations*. Depending on their functions, substations can be grouped into three typologies, in particular:

1. Transformation substations.
2. Distribution substations.
3. Transformation/distribution substations.

An important component inside a substation is the bus, a *redundant system of bars* (generally two bar systems form a bus, with the second one being provided for the purpose of maintenance operations) transferring energy between lines entering or exiting from the station. When the transformation function is required (type 1 and 3 above), two buses at two different voltages are present. For type 3 only, where also power delivery is required, one or both buses are load buses. For distribution substations, the only bus present is a load bus. Buses are the network nodes.

Substations layouts are extremely variable. They can be entirely enclosed in buildings where all the equipment is assembled into one metal clad unit. Other substations have step-down transformers, high voltage switches, oil circuit breakers, and lightning arresters located outside the substation building.

The electric power is delivered to the single customers through distribution circuits, which include poles, wires, in-line equipment, utility-owned equipment at customer sites, above ground and underground conductors. Distribution circuits either consist of anchored or unanchored components.

Finally, loads of power systems are divided into *industrial*, *commercial* and *residential*. Loads are independent of frequency and consume negligibly small reactive power. The real power of loads is expressed in terms of kilowatts (kW) or megawatts (MW).

Functional modelling

The analysis of an EPN in a seismically active environment can be carried out, as for other lifeline systems, at two different levels. The first basic one focuses on connectivity only and can only lead to a binary statement on whether any given node is connected with another node, specifically a source node, through the network. This level of analysis is particularly inadequate for a system such as the EPN since the tolerance on the amount and quality, in terms of voltage and frequency, of the power fed to any demand node for maintaining serviceability is very low. The actual power flow in the node must be determined to make any meaningful statement on the satisfaction of the power demand at the node, not just its state

of continued connectivity. The latter is an intrinsically systemic problem since it depends on the determination of the flows on the entire (damaged) network. Further, before being able to evaluate flows it is necessary to determine what is the EPN portion still up and running after an event. This does not simply mean what components are damaged since damage to components has non-local consequences. Indeed, damage to the components of a substation can lead to a short-circuit that may or may not propagate further away from that substation to adjacent others, generating in extreme cases very large black-outs. Hence, power flow analysis follows the analysis of short-circuit propagation, in which circuit breakers are active components playing a key role in arresting the short-circuit spreading. This is the modelling approach adopted within the SYNER-G general methodology. Moreover, the substations are not modelled as vulnerable points, characterised by an assigned fragility function: their full internal logic is modelled, to account for partial functioning (continued service with reduced power flow) (see report D5.2). The eleven typologies of micro-components composing the load substations are the only elements in the network that are considered vulnerable. For such elements, fragility curves function of peak ground acceleration (PGA) are available and reported in deliverable D3.3.

Within a power-flow analysis the target is to determine the voltage and power in all stations, as well as the current, power and power loss in all transmission lines. Voltage, power and current are phasorial quantities, thus they are complex numbers. The first step is to retrieve the two voltage parts (magnitude and phase) in all stations where they are unknown. To this aim, a set of algebraic non-linear equations are available, representing the active (or real) and reactive power balance in the nodes. The system is written as

$$\begin{aligned} 0 &= -P_i + \sum_{k=1}^{N} |V_i||V_k|\left(G_{ik}\cos\theta_{ik} + B_{ik}\sin\theta_{ik}\right) \\ 0 &= -Q_i + \sum_{k=1}^{N} |V_i||V_k|\left(G_{ik}\sin\theta_{ik} - B_{ik}\cos\theta_{ik}\right) \end{aligned} \tag{2.11}$$

where P_i and Q_i are the real and reactive powers at node i, $|V_k|$ and $|V_i|$ are the voltage magnitude at nodes k and i, G_{ik} and B_{ik} are the real and imaginary parts of the ik term in the bus admittance matrix Y, θ_{ik} is the difference of voltage phases between nodes i and k. The solution is found by using one the classical derivative algorithms, for instance Newton-Raphson. Once known the stations voltages, it is straightforward the computation of the lines currents and powers in both directions, the lines power loss and the powers (real and reactive) in all generation stations. These issues are explained in detail in report D5.2.

Description of the classes

The right part of Fig. 2.8 illustrates the EPN class diagram. In the prototype software, the EPN is modelled as an undirected graph, i.e. a graph in which flow can occur in both directions on all. For this reason, the EPN class is considered as a subclass of the *Undirected* abstract class, that in its turn is a subclass of the *Network* abstract class.

The electric power network is made up of nodes and edges/lines connecting them. As a consequence, the EPN class is the composition of *EPNedge* and *EPNnode* classes, that are both abstract. The first one is the generalization of the OverheadLine and UndergroundLine classes, while the second one is the generalization of the SlackBus, PVGenerator and *LoadBus* classes. The latter is the generalization of the TransformationDistribution and Distribution classes, both of which are composed of the *Component* abstract class. This

latter class is the generalization of eleven classes, one for each micro-component composing the substations.

The following is the list of properties of the EPN class, with the names following the naming convention adopted for variables in developing the prototype software, whereby multi-word names have no blank spaces in between words and the latter are separated by capitalizing the initial letter of each word. The list is split into four parts:

List of pointers

- **overheadLine:** pointers to the overhead transmission lines in the system, objects from the OverheadLine class (underground lines are not yet included in the model)
- **slack:** pointer to the slack bus, one object from the SlackBus class
- **generator:** pointers to all power generators (excluding the slack bus) in the system, objects from the PVGenerator class
- **transfdistr:** pointers to all transformation/distribution substations in the system, objects from the TransformationDistribution class
- **distribution:** pointers to all distribution substations in the system, objects from the Distribution class

Electric Power Network global properties

- **admittanceMatrix:** admittance matrix of the EPN, containing the self and mutual bus admittances, used in power flow evaluation
- **capacityPerCapita:** required average power per inhabitant, for the region of interest
- **baseV:** reference voltage to switch to per-unit system (a way of normalizing quantities appearing in the power flow equations in order to obtain comparable values and improve convergence of the Newton solution strategy, see report D5.2)
- **baseP:** reference power to switch to per-unit system
- **baseY:** reference admittance to switch to per-unit system

Line and bus (node) properties (many of these properties have counterparts in the EPNedge and EPNnode classes. Those in this class are vectors collecting values that are also stored individually within each node and edge object)

- **edgeVoltage:** nominal voltage of lines
- **edgeElectricProp:** electric properties of lines, i.e. resistance, reactance and susceptance, in units consistent with voltage and power units
- **edgeVoltageRatio:** ratio of voltages at the two ends of lines (different from 1 for lines with transformer)
- **busBC:** buses boundary conditions (voltage magnitude and phase for the slack bus, voltage magnitude and real power for generators, real and reactive power for load buses)

Properties that record the state of the EPN for each event

- **states:** n_E×1 collection of properties that describe the current state for each of the n_E events
  - **Ybus:** current admittance matrix

- **X0:** initial guess vector for power flow
- **P:** current vector of real power at buses
- **Q:** current vector of reactive power at buses
- **loss:** current vector of lines complex power losses
- **totalLossP:** total real power loss
- **totalLossQ:** total reactive power loss
- **numSources:** number of power plants connected to load buses
- **numSourcesP:** sum of real power of power plants connected to load buses
- **CL:** Connectivity Loss, system-level **performance** indicator
- **PL: Connectivity** Loss, system-level performance indicator
- **SSI:** System Serviceability **Index**, system-level performance indicator

The following is the list of the methods of the EPN class (some of these are briefly explained):

- **buildAdmittance:** builds the network admittance matrix
- **buildInitialEstimate:** builds an initial guess vector for the Newton-Raphson algorithm.
- **checkIsolatedBuses:** finds and delete buses that are isolated from the slack bus
- **computeDemand:** determines the required real power at all load buses in which the real power is set to 0 in the textual input. The computation for the generic load bus is based on the user-specified average power per inhabitant and the population of its reference cells, if any, i.e. the cells fed by the node itself
- **computeLineCurrFlowLosses:** retrieves the lines current, power flow and power loss, as well as the slack bus real and reactive power and the generators reactive power
- **computePerformanceIndicator**
- **defineStatCompState:** assigns a damage state to all components of a substation
- **deleteBuses:** deletes from the network broken buses
- **noSolutionFound:** assigns zero values to all electrical quantities, when no power flow solution is found, due to damage of the network
- **computeFlow:** performs the computation of voltage and power in all stations, as well as the current, power and power loss in all transmission lines, in both seismic and non-seismic conditions. This method calls the *buildInitialEstimate* method. If a solution is found for the stations voltages, then the *computeLineCurrFlowLosses* method is called, otherwise the *noSolutionFound* sets all quantities to zero for the current event
- **spreadShortCircuitsInEPN**
- **switchToPhysicalUnits:** switch back to the physical units of voltage, power and admittance, in case the user chooses to work with the per-unit system

The EPNedge class and subclasses

The following is the list of properties of the *EPNedge* abstract class. These properties are common to the two subclasses of this class.

- **voltage**
- **voltageRatio**
- **resistance:** line resistance
- **reactance:** line reactance
- **susceptance:** line susceptance
- **longAdmittance:** line longitudinal admittance
- **transAdmittance:** line transversal admittance
- **states:** n_E×1 collection of properties that describe the current state for each of the n_E events
  - **I:** line current
  - **invI:** line inverse current
  - **flow:** line power flow
  - **invFlow:** line inverse power flow
  - **loss:** line complex power loss
  - **shortCircuitOut:** flag indicating if a short circuit spreads over the network starting from the considered line
  - **lineDown:** flag indicating if the considered line is out of service

The *EPNedge* abstract class and its subclasses do not have any methods (only the object constructor for the concrete subclasses).

The EPNnode class and subclasses

The following is the list of properties of the *EPNnode* abstract class. These properties are common to all subclasses of this class.

- **BC**
- **states:** n_E×1 collection of properties that describe the current state for each of the n_E events. For the slack bus and generators, the state only indicates the output of the power flow analysis, while for load buses the properties are:
  - **phi:** voltage phase resulting from power flow (same property for the second bus,in case the station is of transformation/distribution type)
  - **V:** voltage magnitude resulting from power flow (same property for the second bus, in case the station is of **transformation**/distribution type)
  - **primaryIM:** primary intensity measure at node site, as interpolated from the regular grid **points**
  - **localIMs:** secondary or local intensity measures, correlated to the primary IM
  - **brokenComp:** list of flags indicating if the generic component is broken

- **busDown:** flag indicating if the considered bus is out of service (same property for the second bus, in case the station is of transformation/distribution type)
- **isolatedBus:** flag indicating if the considered bus is isolated from the slack bus (same property for the second bus, in case the station is of transformation/distribution type)
- **shortCircuitOut:** flag indicating if a short circuit spreads over the network starting from the considered station
- **shortCircuitIn:** flag indicating if a short circuit, spread over the network, enters the considered station
- **VR:** voltage ratio, ratio of voltage in seismic conditions to voltage in reference **condition**

The abstract subclass *LoadBus* has two further properties, i.e. **component** (list of pointers to components composing the stations) and **refCells** (cells fed by the station). The TranformationDistribution and Distribution classes have further properties indicating the correspondent bus or buses ID numbers and the pointers to lines entering or exiting from the station.

The *EPNnode* abstract class has no methods, while the *LoadBus* abstract class has three methods, present in all its subclasses (TransformationDistribution and Distribution classes).

- **createComponents**
- **spreadShortCircuitsInStation**
- **checkStationDamage**

The *checkStationDamage* method is called inside the *spreadShortCircuitsInStation* method to eventually delete the transmission lines affected by short circuits.

The TransformationDistribution and Distribution classes are composed of the *Component* abstract class, which is the generalisation of eleven classes, one for each micro-component composing the substations. In particular, these classes are:

- **BarSupport**
- **Box**
- **CircuitBreaker**
- **CoilSupport**
- **CurrentTransformer**
- **VoltageTransformer**
- **HorDisconnectSwitch**
- **VertDisconnectSwitch**
- **LightningArrester**
- **PowerSupplyToProtectionSystem**
- **Transformer**

The following is the list of properties of the *Component* abstract class. These properties are common to all subclasses of this class.

- **parent:** this is a pointer to the parent object which is in this case one of the network stations
- mean: log-mean, i.e. the first parameter of the lognormal fragility curve
- **beta:** log-std, i.e. the second parameter of the lognormal fragility curve
- **fragility:** vector of fragility curve values
- **states:** n_E×1 collection of properties that describe the current state for each of the n_E events. For all component is present the flag **broken**. Only for circuit breakers, also the flags **open** and **passive** are present.

The *Component a*bstract class has no methods.

Damageability model

The details about the fragility functions for each EPN components' typology are reported in Deliverable D3.3. As a reminder, the three fragility functions of 230 kV circuit breakers are displayed in Fig. 2.20. They represent the probability of failure, according to three different failure modes, plotted against the peak ground acceleration (PGA).

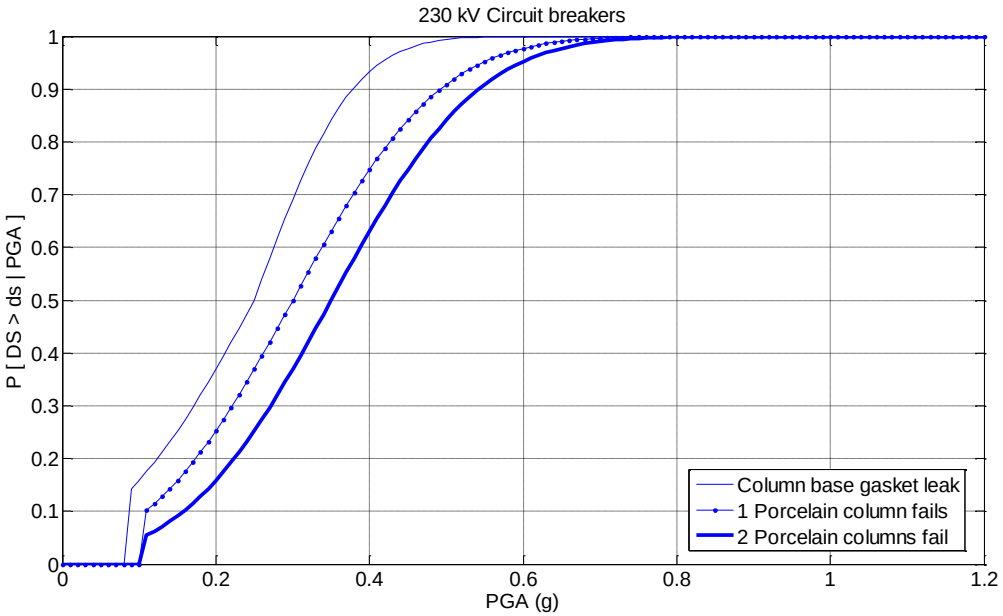

Fig. 2.20 Fragility functions for three failure modes of 230 kV circuit breakers

Demand model

In both reference, non-seismic conditions and in seismic conditions, the power demand is assigned to each load bus based on the reference cells population and a reference value of installed capacity per capita, 2.8 kW/inhab. (see Saadat, H. 2002. *Power system analysis - second edition*. McGraw-Hill Primis Custom Publishing). A more detailed discussion about demand models can be found in deliverable D5.2 "Systemic vulnerability and loss for electric power systems".

2.3.8 Performance indicators

The goal of the SYNER-G methodology is to assess the performance of the Infrastructure and of all its systems and components, when subjected to a seismic hazard. The quantitative measure of this performance is given by Performance Indicators (PIs), that express numerically either the comparison of a demand with a capacity quantity, or the consequence of a mitigation action, or the assembled consequences of all damages (the "impact").

Performance Indicators can be categorized, according to the level within the hierarchy of the Infrastructure to which they refer, into:

- Component-level PIs
- System-level PIs
- System of systems or Infrastructure-level PIs

The following sub-sections give some examples of performance indicators from the literature, divided according to the three categories above. All the PIs considered within SYNER-G are described in the corresponding reports D2.2 to D2.8, which give system components and system functions to evaluate the performance of all systems in the Infrastructure.

Component-level PIs

Examples of component-level PIs include (in this, as well as the following lists of PIs, the initial acronym indicates the system according to the SYNER-G taxonomy):

- WSS: Junctions/Nodes, the **Head Ratio**, or *HR*. For each node, this index is defined as the ratio of the water head in the seismically damaged network to the reference value for non-seismic, normal operations conditions:
  $HR_i = H_{si} / H_{0i}$

  The determination of the water head requires a flow analysis on the network. Hence this index expresses a functional consequence in the *i*-th component of the physical damage to all system components (within the WSS). When interactions with other systems are modeled, HR_i expresses the functional consequence in the *i*-th component of the physical damage to components of all the systems (WSS, EPN, etc), i.e. it is the value of the index that changes due to the inter- and intra-dependencies, not its definition.
- WSS: Pipes, the **Damage Consequence Index**, or *DCI* (Wang *et al*, 2008). This index is defined to measure the *impact of each pipe* on the *overall system serviceability* and to *identify critical links* that significantly affect the system seismic performance. The index is defined at the component level in terms of a system-level PI that measures serviceability, the System Serviceability Index (*SSI*), defined afterwards. Thus, as for the *HR* index, this is a PI that reflects at component-level the functional consequence of damage to all systems' components (and incorporates the effect of the inter- and intra-dependencies, when modeled). The *DCI* for the *i*-th pipe is defined to reflect the consequence from damaging the pipe, including pipe breaks and leaks. It is expressed as:

$$DCI_i = \frac{E\left[SSI\right] - E\left[SSI\middle|L_i\right]}{1 - E\left[SSI\right]} \tag{2.12}$$

in which $E\left[SSI\right]$ is the (unconditional) expected value of *SSI* from a set of simulations in which the *i*-th pipe might or might not be damaged; and $E\left[SSI\middle|L_i\right]$ is the conditional expectation of *SSI* from another set of simulations under the same seismic hazard, but given that the i-th pipe is damaged. As damage to the i-th pipe is certain in the calculation of $E\left[SSI\middle|L_i\right]$, theoretically, $E\left[SSI\middle|L_i\right]$ is always smaller than $E\left[SSI\right]$ where the pipe might or might not be damaged. Therefore, DCI_i is always positive, and it is the percent reduction of *SSI* given that the *i*-th pipe is damaged.

DCI can be effectively estimated as:

$$DCI_i \cong \frac{\frac{1}{m_1}\sum_{i=1}^{m_1} SSI_i - \frac{1}{m_2}\sum_{j=1}^{m_2} SSI_j}{1 - \frac{1}{m_1}\sum_{i=1}^{m_1} SSI_i} \tag{2.13}$$

in which m_1 is the number of all Monte Carlo samples, and m_2 is the number of Monte Carlo samples where damage occurs in the i-th pipe.

- WSS: Pipes, the **Upgrade Benefit Index**, or *UBI* (Wang *et al*, 2008). Similarly to the *DCI*, the index measures the impact of an upgrade of an individual pipe on the overall system serviceability, and reflects at the component level the systemic functional consequence of damage to the whole system(s). It is defined as:

$$UBI_i = \frac{E_{upgrade_i}\left[SSI\right] - E\left[SSI\right]}{1 - E\left[SSI\right]} \tag{2.14}$$

in which $E_{upgarde_i}\left[SSI\right]$ is the expected value of *SSI* given that the i-th pipe is "upgraded." By "upgrade" it is meant that the probability of pipe damage given an earthquake is significantly smaller than its value before upgrade. UBI_i is the percent increase of *SSI* given that the *i*-th pipe is upgraded, and its relative value is a measure of the pipe impact on the overall system serviceability. *UBI* can be used to identify critical links in seismic mitigation, as those with relatively large *UBI* values. The meaning of *DCI*, on the other hand, is complementary to *UBI* but less direct since it is related to the consequence of damage. When the probability of damage in the i-th pipe after upgrade is small compared to its pre-upgrade value, say $P_{upgrade}\left(L_i\right)/P\left(L_i\right) \le 0.1$, and can be approximated as zero, the *UBI* can be effectively evaluated by means of *conditional sample analysis*. In the run for system risk assessment, a subset of the samples in which the i-th pipe is observed *intact* can be treated as an equivalent set of Monte Carlo samples with the pipe upgraded. *UBI* can then be estimated as:

$$UBI_i \cong \frac{\frac{1}{m_2}\sum_{j=1}^{m_2} SSI_j - \frac{1}{m_1}\sum_{i=1}^{m_1} SSI_i}{1-\frac{1}{m_1}\sum_{i=1}^{m_1} SSI_i}$$

in which m_1 is the number of all Monte Carlo samples, and m_2 is the number of Monte Carlo samples where no damage occurs in the i-th pipe.

It can be easily shown (Wang *et al*, 2008) that the *UBI* and *DCI* are related as:

$$UBI_i = DCI_i \frac{P(L_i)}{P(\bar{L}_i)} = DCI_i \frac{P(L_i)}{1-P(L_i)} \tag{2.15}$$

which suggests that, as far as upgrading benefit is concerned, both the consequence of damage (DCI) and the likelihood of damage (the odds ratio $P(L_i)/P(\bar{L}_i)$) should be factored in. For example, for two pipes with equal damage consequence (DCI), the one with high odds of damage should be upgraded first. On the other hand, among the pipes that have the same odds of damage, the one with a high damage consequence has a high upgrade priority. These rather intuitive deductions are consistent with current practices in water system upgrades, whereby priority is given to non redundant links with high flow rate and high repair rate, which correspond to severe damage consequence, DCI, and high damage probability, $P(L_i)/P(\bar{L}_i)$, respectively.

- EPN: **Voltage Ratio**, or *VR*. For each bus inside the substations, this index is defined as the ratio of the voltage magnitude in the seismically damaged network to the reference value for non-seismic, normal conditions:

$$VR_i = V_{i,s}/V_{i,0} \tag{2.16}$$

The voltage computation requires a power-flow analysis on the network. Hence this index expresses a functional consequence in the *i*-th component of the physical damage to all system components. When interactions with other systems are modeled, VR_i expresses the functional consequence in the *i*-th component of the physical damage to components of all the interacting systems, i.e. it is the value of the index that changes due to the inter- and intra-dependencies, not its definition.

DCI and *UBI* can also be defined for the EPN, or for any other system where a *SSI* is defined.

System-level PIs

Examples of system-level PIs include:

- WSS: the **Average Head Ratio,** or AHR. This index is defined as the average over the network nodes of the HR index:

$$AHR = \frac{1}{n_N}\sum_{i=1}^{n_N} HR_i \tag{2.17}$$

where n_N is the number of nodes in the WSS.

- WSS: the **System Serviceability Index**, or SSI (Wang *et al*, 2008). The index is defined as the ratio of the sum of the satisfied customer demands after an earthquake to that before the earthquake:

$$SSI = \frac{\sum_{i=1}^{n} Q_i}{\sum_{i=1}^{n_0} Q_i} \tag{2.18}$$

where n and n_0 are the number of satisfied demand nodes after and before the earthquake, and Q_i is the demand at the i-th node. The SSI varies between 0 and 1. A single value can be determined for a given condition of the network. Its probabilistic characterization, in terms of either it full distribution or its expected value $E[SSI]$ that enters in the definitions of DCI and UBI, requires running multiple simulations for different earthquake realizations.
The above definition from (Wang *et al*, 2008) assumes that the demand remains fixed before and after the earthquake, since it looks only at a single system, without considering the interactions of the WSS with the other systems.

- EPN: the **System Serviceability Index**, can be defined for EPNs as in (Vanzi, 1995), by the ratio of the sum of the real power delivered from load buses after an earthquake, to that before the earthquake:

$$SSI = \frac{\sum_{i=1,\ldots,N_D} P_{i,0} \cdot (1 - R_i) \cdot w_i}{\sum_{i=1,\ldots,N_D} P_{i,0}} \tag{2.19}$$

where $P_{i,0}$ is the real power delivered from the *i*-th load bus in non-seismic conditions, i.e. the demand. In order to compute the eventually reduced power delivered in seismic conditions, two factors are considered. The first one, $R_i = \frac{|V_{i,s} - V_{i,0}|}{V_{i,0}}$, with $V_{i,s}$ and $V_{i,0}$ the voltage magnitudes in seismic and non-seismic conditions, is the percent reduction of voltage in the *i*-th load bus and if $V_{i,s} < V_{i,0}$ one has $1 - R_i = VR_i$. The second factor, w_i, is a weight function accounting for the small tolerance on voltage reduction: in particular, its value is 1 for $R_i \leq 10\%$ and 0 otherwise. The *SSI* index varies between 0 and 1, assuming the value 0 when there is no solution for the power-flow analysis and 1 when the EPN remains undamaged after the earthquake.

The above definition assumes that the demand remains fixed before and after the earthquake, since the index looks only at a single system, without considering the interactions of the EPN with the other infrastructure systems. It can be improved upon and redefined as the *ESSI* that follows.

- EPN: **Enhanced System Serviceability Index**, or *ESSI*, is an enhancement of the *SSI*, defined to capture the interaction of the EPN with the built area of the study region. In order to model this interaction, the power demand is eventually reduced of the fraction corresponding to collapsed buildings. The *ESSI* is defined as:

$$ESSI = \frac{\sum_{i=1,\ldots,N_D} P_{i,0} \cdot (1-R_i) \cdot w_i \cdot \frac{\sum_{j \in I_i} N_{j,\overline{CO}}}{\sum_{j \in I_i} N_j}}{\sum_{i=1,\ldots,N_D} P_{i,0} \cdot \frac{\sum_{j \in I_i} N_{j,\overline{CO}}}{\sum_{j \in I_i} N_j}} \tag{2.20}$$

where I_i is the set of tributary cells for the *i*-th load bus, N_j is the total number of buildings inside the *j*-th tributary cell and $N_{j,\overline{CO}}$ is the number of not collapsed buildings inside the *j*-th tributary cell. As the *SSI*, also the *ESSI* index varies between 0 and 1, assuming the value 0 when there is no solution for the power-flow analysis or all buildings in the study region are collapsed and 1 when the EPN remains undamaged after the earthquake.

- RDN: the **Driver's Delay**, or DD (Shinozuka *et al*, 2003). This system-level performance index is defined as the increase in total daily travel time (hours/day) for all travellers, not distinguishing between commuters and commercial vehicles:

$$DD = \sum_a x'_a t'_a (x'_a) - \sum_a x_a t_a (x_a) \tag{2.21}$$

where x_a and x'_a denote the traffic flows (in PCU/day[4]) on the *a*-th link in the pre-event undamaged and the damaged conditions, respectively, while $t_a(x_a)$ and $t'_a(x'_a)$ denote the corresponding travel times (hours/PCU), which depend on the congestion level through the model:

$$t_a = t_a^0 \left[1 + \alpha \left(\frac{x_a}{c_a} \right)^{\beta} \right] \tag{2.22}$$

where c_a is the "practical capacity" of the link, t_a^0 is the travel time at "zero" flow in the link, and α and β are model parameters (frequently assigned values for α and β are 0.15 and 4, respectively).

- HCS: the **Hospital Treatment Capacity**, or *HTC* (Lupoi *et al*, 2008). This system-level index expresses the number of patients that can be given surgical treatment per hour. It is defined as:

$$HTC = \frac{\alpha \cdot \beta \cdot \gamma_1 \gamma_2}{t_m} \tag{2.23}$$

where α and β are factors accounting for organizational and human macro-components of the hospital system, γ_1 is the number of undamaged operating theatres, γ_2 a Boolean variable that takes upon the value of one when essential utilities needed for the functioning of the operating theatres are properly working, zero otherwise, and t_m is the average duration of surgical treatment. The performance of

[4] PCU=Passenger Car Unit.

the system relative to its pre-earthquake state can be measured through *HTC* either by taking its ratio to the pre-earthquake value $HTCR = HTC/HTC_0$, or by taking its ratio to the corresponding demand HTC/HTD.

Infrastructure-level PIs

Examples of Infrastructure-level PIs include:

- The **Total Infrastructure Loss**, or *TIL*. This performance indicator is an assembled measure of the systemic consequences, or impact, of an earthquake on a region. It is defined as the sum of all *direct* and *indirect* economic loss over the Infrastructure:
  $TIL = L_D + L_I$
  Direct loss is defined as the sum over all systems' components of the economic value of repair/replacement of the component as a function of its state of physical damage. In the crudest of forms this term can be assessed even with a simple *portfolio* study, without considering the inter- and intra-dependencies. Its evaluation requires cost functions, ideally affected by uncertainty, relating physical damage states to the cost. Since repair and replacement are operated by a finite number of agents in a given period of time and with external constraints of the availability of basic materials, these costs cannot be predicted in principle based on the pre-earthquake market conditions. Hence, even the estimate of direct loss requires a systemic approach, to be realistic.
  Indirect loss is the sum of the economic value of all functional consequences of the physical damage, and its evaluation obviously requires a systemic study. An example of a term that contributes to this sum is the cost of additional time spent travelling, expressed as Driver's delay times a unit cost of time (€/hour). The indirect loss term includes the cost of business interruption, cost of reduced production, etc.
- The **Shelter-seeking population** or *SSP*. This index is an example of non-economic Infrastructure-level PI. It is defined as the total number of people seeking public shelter in the aftermath of the event and its evaluation within the presented SYNER-G general methodology follows the scheme shown in Fig. 2.1.

2.4 SEISMIC HAZARD MODEL

2.4.1 Introduction

The seismic vulnerability assessment of an Infrastructure of regional extension requires fragility models for a large number of different components. These fragility models take an intensity measure, scalar or vector, and provide the probability of each damage state. In general multiple different components may share the same site. Thus, in order to assess the damage state of the Infrastructure for any given event, it is necessary to predict a vector of IMs at all sites where one or more vulnerable components are present. This is the purpose of the seismic hazard model.

The vector $\mathbf{s} = \left\{ \mathbf{s}_1 \quad \cdots \quad \mathbf{s}_n \right\}$ of length $m = \sum m_i$, where $\mathbf{s}_i$ is the vector of length m_i of seismic IMs at the *i*-th site, exhibits a variable degree of statistical dependence between its

components, decaying with the distance between the sites, and usually larger between the components within each $\mathbf{s}_i$ (zero distance).

There is sufficient statistical support for adopting a joint lognormal distribution for $\mathbf{s}$. Under this assumption the statistical dependence is fully described in terms of the correlation matrix of **s**. Available data from past earthquakes have been exploited to estimate models for the *within-site* correlation between different IMs (notably, spectral ordinates, e.g. Inoue and Cornell 1990, Baker and Cornell 2006), and to estimate models of *across-sites* correlation for the same IM (Jayaram and Baker, 2009). More recently (Goda and Hong, 2008)(Loth and Baker, 2012) and also within SYNER-G (report D2.13) cross-IM spatial correlation models have been proposed. With such a cross-IM model fully developed it would be possible to sample spatially distributed seismic intensities (shake-fields as they are defined in D2.13) directly from the probability density of $\mathbf{s}$. Within this document an alternative approach is described which does not rely on cross-IM spatial correlation.

Section 2.4.2 illustrates the model for generating events in terms of magnitude and localization. Section 2.4.3 describes how fields of spatially distributed intensity measures are predicted for a single event, while Section 2.4.4 illustrates how local site effects are incorporated in the predicted intensity fields. Further discussion on efficient ways to sample seismic scenarios (event and corresponding spatially distributed intensities) is presented in Section 2.5.2.

2.4.2 Model for event generation

The seismicity of a region is usually described in terms of a number of zones, characterized by approximately homogeneous seismo-tectonic features and hence activity, or, in some parts of the world, in terms of faults of simple or complex geometry, and in some cases of both (with areas employed to model so-called background seismicity). In both cases the activity is described by a magnitude-recurrence law, which most often follows the truncated Gutenberg-Richter law:

$$\lambda_i\left(m\right)=\lambda_{0,i}\left[1-F_M\left(m\right)\right]=\lambda_{0,i}\frac{e^{-\beta_i m}-e^{-\beta_i m_{u,i}}}{e^{-\beta_i m_{l,i}}-e^{-\beta_i m_{u,i}}} \tag{2.24}$$

where $\lambda_{0,i}$ is the mean annual rate of all events with magnitude between the lower bound magnitude $m_{l,i}$ and the upper bound magnitude $m_{u,i}$, and β_i is the rate of decay of the mean annual frequency with magnitude.

By definition, within each zone earthquake epicenters are uniformly distributed. Also, the activity of the zones are assumed to be independent of each other. Source models for faults have also been developed within SYNER-G, and incorporated within the Tololbox, but are not described here. The interested reader can consult report D2.13.

2.4.3 Model for the spatially distributed intensities (ShakeFields) on rock

The local intensity at a site *i*, s_i, is the output of models called *attenuation laws* or *ground-motion prediction equations* (GMPEs), which take as an input earthquake and site characteristics such as magnitude *M*, faulting style *F*, source-to-site distance *R* and local soil properties (e.g. through shear-wave velocity *V*). In general GMPEs have the form:

$$\ln s_i = \mu_{\ln s}\left(M,R_i,F,V_i\right) + \varepsilon_i\sigma_i + \eta_i\tau_i \tag{2.25}$$

where $\mu_{\ln s}\left(M,R_i,F,V_i\right)$ is the mean of the logarithm of the intensity, $\varepsilon_i\sigma_i$ is the *intra-event model error* term at site *i* (ε_i being the standard Gaussian normalized error) and $\eta_i\tau_i$ is the *inter-event model error* term (η_i being the standard Gaussian normalized error). The total variability of the intensity around the predicted log-mean is split in two terms, the intra-event which varies from site to site, for a given earthquake, and the inter-event error which varies from event to event but is constant for all sites (the product $\eta_i\tau_i$ is constant, i.e. $\eta_i\tau_i = \eta_k\tau_k$ with *i* and *k* denoting two different sites, but the standard deviation τ_i varies as a function of structural period, when applicable, and, in some models, also function of *M* and *R*).

Spatial correlation is usually described through models of decay with distance of the form:

$$\rho_{\varepsilon_i\varepsilon_j}\left(h\right) = e^{\frac{-bh}{r}} \tag{2.26}$$

where *b* and *r* (the so-called “range”, or correlation distance) are the model parameters.

As anticipated prediction of shake-fields or maps of spatially distributed intensities has been split in the sequence of two steps.

Step 1: an intensity measure is selected as the “primary IM”, among those for which a spatial correlation model is available. A regular grid that covers the region of interest is identified based on the correlation structure of this IM, i.e. a grid with a subdivision that is adequately smaller of its correlation length. It is emphasized how this grid depends on the extension of the study region, but in general its nodes do not coincide with any of the sites of the Infrastructural components. The number of its nodes and their average distance are independent of the number and location of the sites of vulnerable components. The advantage of this choice is that the grid uses only the necessary and sufficient number of nodes to describe the spatial variation of the IM, which is usually a smooth function of distance, making its evaluation independent of the refinement in the modelling of the Infrastructure. The value of the primary IM at each site is obtained interpolating the grid values. A second advantage is that possible singularity problems in the correlation matrix are mostly avoided, since nodes are regularly spaced and never “too close” to each other. Fig. 2.21 shows the simulation of one map for a scenario event (the figure, taken from D2.13, shows the map for an event on a fault, generated with the planar fault model described in D2.13 and implemented in the SYNER-G toolbox).

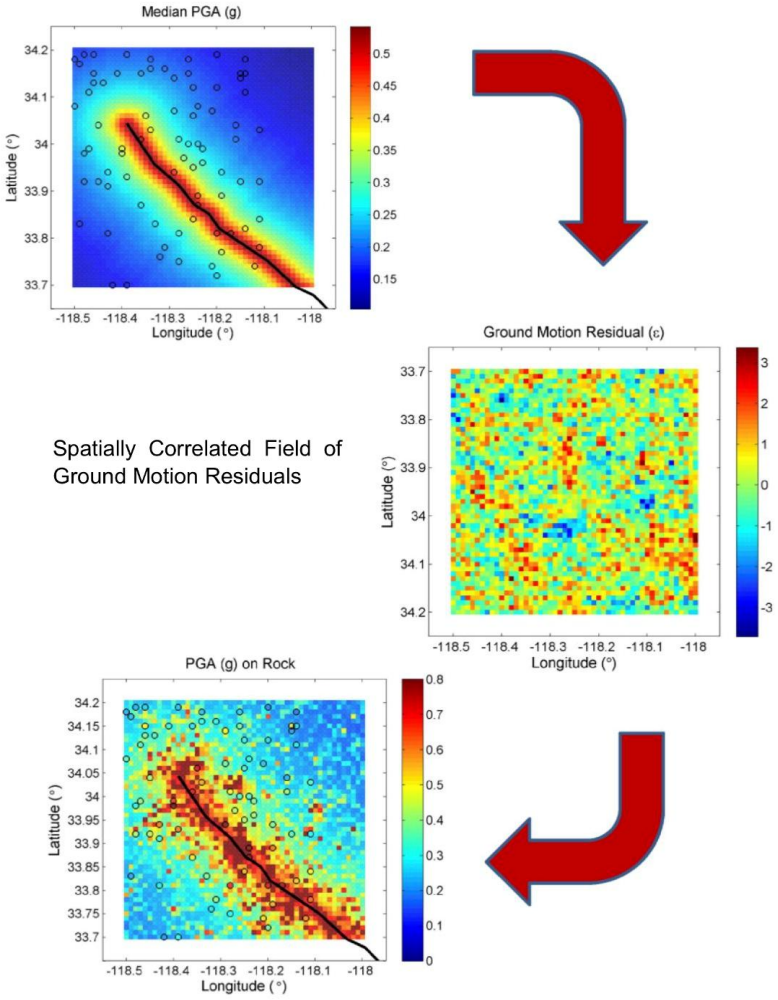

Fig. 2.21 (from D2.13) Overview of the Shakemap process for strong motion on rock: attenuation of median ground motion (top), generation of field of spatially correlated ground motion residuals (middle) and calculation of ground motion on rock (bottom). Fault source indicated by black line, target sites indicated by black circles

Step 2: at each site, the vector $\mathbf{s}_i = \left\{ s_{i1} \quad \mathbf{s}_{i2} \right\}$ of the local IMs, partitioned in the primary IM s_{i1} (simply s_1 in the following) and the sub-vector $\mathbf{s}_{i2}$ of the secondary IMs (simply $\mathbf{s}_2$ in the following), is described by means of its joint distribution $f(\mathbf{s})$. Values of $\mathbf{s}_2$ can be sampled from its conditional distribution $f(\mathbf{s}_2|s_1)$ given the value of the primary IM s_1 (sampled on the grid and interpolated at the site). Under the assumption that $f(\mathbf{s})$ is lognormal, all marginal and conditional distributions of lower order are still lognormal. Hence $f(\mathbf{s}_2|s_1)$ reads:

$$f(\mathbf{s}_2|s_1) = \frac{1}{(2\pi)^{-n/2}\sqrt{\det \mathbf{R}_{\ln \mathbf{s}_2 \ln \mathbf{s}_2|\ln s_1}} \prod s_{2j}\sigma_{\ln s_{2j}|\ln s_1}} \cdot \exp\left[-\frac{1}{2}\left(\ln \mathbf{s}_2 - \mu_{\ln \mathbf{s}_2|\ln s_1}\right)^T \mathbf{C}_{\ln \mathbf{s}_2 \ln \mathbf{s}_2|\ln s_1} \left(\ln \mathbf{s}_2 - \mu_{\ln \mathbf{s}_2|\ln s_1}\right) \right] \quad (2.27)$$

where the conditional mean vector, and the conditional covariance and correlation matrices are:

$$\mu_{\ln \mathbf{s}_2|\ln s_1}(M,R,F,V) = \mu_{\ln \mathbf{s}_2}(M,R,F,V) + \mathbf{C}_{\ln \mathbf{s}_2|\ln s_1} \frac{\ln s_1 - \mu_{\ln s_1}(M,R,F,V)}{\sigma_{s_1}^2} \tag{2.28}$$

$$\mathbf{C}_{\ln \mathbf{s}_2 \ln \mathbf{s}_2|\ln s_1} = \mathbf{C}_{\ln \mathbf{s}_2 \ln \mathbf{s}_2} - \frac{\mathbf{C}_{\ln \mathbf{s}_2 \ln s_1} \mathbf{C}_{\ln s_1 \ln \mathbf{s}_2}}{\sigma_{s_1}^2} \tag{2.29}$$

$$\mathbf{R}_{\ln \mathbf{s}_2 \ln \mathbf{s}_2|\ln s_1} = \mathbf{D}^{-1}_{\ln \mathbf{s}_2 \ln \mathbf{s}_2|\ln s_1} \mathbf{C}_{\ln \mathbf{s}_2 \ln \mathbf{s}_2|\ln s_1} \mathbf{D}^{-1}_{\ln \mathbf{s}_2 \ln \mathbf{s}_2|\ln s_1} \tag{2.30}$$

with:

$$\mathbf{C}_{\ln \mathbf{s} \ln \mathbf{s}} = \begin{bmatrix} \sigma_{s_1}^2 & \mathbf{C}_{\ln s_1 \ln \mathbf{s}_2} \\ \mathbf{C}_{\ln \mathbf{s}_2 \ln s_1} & \mathbf{C}_{\ln \mathbf{s}_2 \ln \mathbf{s}_2} \end{bmatrix} = \mathbf{D}_{\ln \mathbf{s} \ln \mathbf{s}} \mathbf{R}_{\ln \mathbf{s} \ln \mathbf{s}} \mathbf{D}_{\ln \mathbf{s} \ln \mathbf{s}} \tag{2.31}$$

$$\mathbf{D}_{\ln \mathbf{s} \ln \mathbf{s}} = \begin{bmatrix} \sigma_{s_1} & \cdots & 0 \\ \vdots & \ddots & \vdots \\ 0 & \cdots & \sigma_{s_n} \end{bmatrix} \tag{2.32}$$

$$\mathbf{R}_{\ln \mathbf{s} \ln \mathbf{s}} = \begin{bmatrix} 1 & \cdots & \rho_{\ln s_1 \ln s_n} \\ \vdots & \ddots & \vdots \\ \rho_{\ln s_n \ln s_1} & \cdots & 1 \end{bmatrix} \tag{2.33}$$

The standard deviations in Eq. (2.32) are *total* standard deviations $\sigma_T = \sqrt{\sigma^2 + \tau^2}$. Models for the correlation coefficients in Eq. (2.33) are available in the literature, e.g. for spectral accelerations at different periods, as in Baker and Cornell (2006) or Inoue and Cornell (1990), the latter having the simple form (valid for periods between 0.1s and 4.0s):

$$\rho_{\ln s_i \ln s_j} = 1 - 0.33 \ln\left(T_j / T_i\right) \tag{2.34}$$

2.4.4 Modelling of site effects

Several models are available for describing the amplification of ground motion at the site as a function of the local properties of the upper soil layers. Preference of a model over another strongly depends on the information available to characterise the geotechnical properties of the sites under consideration, the quality and quantity of which may be hard to anticipate. It is expected that, at the minimum, it should be possible to map the shallow geology in terms of design code site classes, such as those in Eurocode (CEN, 2004) and/or NEHRP. The option may also be available to characterise 30-m shear wave velocity (V_{s30}), values for which can be derived directly by topographic or geological proxy. The accuracy of site parameters estimated from proxies may not be sufficient for application on an urban scale. At the upper end in terms of quality and quantity of information, it may be the case that an

extensive micro-zonation study is available with detailed geotechnical characterization of soil profiles on a grid that cover that study area.

In general, as reported in more detail in D2.13, the available options are:

- **GMPE amplification model**
  - This approach considers only amplification factors associated with the GMPE used for the hazard analysis, and may be implemented in one of two ways, the preference for which may depend on the GMPE in question:
    - The first approach assumes that each point where the motion is predicted can be characterised according to the site classification scheme adopted and modelled within the GMPE.
    - The second approach is preferred when a ground motion field is interpolated between neighbouring points, e.g. when generating ground motion values for an unevenly distributed set of points, from a fixed grid of ground motion points, such as is the case for the procedure presented in the previous section. In this case the GMPE is used assuming a constant reference condition (usually rock) and the amplification factor is applied after interpolation.
  - Advantage(s): the approach requires a *minimum amount of information* within the site characterisation. In most cases each site need only be categorised according to a design code site class, or in terms of V_{s30} (see Appendix A of D2.13 for classification schemes). Such broad categorization makes application to an urban scale relatively simple.
  - Shortcoming(s): The most obvious is that application is limited to sites that can be classified according to the (usually gross) scheme applied in the GMPE. Often the set of records used for deriving the GMPE will not adequately represent all the site classes of interest (most likely very soft or liquefiable soils will be underrepresented to model amplification reliably), as is the case for many existing European models. Other models, such as Boore et al, 1997, or the recent NGA set of GMPEs (Abrahamson & Silva, 2008; Boore & Atkinson, 2008; Campbell & Bozorgnia, 2008; Chiou & Youngs, 2008), prefer to characterise site according to V_{s30}, some including additional parameters to model the response of basin resonance. These models may capture a wider range of site effects, but they too may be limited to a narrower range of V_{s30} than required for the vulnerability analysis, particularly for soft soil sites. Furthermore, many models of this type adopt nonlinear site amplification scaling factors that may be functions of both V_{s30} and expected ground motion on reference rock.
- **Design-code amplification model**
  - In certain applications site amplification is estimated using factors specified in design codes. Such an approach can be found in the current HAZUS methodology, which uses the amplification factors specified in the 1997 NEHRP Provisions. Although not stated in the original NEHRP Provisions (FEMA 450), the HAZUS manual applied FA to scale PGA and FV to PGV. Similar amplification factors can be derived from the Eurocode 8 classification, or indeed any other design code relevant to the application in question.

- Advantage(s): this method is *simple and has relatively minimal requirements* in terms of the site classification, as the GMPE-based approach. It is relatively easy to implement across a region. The issue of linear or nonlinear amplification need not be addressed directly, as nonlinearity may be implicit in the code amplification factors, as they are for the NEHRP Provisions.
- Shortcoming(s):
    - by implementing code-based amplification factors, this approach is limited to site categories for which the code supplies such factors, again as for the GMPE-based approach. This is particularly problematic for complex soil conditions or liquefiable soils, for which ad-hoc investigation is usually required in codes. As such, for potentially liquefiable sites this is a significant shortcoming. An additional limitation is that design codes are extremely unlikely to provide amplification factors for IMs other than PGA or spectral acceleration. This limits the extension of the code-based site amplification approach to less common IMs which, however, are needed for the fragility of many lifelines components.
    - Deterministic application of site factors, when this are nonlinear (intensty-dependent) has been shown to underestimate ground motion intensities evaluated probabilistically for return periods of engineering interest (Goulet and Stewart, 2009). Reasons include different standard deviation terms for rock and soil sites, different controlling earthquakes, and overestimation of the nonlinear component of the site response in the deterministic procedure. When this is the case one should resort by including the site factors amongst the random variables with appropriate consideration of nonlinear site response in the simulation of the shake fields.

- **Generic amplification model from site-response simulations**
    - One such approach is implemented in Walling *et al.* (2008). In their application the amplification factors are calculated using a 1D equivalent linear analysis model of site amplification, applied to a synthetic time history generated by point source stochastic simulation. Multiple randomly-generated site profiles are used to characterise each of the NEHRP classes, with given properties. The approach of Walling *et al*. (2008) represents a way of characterising a generic site amplification model, on the basis of ground motion simulations, for a broader range of site classes than is typically represented in observed strong motion records.
    - Advantage(s): the required input data to characterise the site condition is only the V_{s30}.
- **Application-specific amplification model from site-response simulations**
    - It may be the case that extensive micro-zonation studies have been undertaken for the region of application. When this detailed information is available it is possible to define site-specific amplifications factors. It may be expected that a detailed micro-zonation study of a region would produce a set of geotechnical profiles that characterise the site condition (variation in V_s and density with depth, as well as describing both static and dynamic material properties for each layer) at many locations within the area in question. From this, it is possible to classify

particular zones or areas with similar site profiles, using e.g. a clustering technique. For each micro-zone a characteristic site profile may be then developed. From this profile, and using a 1D numerical amplification tool (a particularly useful summary of the available tools is given in (Faccioli, 2007)), it is possible to estimate an amplification factor (F_{ij}) particular to the micro-zone via the formulation of Bazzuro & Cornell (2004a,b). With the latter technique it is also possible to account for non-linear scaling. As for the Walling *et al* (2008) approach, multiple 1D analyses are performed for different rock input motions and randomly generated variations of the micro-zone characteristic site profile. As many 1D analyses may be needed for each zone, the relatively simple and efficient 1D equivalent linear approach (Schnabel et al, 1972; Robinson et al, 2006), should be preferred for computational convenience to the more complex nonlinear amplification tools. Ground motions for the rock site may be taken from observed rock records or could be generated via stochastic simulation of ground motions relevant to the controlling earthquakes of the region in question (e.g. Boore, 2003; Motazedian & Atkinson, 2005; Rezaeian and Der Kiureghian 2008, 2010). Depending on the likely hazard within a given region, it may be prudent to separate the rock ground motion records into bins according to PGA, and to develop separate amplification factors for each bin. This may better capture any nonlinear amplification effects at a given site.

- Advantage(s): This approach has several benefits over the generic amplification models to site amplification considered previously. The main benefit is that a greater quantity of geotechnical information is integrated into the analysis. Whilst a greater computational effort is required to develop the amplification functions, they remain characteristic for the region in question, hence this is one-time cost. Implementation of the site amplification within the stochastic earthquake hazard simulation is a relatively simple and computationally efficient procedure. For the purpose of the current application we can incorporate cross-spectral (or cross-IM) correlation in the amplification function, however, no spatial correlation can be estimated for the residuals if synthetic rock motions are used to estimate the amplification. The strength of this assumption is difficult to test from observed strong motion records, but may be better constrained in future.

As already stated, in order to preserve the generality of the developed methodology it is paramount to devise a scheme capable of accommodating information with varying degree of detail. In many practical applications there will not be enough data to adopt an application-specific amplification model.

In any case, the general scheme will be that of modelling the amplification of the required IMs at the site through random amplification functions, denoted by “A” in the following. These will be either generic or site-specific, from (randomised) profiles of the sites.

2.4.5 Geotechnical hazards

In modelling the seismic risk to lifeline systems, the consideration of hazard from permanent deformation of the ground (PGD_f) is paramount. For pipelines and similar systems with linear elements, fragility models are generally given in terms of PGD_f, as they are most vulnerable to the permanent displacement of the ground rather than transient shaking. For application within SYNER-G, four primary causes of permanent ground displacement are considered:

liquefaction-induced lateral spread, liquefaction-induced settlement, slope displacement and coseismic fault rupture (see Fig. 2.6).

Geotechnical hazard from earthquakes has been the subject of a considerable amount of investigation in recent decades. There are many models available that are intended to relate the degree of deformation and the probability of the geotechnical hazard occurring, to the strength of the ground motion. Implementation within a study of earthquake risk for an urban area requires a holistic approach; one capable of modelling all the likely phenomena concurrently. Such an approach will obviously impose limitations on the type of models used. As with the characterisation of site amplification, for consideration of spatially distributed systems the main limiting factor will be the availability of geotechnical information for the sites in question. Many theoretical and empirical models relating PGD_f to strong shaking require a level of geotechnical detail that may be impractical to obtain for a spatially distributed set of sites. As such, it is more appropriate to consider a "baseline" model that can be implemented in the widest variety of applications. Some considerations can then be given to measures that may be taken to improve the geotechnical hazard models. The "baseline" approach that will be considered here is that implemented in the HAZUS methodology, for each of the geotechnical hazards. The adopted object-oriented framework provides for extension to higher-level models when supporting data are available (the classes for CoseismicRupture, Landslide and Liquefaction are all abstract ones).

Probability of Liquefaction

Within the HAZUS methodology, the estimation of the probability of liquefaction is based on the analysis of Youd and Perkins (1978), who introduced classes of *liquefaction susceptibility*. These classes (Very High, High, Moderate, Low, Very Low and None) are categorised on the basis of deposit type, age and general distribution of cohesionless sediments. Each liquefaction susceptibility category (*SC*) has an associated conditional probability of liquefaction for a given PGA (P[*L*|PGA=*a*]), and a proportion of map unit susceptible to liquefaction (P_{ml}). This last term is intended to take into account the variability of soil properties within any given sedimentary class, which may act to inhibit liquefaction at a site. The probability of liquefaction for a given susceptibility category (P[L_{SC}]) is defined as:

$$P\left[L_{SC}\right] = \frac{P\left[L|PGA = a\right]}{K_M K_W} P_{ml} \tag{2.35}$$

where K_M is the moment magnitude correction factor (to account for duration-effects), calculated from Seed and Idriss (1982):

$$K_M = 0.0027 M_W^3 - 0.0267 M_W^2 - 0.2055 M_W + 2.9188 \tag{2.36}$$

and K_W is the correction factor for groundwater depths other than five feet, calculated via:

$$K_W = 0.022 d_W + 0.93 \tag{2.37}$$

where d_W is the depth (in feet) to the groundwater.

This formulation may be the simplest approach, requiring only the susceptibility class (which can be inferred from a geological map), PGA and magnitude (from the generated event and corresponding shake-field) and depth to the groundwater. Values of P[*L*|PGA=*a*] and P_{ml} are

given in the HAZUS manual. These are derived, in part, from the empirical models of Liao et al. (1988), which relate the probability of liquefaction to the SPT resistance ($(N_1)_{60}$) and load.

To determine whether liquefaction occurs, a uniformly distributed random variable in the range 0 to 1 is determined, independently for each site. If this variable is less than the liquefaction probability, then liquefaction is assumed to occur at the site.

A review of additional models can be found in report D2.13.

Liquefaction-Induced lateral spread

The HAZUS methodology calculates the expected amount of lateral displacement in inches ($E[PGD_{SC}]$) via:

$$E\left[PGD_{SC}\right]=K_{\Delta}\cdot E\left[PGD_f|PGA/PGA_t\right] \tag{2.38}$$

where $E[PGD_f|PGA/PGAt]$ is the expected PGD_f for each susceptibility category under the normalised level of shaking defined by PGA/PGA_t where PGA_t is a SC-dependent threshold PGA. The factor K_{Δ} is a magnitude-dependent displacement correction term calculated from Seed and Idriss (1982):

$$K_{\Delta}=0.0086M_W^3-0.0914M_W^2+0.4698M_W-0.9835 \tag{2.39}$$

The primary advantage of the HAZUS methodology is the simplicity and the dependence on few site-specific factors. It may be considered only a first order estimate on the amount of displacement associated with lateral spreading at a site. It is evident, however, that the characterisation of PGD_f via the HAZUS methodology is only a deterministic estimate (an expected value), and does not take into account uncertainty in the relation with intensity measures. If the ground conditions can be better constrained for the site in question, other empirical models, including those that characterise uncertainty, could alternatively be applied. Examples are presented in report D2.13.

Liquefaction-Induced settlement

Despite being a commonly observed liquefaction phenomenon, there are fewer established models that are used in assessment of ground settlement. It has been suggested by Tokimatsu and Seed (1987) that the extent of settlement shows little dependence on the strength of ground motion. This makes characterisation in a hazard framework substantially more challenging. In the HAZUS methodology a characteristic settlement is attributed to each susceptibility class, thus making the expected settlement a product of the liquefaction probability and the characteristic settlement (in any given scenario, however, liquefaction will either occur or not occur and the settlement will be equal to its characteristic value for the SC in the former case, or to zero in the latter). The actual values of the characteristic settlement were determined from the process described by Tokimatsu and Seed (1987). The process by which the characteristic values were obtained requires careful interpretation of observational data and detailed geotechnical characterisation of the site. Clearly such an approach is challenging to implement on a spatial scale. Modelling of settlement is a more complex procedure that requires integration of the volumetric strain (ε_V) over the soil profile, taking into account static properties of each soil layer and the increase in confining pressures with depth. Alternative models are briefly described in report D2.13. However, for implementation over a spatially distributed system the HAZUS methodology (including the

characteristic values for volumetric settlement) may be the most widely applicable, in spite of the relative crudeness of the model.

Slope Displacement

The HAZUS approach to characterisation of slope displacement mirrors, in concept, that of liquefaction displacement. This is a two-step process that determines, for each shake-field, whether displacement is observed at a site and its magnitude. Parameters for the first step are assigned via the classification of *landslide susceptibility*. The susceptibility class is selected from a ten-point scale and assigned on the basis of geology, slope angle and the position of groundwater with respect to the level of sliding (essentially a wet/dry distinction). For each susceptibility class, a critical acceleration is defined; hence, if PGA exceeds the critical acceleration then a landslide is observed. The probability of a landslide occurring is modified by a term to determine the percentage of the map area having a landslide susceptible deposit. The occurrence of a landslide at a location may be determined via uniformly distributed random variable. If this is below the probability level of observing a landslide then the landslide is assumed to occur.

The expected displacement for a seismically induced landslide ($E[PGD_f]$) is determined via:

$$E\left[PGD_f\right] = E\left[d|a_{is}\right] \cdot a_{is} \cdot n \tag{2.40}$$

where $E[d|a_{is}]$ is the expected displacement factor, which is a function of the induced acceleration (a_{is}), more generally represented as PGA (g). The number of cycles (n) is determined via the relation of Seed and Idriss (1982) as a function of magnitude:

$$n = 0.3419M_W^3 - 5.5214M_W^2 + 33.6154M_W - 70.7692 \tag{2.41}$$

Once again, the simplicity is the relative advantage of the HAZUS approach. The crucial parameter needed for estimation of slope displacement is the yield coefficient (k_y), which corresponds to the threshold acceleration above which slope displacement is initiated. This may be estimated via many different ways, taking into consideration the properties of the slope. Estimation of this parameter may not be a necessary input for a geotechnical risk analysis software, so it may be prudent to assume that the yield coefficient is specified by the user *a priori*, or assigned according to the HAZUS susceptibility classes.

As with the case of liquefaction, the HAZUS estimator of PGD_f is deterministic, and does take into consideration variability of the model. Alternative empirical models exist that may better constrain the uncertainty, whilst retaining practicality for use with common intensity measures. Such examples, briefly presented in report D2.13, may be the simplest extension of the slope displacement calculation already implemented in HAZUS. It is noted that these models are largely derived from Newmark's (1965) sliding block method for assessment of slope displacements. This formulation is a simplification of the process of slope displacement and does not take into account other potential hazards such as coseismic rock fall. Nevertheless, the sliding mass may be sufficient to characterise the most likely type of slope displacement expected to result in damage to infrastructural elements in a region.

Coseismic Rupture

The final source of ground displacement considered within the HAZUS methodology is coseismic rupture of the fault at the surface. The most common approach to do this is via

empirical models of peak displacement for a given magnitude, such as those of Wells and Coppersmith (1994):

$$\log\left(\max\left\{PGD_f\right\}\right) = -5.42 + 0.82M_W \pm 0.42\varepsilon \quad (2.42)$$

As is noted within the HAZUS documentation, it is recognised that the maximum displacement may occur at any point along the fault, although displacement must taper to zero at the fault ends. As a consequence, displacement for a point along the fault rupture is sampled from a uniform probability distribution between half the maximum and the maximum displacement.

The characterisation of coseismic surface rupture should depend on, or at least be consistent with, the description of the fault source. It may be suggested that fault rupture should only be considered for larger (M_W > 6.0) events occurring on a defined fault source. This means that coseismic rupture displacement should not be considered for area source zones, even for large earthquakes. Alternative empirical models correlating displacement and magnitude may be used if required, although the Wells and Coppersmith (1994) models remain a common standard in many seismic hazard codes.

A more nuanced approach to characterising coseismic fault displacement has been undertaken in the analysis of strike-slip faults by Petersen et al. (2011). Their empirical analysis of displacements along seven well-mapped strike-slip ruptures, yields several regression equations that may be pertinent for use in fault displacement hazard analysis and also defines an empirical model for off-fault ruptures. It should be recognised, however, that the empirical models presented here correspond only to strike-slip faults, and that the behaviour of slip on normal or reverse faults may require different functional forms, and will almost certainly yield different coefficients, from those considered here. Such analysis may need to be a focus of future research.

2.5 PROBABILISTIC ANALYSIS

2.5.1 Uncertainty modelling

The uncertainties entering the regional seismic vulnerability analysis have been briefly described in the previous sections. Here are summarized for convenience:

- Seismic activity of the seismo-genetic sources/faults (modelled through magnitude-recurrence laws, Section 2.4.2 and report D2.13)
- Local seismic intensities at the sites (modelled through ground-motion prediction equations, spatial correlation models, cross-IM correlation models and site amplification models, Sections 2.4.3 and 2.4.4 and deliverable D2.13)
- Physical damageability of the components of the Infrastructure (modelled by fragility models, e.g. Sections 2.3.4, 2.3.6 and 2.3.7, more generally all reports from WP3)
- Uncertainty in the *functional consequences* at component and/or system level of the *physical damage* at the component level (see Section2.3.3)
- Uncertainty in the socio-economic consequences of physical damage (non-structural components fragility models, probabilistic cost models, etc, reports from WP4)
- Epistemic uncertainty in all the above models.

The goal of the analysis is to evaluate probabilities or mean annual rates of events *E* defined in terms of performance-indicators of the types presented in Section 2.3.8. This requires the joint probability model (distribution) of all the above uncertainties, denoted by $f(\mathbf{x})$, where $\mathbf{x}$ is the vector that collects all random variables in the problem. The latter variables form a sequence of cause and effect and this sequence can be represented graphically in the form of a directed acyclic graph as shown in Fig. 2.22, which illustrates the flow from the rupturing fault/source, to event location and magnitude, the local intensities, the components' state of physical damage, the functional consequences at system-level and finally the value of the performance indicators at the highest, Infrastructure, level.

Additional uncertainty in the results of the analysis comes from the epistemic uncertainty on the models. This uncertainty is of two types. The first type is that characterizing the parameters θ of the probabilistic models employed, e.g. those of the magnitude-recurrence laws, or the parameters of the fragility models, etc. This uncertainty can be included in the overall scheme, by enhancing the joint probabilistic model, as shown in Fig. 2.22 by the grey variables.

The second type refers to the model form itself, since, in general, for each uncertainty component alternative models are available (e.g. different fragility models for pipes, see Section 2.3.4). The latter form could be dealt with by repeating the whole analysis for different choices of the models, effectively setting up a logic tree of model alternatives, as it is done for instance in Engineering Seismology for hazard assessment, weighting different GMPEs, hypotheses on the boundaries of seismo-genetic sources, etc.

Finally, Fig. 2.22 (light blue *N* variables, or "Non-deterministic link" variables) also shows how the soft links (Section 2.3.3) can be included as additional random terms that enter in the relation between the physical damage state *D* and the performance *PI*. The scheme shows how these links can be at any level, from the component to the system, or system of system level.

Fig. 2.23 summarizes in very general terms what are the inputs and outputs exchanged by the three models for hazard, physical vulnerability and systemic consequences.

Fig. 2.22 refers to the simple system shown in Fig. 2.24, where the Infrastructure is made up of two systems: an EPN with a generator (vulnerable component number 1) and distribution sub-station (vulnerable component 2), connected by an overhead line of negligible vulnerability; a WSS with a pumping station working with power from the adjacent distribution station in the EPN, and feeding water to an end-user or demand node (tributry building cell shown but not considered in the example).

Within this simple example shown in the figure the random variable *M* desribes the event magnitude, the discrete r.v. *S* describes the seismo-genetic sources (and depends on the magnitude since not all sources can generate event for a given magnitude), the r.v. *L*, whose distribution depends on the source, describes the event location (epicentre, hypocentre), variables η and $\boldsymbol{\varepsilon}$ (the vector is represented as dependent on a standard normal vector $\boldsymbol{u}$, because this is usually the way correlated normal vectors are sampled) describe the inter-event and intra-event errors, $S_{gi,r}$ are the values of the primary IM at the *grid* points, still on rock/stiff-soil, S_{ri} are the primary IM values interpolated at the components' location, on rock/stiff-soil, A_i are the *amplification* functions for each site, $\boldsymbol{S}_{si}$ is the vector of IMs needed at each site, incorporating the site effects, D_i is and the i-th component physical *damage* state, whose randomness is described by the set of fragility functions for increasing performance levels/limit-states.

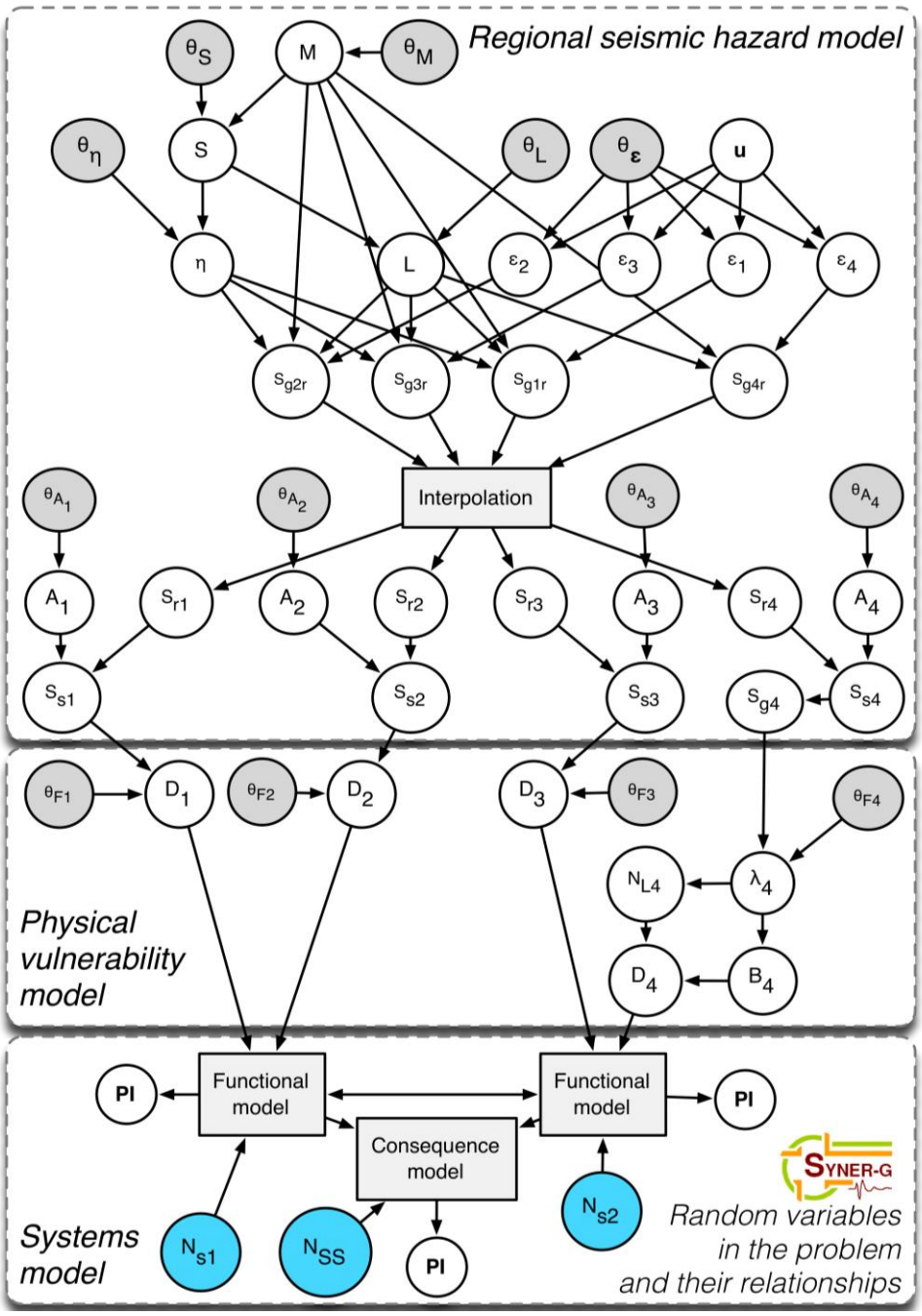

Fig. 2.22 The network of random variables modelling the uncertainty in the regional seismic vulnerability assessment problem

At some locations a geotechnical hazard model is used to sample geotechnical IMs such as peak ground displacement (variable S_{g4} in Fig. 2.22) for components whose fragility model requires one, such as the pipe (component 4) in Fig. 2.24. Physica damage is then sampled from the respective distribution differently for point-like and line-like components: for the first three components (the generatoion plant and the sub-station in the EPN, as well as the pump in the WSS) a damage state is determined from a discrete probability distribution function of the sampled IM values, as shown for buildings in Section 2.3.4; for the last, fourth component, the pipe, a repari rate or damage rate per unit length is determined as a function of e.g. peak ground deformation and/or velocity, and this determines the porbability of

rupture and of leak number, used to sample the boolean variable B_4 (rupture/unruptured) and the number of leaks N_{L4}. If unruptured (B_4=0) the pipe is assigned a leakege area equal to the sum of the areas at each of the N_{L4} leaks, and the corresponding additional demand is lumped at the end node of the sub-segment (produced by the discretization algorithm and to which an initial zero demand is assigned), otherwise the pipe is removed from the damaged network.

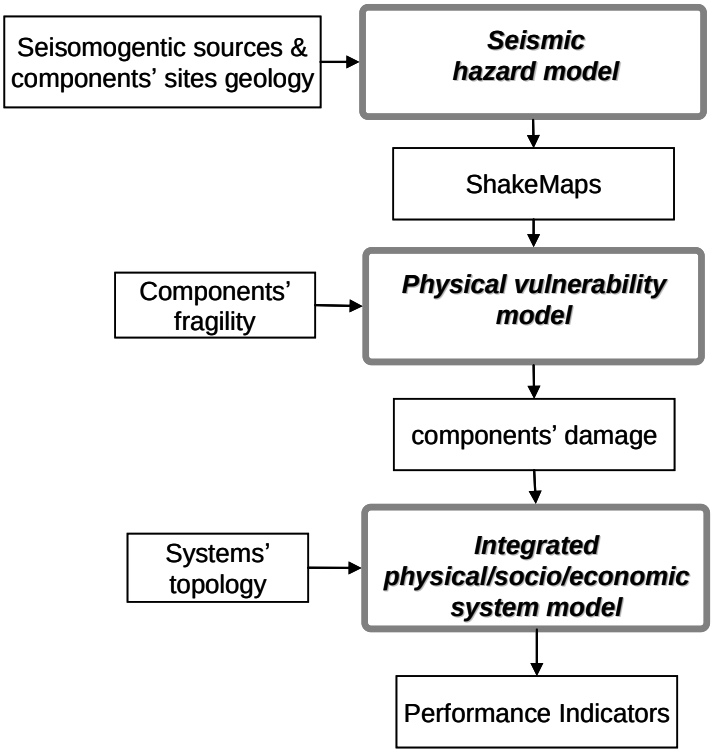

Fig. 2.23 The sequence of models with associated input and output quantities

Given the state of physical damge systems are evaluated according to their functional models and they all concur to determine the performance of the Infrastructure. Vectors of performance indicators for each system and for the Infrastructure as a whole are computed at this last stage.

It can also be observed how the above graphical representation allows an efficient writing of the joint density $f(\mathbf{x})$, by highlighting the *statistical dependencies* between the variables. In particular, the diagram describes a directed acyclic graph (DAG) and represents a Bayesian hyerarchical model. In this work, no Bayesian updating is performed, and hence, the graph is used just as a description of the sampling sequence within the typical simulation run, as explained in the next section.

The joint density can be written as a product of a set of conditional distributions in the form:

$$\begin{aligned} f(\mathbf{x}) &= f(x_n | x_1,\ldots,x_{n-1}) f(x_1,\ldots,x_{n-1}) = \\ &= f(x_n | x_1,\ldots,x_{n-1}) f(x_{n-1} | x_1,\ldots,x_{n-2}) f(x_1,\ldots,x_{n-2}) = \\ &= f(x_1) \prod_{i=2}^{n} f(x_i | x_1,\ldots,x_{i-1}) \end{aligned} \tag{2.43}$$

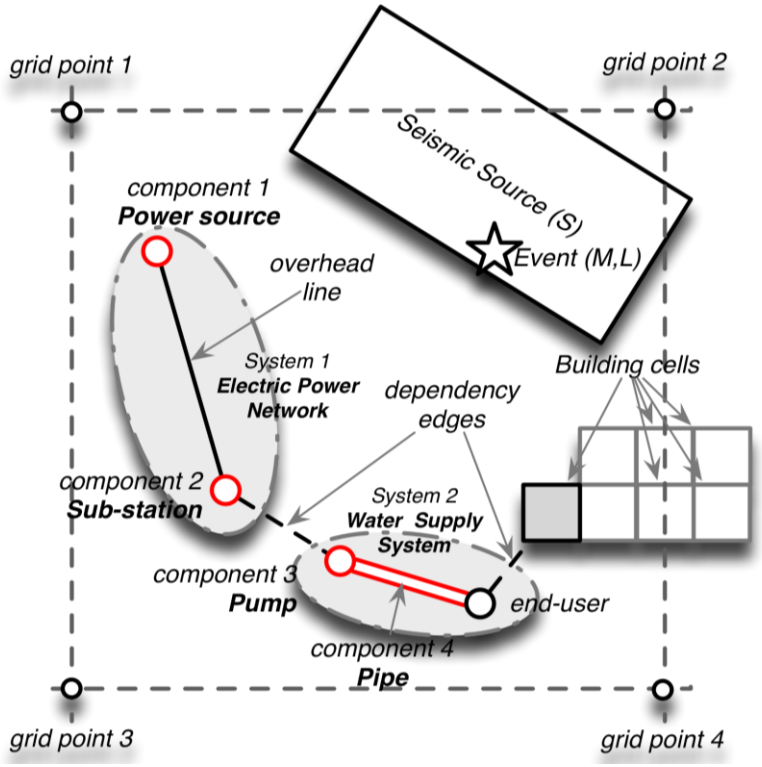

Fig. 2.24 Sample physical system for Fig. 2.22

The network of statistical dependencies represented above allows a drastic reduction in the terms of Eq.(2.43), which can be rewritten neglecting epistemic uncertainties as:

$$\begin{aligned} f(\mathbf{x}) &= f_{SYS|PhVM}(\mathbf{x}_{SYS}|\mathbf{x}_{PhVM}) f_{PhVM|SH}(\mathbf{x}_{PhVM}|\mathbf{x}_{SH}) f_{SH}(\mathbf{x}_{SH}) = \\ &= f(\mathbf{PI}|\mathbf{D}) \cdot \prod_{i=1}^{4} f(D_i|\mathbf{S}_i) \left[\cdot \prod_{i=1}^{4} f(\mathbf{S}_i|M,L,\varepsilon_i,\eta) f(\varepsilon_i|\mathbf{u}) f(L|S) f(\eta|S) f(S|M) f(M) \right] \end{aligned} \tag{2.44}$$

and accounting for them as:

$$\begin{aligned} f(\mathbf{x}) &= f_{SYS|PhVM}(\mathbf{x}_{SYS}|\mathbf{x}_{PhVM}) \cdot f_{PhVM|SH}(\mathbf{x}_{PhVM}|\mathbf{x}_{SH}) \cdot f_{SH}(\mathbf{x}_{SH}) = \\ &= \left[f(\mathbf{PI}|\mathbf{D},\mathbf{N_S}) f(N_{S1}) f(N_{S2}) f(N_{SS}) \right] \cdot \\ &\cdot \left[\prod_{i=1}^{4} f(D_i|\mathbf{S}_i,\theta_{F_i}) f(\theta_{F_i}) \right] \\ &\cdot \left[\left(\prod_{i=1}^{4} f(\mathbf{S}_i|M,L,\varepsilon_i,\eta) f(\varepsilon_i|\mathbf{u},\theta_{\varepsilon_i}) f(\theta_{\varepsilon_i}) \right) \cdot \right. \\ &\left. \cdot f(L|S,\theta_L) f(\theta_L) f(\eta|S,\theta_\eta) f(\theta_\eta) f(S|M,\theta_S) f(\theta_S) f(M|\theta_M) f(\theta_M) \right] \end{aligned} \tag{2.45}$$

Comments:

- The SYNER-G software toolbox written to illustrate the methodology in its current stage of development does not account for the epistemic uncertainties in the models, or for the soft links (additional variables in Fig. 2.22).

- The uncertainty related to the socio-economic portion of the integrated model is not represented, nor included yet. Characterization of the uncertainty associated with models such as the casualty and displaced population ones described previously still requires fundamental research and represents a direction for future efforts.

2.5.2 Simulation methods

Probabilistic evaluation of the performance of the Infrastructure can be carried out with different methods. These can be classified in two general classes: simulation methods, described in this section, and non-simulation methods described in Section 2.5.3. Simulation methods have been adopted and implemented within the SYNER-G software toolbox.

Plain Monte Carlo method and variance-reduction techniques

Simulation is a robust way to explore the behaviour of systems of any complexity. It is based on the observation of system response to input **x**. Simulation of a set of inputs from $f(\mathbf{x})$ and evaluation of corresponding outputs allows to determine through statistical post-processing the distribution of the output.

The probability of an event *E* can be expressed as (the "reliability integral"):

$$p_E = \int_{\Omega_E} f(\mathbf{x}) d\mathbf{x} \tag{2.46}$$

where Ω_E is the portion of the sample space (the space where **x** is defined) collecting all **x** values leading to the event *E*.

Simulation methods start from Eq. (2.46) by introducing the so-called "indicator function" $I_E(\mathbf{x})$, which equals one if **x** belongs to *E*, zero otherwise. It is apparent that p_E is the expected value of I_E:

$$p_E = \int_{\Omega_E} f(\mathbf{x}) d\mathbf{x} = \int I_E(\mathbf{x}) f(\mathbf{x}) d\mathbf{x} = \mathrm{E}\left[I_E(\mathbf{x})\right] \tag{2.47}$$

Monte Carlo (MC) simulation (Rubinstein, 1981) is the crudest possible way of approximating p_E, in that it amounts to estimating the expectation of I_E as an arithmetic average $\hat{p}_E$ over a sufficiently large number *N* of **x** samples:

$$p_E = \mathrm{E}\left[I_E(\mathbf{x})\right] \cong \frac{1}{N}\sum_{i=1}^{N} I_E(\mathbf{x}_i) = \frac{N_E}{N} = \hat{p}_E \tag{2.48}$$

The problem is thus reduced to that of sampling realizations $\mathbf{x}_i$ of **x** from the distribution $f(\mathbf{x})$, and evaluating the PI for each realization in order to assign a value to the indicator function.

Sampling of realizations from the joint distribution $f(\mathbf{x})$ can be performed according to different algorithms. These are not independent of the simulation method and, actually, "smart" sampling of the realizations can result in drastic improvements of efficiency, in terms of the required computational effort. For the problem at hand, and plain Monte Carlo simulation, sampling is carried out in a conditional fashion, according to the representation of the joint density given in Eq.(2.44): the first variable to be sampled is the magnitude *M*, then, conditional on the sampled magnitude, the source *S*, the location *L* within the source and

inter-event error η are sampled from the appropriate conditional distribution. Finally at each site S_i follows, together with the component damage state *D*i, etc.

A basic well-known result about plain MC simulation is that the *minimum* number of samples required for a specified confidence in the estimate (in particular to have 30% probability that $\hat{p}_E \in [0.77,1.33] \cdot p_E$) is given by:

$$N \geq 10 \frac{1-p_E}{p_E} \cong \frac{10}{p_E} \tag{2.49}$$

In order to reduce the required minimum *N* one must act on the variance of $\hat{p}_E$. This is why the wide range of enhanced simulation methods that have been advanced in the last decades fall under the name of "variance reduction techniques". One such technique is *Importance sampling* (IS). This is a form of simulation based on the idea that when values of **x** that fall into Ω_E are rare and difficult to sample, they can be conveniently sampled according to a more favourable distribution, somehow shifted towards Ω_E. Of course the different way **x** values are sampled must be accounted for in estimating p_E according to:

$$\begin{aligned} p_E &= \int I_E(\mathbf{x}) f(\mathbf{x}) d\mathbf{x} = \int I_E(\mathbf{x}) \frac{f(\mathbf{x})}{h(\mathbf{x})} h(\mathbf{x}) d\mathbf{x} = \\ &= \mathrm{E}_h \left[I_E(\mathbf{x}) \frac{f(\mathbf{x})}{h(\mathbf{x})} \right] = \mathrm{E}_h \left[I_E(\mathbf{x}) \alpha(\mathbf{x}) \right] \cong \frac{1}{N} \sum_{i=1}^{N} I_E(\mathbf{x}_i) \alpha(\mathbf{x}_i) \end{aligned} \tag{2.50}$$

where now p_E is expressed as the expectation of the quantity $I_E(\mathbf{x})\alpha(\mathbf{x})$ with respect to the distribution $h(\mathbf{x})$, called sampling density. The IS ratio $\alpha(\mathbf{x})$ corrects the estimate to account for the different probability content of the neighbourhood of **x** assigned by the original and the sampling density. The difficulty with the IS method is to devise a good sampling density $h(\mathbf{x})$, since it inevitably requires some knowledge of the domain *E*. One way to do this is to start with a sampling density and change it during the simulation while samples closer to *E* occur. This is called *adaptive importance sampling*.

Both plain MC simulation and a highly effective brand of IS specifically developed for distributed Infrastructure analysis (Jayaram and Baker, 2010) are implemented in the SYNER-G toolbox. The latter method is explained in some detail in the following section closely following the original work by (Jayaram and Baker, 2010).

Importance sampling with K-means clustering

Jayaram and Baker (2010) propose a simulation-based framework for developing a small but stochastically representative catalogue of earthquake ground-motion intensity maps that can be used for risk assessment of spatially distributed systems. In this framework, Importance Sampling is used to preferentially sample 'important' ground-motion intensity maps, and K-Means Clustering is used to identify and combine redundant maps in order to obtain a small catalogue. The effects of sampling and clustering are accounted for through a weighting on each remaining map, so that the resulting catalogue is still a probabilistically correct representation.

While Crowley and Bommer (2006) are perhaps the first to point out the need for using a model such as that in Eq.(2.25) within the framework of MCS of a spatially distributed

system, though they do not account for the spatial correlation amongst intra-event errors, Kiremidjan *et al* (2007) are the first to employ IS to selectively sample in the larger magnitude range. The inter- and intra-event errors, however, are still sampled using plain MCS. The method by Jayaram and Baker (2010) instead, employs a sampling density for magnitude as well as for the above error terms. This IS technique leads to a reduction of two orders of magnitude in the required number of maps.

The second step of the procedure, the K-means clustering, is even more important then the first and, as explained later, is instrumental in maintaining probabilistic consistency of the reduced set of intensity maps with the hazard model in Section 2.4. Indeed, previous attempts can be found in the literature to drastically reduce the number of scenarios to represent the regional seismicity: Shiraki et al. (2007), within an MCS-based approach to estimate earthquake-induced delays in a transportation network, generated a catalogueue of 47 earthquakes and corresponding intensity maps for the Los Angeles area and assigned probabilities to these earthquakes such that the site hazard curves obtained using this catalogueue match with the known local-site hazard curves obtained from PSHA. In other words, the probabilities of the scenario earthquakes were made to be *hazard consistent*. Only median peak ground accelerations were used to produce the ground-motion intensity maps corresponding to the scenario earthquakes, however, and the known variability about these medians was ignored. While this approach is computationally highly efficient on account of the use of a small catalogue of earthquakes, the selection of earthquakes is a somewhat *subjective* process, and the assignment of probabilities is based on hazard consistency rather than on actual event likelihoods. Moreover, the procedure does not capture the effect of the uncertainties in ground-motion intensities. The K-means clustering technique solves this problem by providing a scenario selection algorithm, thus removing subjectivity, and values of the scenarios probabilities that account for the full variability in the model.

Importance sampling density

As already stated the method uses an importance sampling density h on magnitude, inter-event error η and intra-event errors ε. This is built as the product of three sampling densities on each variable.

The original density for M is defined starting from the densities $f_i(m)$ (e.g., for sources whose activity is specified in terms of the truncated Gutenberg-Richter law, the absolute value derivatives of the ratio of exponentials in the equation (2.24) specified for each of the n_f active faults/sources and the corresponding activation frequencies λ_i:

$$f(m) = \frac{\sum_{i=1}^{n_f} \lambda_i f_i(m)}{\sum_{i=1}^{n_f} \lambda_i} \tag{2.51}$$

Given that an earthquake with magnitude *M=m* has occurred the probability that the event was generated in the i-th source is:

$$P(i|m) = \frac{\lambda_i f_i(m)}{\sum_{j=1}^{n_f} \lambda_j f_j(m)} \tag{2.52}$$

To devise the sampling density for the magnitude, $h(m)$, consider the range $[m_{\min}, m_{\max}]$ of the magnitudes of interest and its partition (stratification) into n_m intervals:

$$[m_{\min}, m_{\max}] = [m_{\min}, m_2)[m_{\min}, m_2) \bigcup \ldots \bigcup [m_{\min}, m_{\max}] \tag{2.53}$$

where the partitions are chosen so as to be small at large magnitudes and large at small magnitudes. The procedure, also referred to as *stratified sampling*, then requires sampling a magnitude value from each partition using within each partition the original density. These leads to a sample of n_m magnitude values that span the range of interest, and adequately cover important large magnitude values. The IS density $h(m)$ for *m* lying in the k-th partition is then:

$$h(m) = \frac{1}{n_m} \frac{f(m)}{\int_{m_k}^{m_{k+1}} f(m)\, dm} \tag{2.54}$$

Once the magnitudes are sampled using IS, the rupture locations can be obtained by sampling faults using fault probabilities $P(i|m)$, which will be non-zero only if the maximum allowable magnitude on fault *i* exceeds *m*. Let $n_f(m)$ denote all such faults with non-zero values of $P(i|m)$. If $n_f(m)$ is small (around 10), a more efficient sampling approach will be to consider each of those $n_f(m)$ faults to be the source of the earthquake and consider $n_f(m)$ different earthquakes of the same simulated magnitude. It is to be noted that this fault sampling procedure is similar to the IS of magnitudes (i.e. it is stratified). The IS ratio for fault *i* chosen by this procedure is computed as:

$$\alpha(i|m) = \frac{f(i|m)}{h(i|m)} = \frac{P(i|m)}{1/n_f(m)} \tag{2.55}$$

It has been observed that a consequence of the above choice for the density is that it is difficult to separate fault/source contributions and, hence, the mean annual frequency of a PI exceeding a predefined level, normally written and evaluated fault by fault:

$$\lambda_{PI} = \sum_{i=1}^{n_f} \lambda_i P(PI \geq u|i) \tag{2.56}$$

must be rewritten as:

$$\lambda_{PI} = \sum_{i=1}^{n} \lambda_i \frac{\sum_{i=1}^{n_f} \lambda_i P(PI \geq u|i)}{\sum_{i=1}^{n_f} \lambda_i} = \lambda_0 \sum_{i=1}^{n} \frac{\lambda_i}{\lambda_0} P(PI \geq u|i) = \lambda_0 P(PI \geq u) \tag{2.57}$$

where $\lambda_0 = \sum \lambda_i$ is the mean annual rate of all events, from any fault/source, and λ_i / λ_0 is the probability that given an event, it occurs on the i-th fault/source. The use of the maps generated by the present method ensures that $P(PI \geq u)$ is evaluated with the correct distribution of events over the active faults.

The intra-event normalized errors ε have a multivariate correlated standard normal distribution, with correlation specified as a function of distance (See Section 2.4.4). A good

sampling density is a multivariate normal with the same covariance matrix $\mathbf{C}_{\varepsilon\varepsilon}$ but mean vector μ_ε shifted towards positive values:

$$h(\varepsilon) = (2\pi)^{-n/2} \left|\mathbf{C}_{\varepsilon\varepsilon}\right|^{-1/2} \exp\left[-\frac{1}{2}(\varepsilon - \mu_\varepsilon)^T \mathbf{C}_{\varepsilon\varepsilon}^{-1}(\varepsilon - \mu_\varepsilon)\right] \quad (2.58)$$

As described in the original paper, the choice of an adequate shifted mean vector is a delicate matter and the result of a compromise between the likelihood of the generated maps and the desire of sampling large epsilon values. In general, numerical tests show that an optimal value of the shift is a function of the number of sites, their average separation distance and the range of the exponential decay function describing spatial correlation.

Fig. 2.25 shows the sampling densities for magnitude (stratified sampling) and intra-event errors (shifted normal, marginal view).

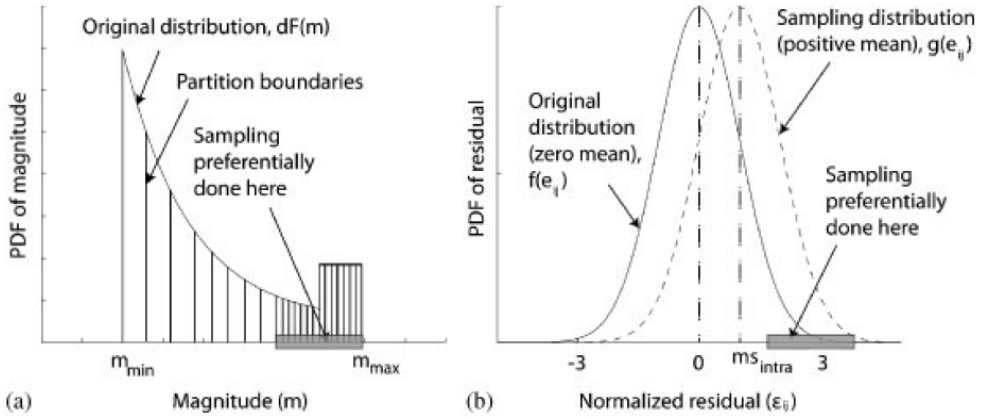

Fig. 2.25 Sampling densities for the magnitude and intra-event errors/residuals (from Jayaram and baker 2010)

The inter-event normalized error η is a standard normal variable. Following standard conventions, since the inter-event error is a constant across all the sites during a single earthquake, the simulated normalized inter-event residuals should satisfy the following relation (which does not assume that the that τ is a constant, in order to be compatible with ground-motion models such as that of Abrahamson and Silva, 2008):

$$\eta_i = \eta_1 \frac{\tau_1}{\tau_i} \quad (2.59)$$

Thus, the normalized inter-event residuals can be simulated by first simulating η_1 from a univariate normal distribution with zero mean and unit standard deviation, and by subsequently evaluating with the above equations the values at the other sites. The IS density is chosen simply as a shifted univariate normal, with shifted mean μ_η.

In conclusion, the IS ratio is given by the product of the corresponding ratios for M, δ and η:

$$\alpha = \frac{f(m)}{h(m)}\frac{f(i|m)}{h(i|m)}\frac{f(\varepsilon)}{h(\varepsilon)}\frac{f(\eta)}{h(\eta)} = \\ = \frac{\int_{m_k}^{m_{k+1}} f(m)dm}{n_m}\frac{P(i|m)}{1/n_f(m)}\exp\frac{1}{2}\left[(\varepsilon-\mu_\varepsilon)^T\mathbf{C}_{\varepsilon\varepsilon}^{-1}(\varepsilon-\mu_\varepsilon)-\varepsilon^T\mathbf{C}_{\varepsilon\varepsilon}^{-1}\varepsilon+(\eta-\mu_\eta)^2-\eta^2\right] \quad (2.60)$$

K-means clustering

K-means clustering is a technique that groups a set of observations into K clusters such that the dissimilarity between the observations (typically measured by their Euclidean distance) within a cluster is minimized (McQueen, 1967).

Let $\mathbf{S}_1,\ldots,\mathbf{S}_r$ denote *r* maps generated using IS, each map $\mathbf{S}_j$ being a *p*-dimensional vector (*p* being the number of points in the grid used to sample the primary IM) defined as $\mathbf{S}_j=\left[s_{11j},\ldots,s_{1ij},\ldots,s_{1pj}\right]$, where s_{1ij} is the value of the primary IM (denoted as s_1) for the *i*-th site/component in the *j*-th map.

The K-means method groups these maps into clusters by minimizing V, which is defined as follows:

$$V=\sum_{i=1}^{K}\sum_{\mathbf{S}_j\in S_i}\left\|\mathbf{S}_j-\mathbf{C}_i\right\|^2=\sum_{i=1}^{K}\sum_{\mathbf{S}_j\in S_i}\sum_{q=1}^{p}\left(s_{1qj}-C_{qi}\right)^2 \quad (2.61)$$

where K denotes the number of clusters, S_i denotes the set of maps in cluster *i*, $\mathbf{C}_i=\left[C_{1i},\ldots,C_{qi},\ldots,C_{pi}\right]$ is the cluster centroid obtained as the mean of all the maps in cluster *i*, and $\left\|\mathbf{S}_j-\mathbf{C}_i\right\|^2=\sum_{q=1}^{p}\left(s_{1qj}-C_{qi}\right)^2$ denotes the Euclidean distance between the map *j* and the cluster centroid and adopted, as explained, to measure maps dissimilarity.

In its simplest version, the K-means algorithm is composed of the following four steps:

- Step 1: Pick K maps to denote the initial cluster centroids. This selection can be done randomly.
- Step 2: Assign each map to the cluster with the closest centroid.
- Step 3: Recalculate the centroid of each cluster after the assignments.
- Step 4: Repeat steps 2 and 3 until no more reassignments take place.

Once all the maps are clustered, the final catalogue can be developed by randomly selecting a single map from each cluster, which is used to represent all maps in that cluster on account of the similarity of the maps within a cluster. In other words, if the map selected from a cluster produces a value PI=u of the performance indicator, it is assumed that all other maps in the cluster produce the same value by virtue of similarity. The maps in this smaller catalogue can then be used in place of the maps generated using IS for the risk assessment (i.e. for evaluating $P(PI\geq u)$), which results in a dramatic improvement in the computational efficiency. This procedure allows us to select K strongly dissimilar intensity maps as part of the catalogue (since the maps eliminated are similar to one of these K maps in the catalogue), but will ensure that the catalogue is *stochastically representative*. Because only one map from each cluster is now used, the total weight associated with the map should be equal to the sum of the weights of all the maps in that cluster:

$$\alpha_i = \sum_{\mathbf{s}_j \in S_i} \alpha\left(\mathbf{S}_j\right) \tag{2.62}$$

where $\alpha\left(\mathbf{S}_j\right)$ is evaluated according to Eq.(2.60).

2.5.3 Non-simulation methods

Reliability methods other than simulation-based ones have been applied to the analysis of infrastructural systems. In particular, these are the so-called Matrix System Reliability Method (Song and Kang, 2009) (Song and Ok, 2010) and the model of Bayesian Networks (Nielsen 2007) (Straub et al, 2008) (Der Kiureghian, 2009) (Straub and Der Kiureghian, 2009) (Bensi et al, 2009). The former method hits its limits when dealing with capacitive (flow) modelling of networks (applications are limited to connectivity problems, Kang et al 2008), while the latter, which seems very promising in perspective, especially for dealing with the problem of real-time or near-real-time decision-making (observer within the time-window of interest, in the language adopted in Section 1.3), appears to be not mature for dealing with problems of realistic dimensions. The strength of this modelling approach resides in the capability of the model of updating the probabilities associated with its states in real-time under a continuous stream of incoming information on the states of an enlarging sub-set of its components (the typical situation in the aftermath of an earthquake). The problem with this modelling technique is the computational effort, which is large since the system state must be known in advance for all possible combinations of the components' states. As it is somewhat candidly put in (Der Kiureghian 2009*): After an earthquake, the [system] assumes one of $N=m_1m_2\ldots m_n$ distinct configurations, where n denotes the number of components. For example a [system] with two-state components, has $N=2^n$ distinct configurations. […] For each of these distinct configurations one can perform disciplinary analysis (e.g., water, power, traffic connectivity or flow analysis) to determine the state of the infrastructure and whether or not it performs the intended function. […] It should be obvious that a [system] with a large number of components can have an extremely large number of distinct configurations. Therefore, disciplinary analysis will have to be performed for a very large number of cases. One of the challenges in infrastructure risk assessment is to devise methods to handle the large amount of computations.*

Pragmatically, with the current state of knowledge in mind, the option adopted within the SYNER-G project to deal with the uncertainty is to resort to simulation methods and to reduce the required number of system evaluations by using advanced variance reduction techniques in order to arrive at probability estimates of the performances of interest.

3 A pilot application

3.1 THE TEST CASE

The methodology described in chapter 2 and implemented in the SYNER-G software toolbox is shortly illustrated in the following with reference to the small, idealized Infrastructure shown in Fig. 3.1. This example is *complete*, in that it contains all elements of the taxonomy for each of the selected systems (a sub-set of all systems in the Taxonomy), and has a *minimum-size*, i.e. the smallest possible dimensions to be still meaningful while constraining complexity while developing the methodology and implementing the software (the example has been used as a test case before actual applications and validation studies have been performed). The systems that have been included are: BDG, RDN, WSS, EPN, HCS (RDN and HCS not shown herein) shown in Fig. 3.1.

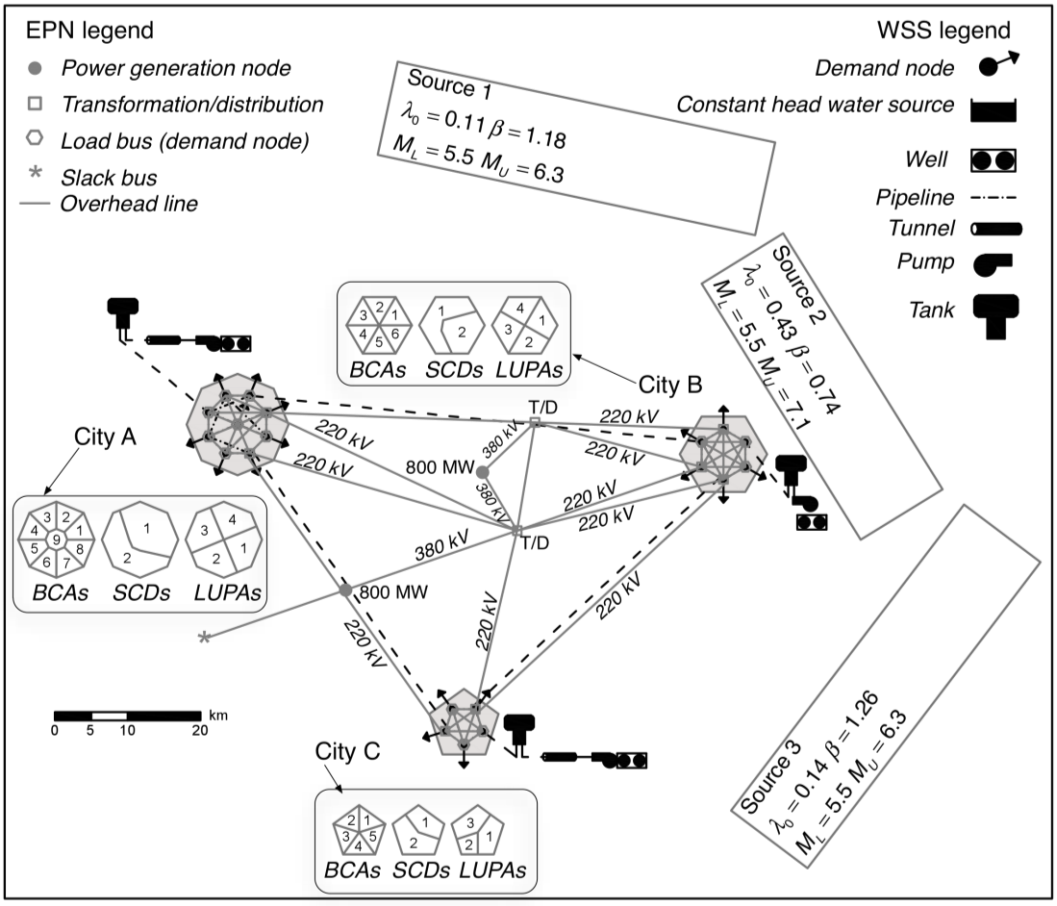

Fig. 3.1 The ideal Infrastructure

3.1.1 Seismic hazard

The region is subject to seismic hazard due to three active seismo-genetic sources/zones of rectangular geometry, denominated SZ1 to SZ3 in Fig. 3.1, which also reports the activity parameters for the truncated Gutenberg-Richter model.

Shake-fields at all locations of interest are simulated employing the Akkar-Bommer (2010) ground motion prediction equation, including inter- and intra-event error terms, valid for Europe, and the Jayaram and Baker (2009) model of spatial correlation of the intra-event errors, with parameters calibrated for Italy (Esposito and Iervolino, 2011).

3.1.2 Cities (BDG)

The example represents a small region with three urban areas, denominated City A to C in Fig. 3.1. The three cities have approximately circular shape, with diameters of 14, 12 and 10 km, respectively. The total population has been determined starting from a population density of about 2 000 inhab./km^2 for the larger city down to about 1 200 inhab./km^2 for the smaller one, resulting in populations of 307 000, 226 000 and 97 000, respectively.

Socio-economic data, as well as data on building type and distribution for European cities are usually available from *Eurostat* through the *European Urban Audit* (EUA) and the *Building Census* (BC), respectively. Data on land use are available on a local basis in the form of a *Land Use Plan* (LUP). For the sake of designing the prototype infrastructure, fictitious realistic EUA, BC and LUP zonations have been created.

Some simplifying assumptions have been made:

- Building Census: Only two building typologies are present in the example for all three cities: old, unreinforced masonry construction and RC construction from the 1960s on. The proportion of each typology varies from city to city and total number of buildings and percentage per typology in each BC area, for all three cities is reported in Table 3.1. Each typology is characterised by a set of fragility curves for increasing state of damage, provided in reports D3.1 and D3.2. Table 3.2 reports the parameters for the fragility sets of the two considered typologies.
- European Urban Audit: only two SCDs per city have been considered, representing two different socio-economic levels in terms of average income, education, etc. (Table 3.3).

Fig. 3.2 shows summary information on the three cities. For clarity of presentation the three different subdivisions of the urban territory according to the three data sources are shown separately, while they obviously overlap.

As far as the Land Use Plan is concerned, four area types are identified: green (G), residential (R), commercial (C) and Industrial (I). **Error! Reference source not found.** eports the use of each area of the three cities according to the LUP.

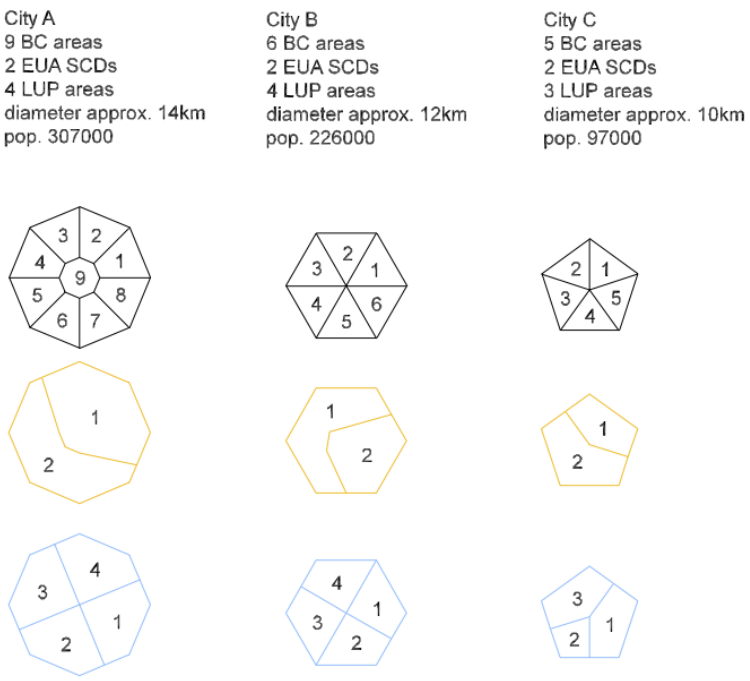

Fig. 3.2 The three cities in the idealized infrastructure

Table 3.1 Building population distribution in the BC areas, per typology

City	BC area	N_{bldg}	% type 1	% type 2
A	1	42500	40	60
	2	42700	45	55
	3	42000	30	70
	4	43000	80	20
	5	40000	75	25
	6	41000	77	23
	7	42000	70	30
	8	42700	20	80
	9	26700	25	75
B	1	45000	50	50
	2	43000	70	30
	3	44000	75	25
	4	42500	80	20
	5	43600	45	55
	6	44700	30	70
C	1	36000	50	50
	2	36500	40	60
	3	37000	75	25
	4	35600	70	30
	5	34400	45	55

Table 3.2 Fragility curves parameters for each building typology (the IM is PGA)

Typology	Limit state	Log-mean	Dispersion
1 – Old masonry	1 (yield)	-2.041	0.574
	2 (collapse)	-1.269	0.550
2 – RC construction	1 (yield)	-1.832	0.474
	2 (collapse)	-1.091	0.485

Table 3.3 Socio-economic data (part 1)

Socio-Economic Factors	Urban Audit Indicators	City A		City B		City C	
		1	2	1	2	1	2
Population	Total Resident Pop.	163000	144000	124000	102000	37600	56400
Children	Aged 0-4 (%)	3,98	4,33	3,45	4,22	4,96	4,84
Elderly	Aged 75 and over (%)	11,11	7,06	13,45	8,09	7,38	6,15
Education	Working-age pop. qualified at level 3 or 4 ISCED (%)	8,38	12,41	9,32	6,29	4,12	2,07
Lone Parent with Children	Lone-parent households (%)	2,21	2,15	2,45	2,66	2,39	3,36
Migration/ Ethnicity	Residents not EU Nationals and citizens of a medium/low HDI Country (%)	2,06	1,01	5,15	3,09	6,19	11,22
Income	Population with less than 60% national media annual income (%)	2,71	1,21	3,17	4,04	8,52	12,77
Substandard Housing	Dwellings lacking basic amenities (%)	1,17	1,08	2,15	1,09	2,21	3,72
Crime	Recorded Crimes per 1000 population	20,5	30,4	13,2	4,0	60,8	77,9

Table 3.4 Socio-economic data (part 2)

City	SCD	Population
A	1	163000
	2	144000
B	1	124000
	2	102000
C	1	37600
	2	56400

Table 3.5 Land Use Plan

City	Area	Use
A	1	I
	2	C
	3	G
	4	R
B	1	C
	2	R
	3	I
	4	G
C	1	R
	2	G
	3	C

3.1.3 The water supply system (WSS)

The water-supply system includes the distribution networks of the three cities as well as aqueducts connecting them. Each demand serves an entire BC area: the lower level pipes from these demand nodes to single buildings are not included in the model.

The distribution networks of City A and B are fed by a *river* and a *dam basin*, respectively, both modelled as *constant head water sources*. City C is fed by a *well field*, equipped with submersible pumps for water lifting; the pump feed pipe runs into a tunnel and conveys water to a tank, modelled as a *variable head water source*.

The daily equipment of water has been set to 250 litres per inhabitant per day. This figure is employed to compute the demand flows at nodes on the base of the population they serve.

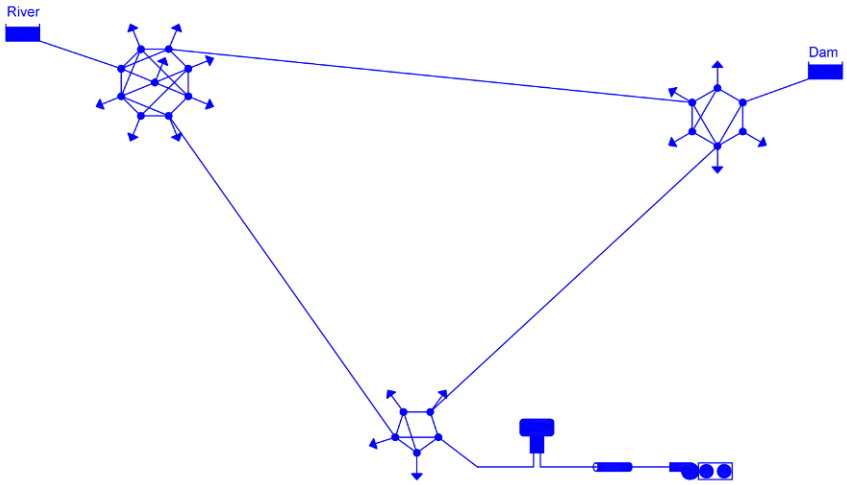

Fig. 3.3 The WSS of the idealized Infrastructure (legend in Fig. 3.1)

3.1.4 The electric power network (EPN)

The electric power network is composed of stations or nodes and the transmission lines connecting them. One balance node, two generation nodes and several load nodes are present. These latter are distinguished into two typologies, i.e. transformation/distribution and distribution, depending on the presence or absence of transformers.

The transmission lines are classified into three types on the base of their nominal voltage. Three high voltage levels are considered, in particular 380 kV, 220 kV and 60 kV. Only the grid-like transmission system is considered (distribution system not included in the model.

The installed capacity per capita has been set to 2.8 kW per inhabitant and can be used in the prototype software to compute the demand at nodes on the base of the population they serve.

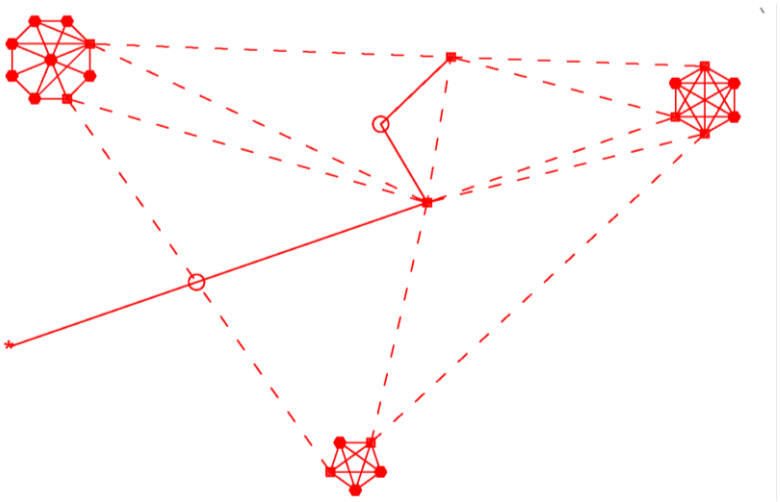

Fig. 3.4 The EPN of the idealized infrastructure (legend in Fig. 3.1)

3.2 VULNERABILITY ANALYSIS

3.2.1 Introduction

This chapter demonstrates some of the results obtainable through the application of the methodology implemented in the SYNER-G software toolbox. The next sections describe: the graphical echo of the input (Section 3.2.2), results for the reference non-seismic conditions (Section 3.2.3**Error! Reference source not found.**), results for a single selected cenario event (fixed epicentre location and magnitude) and for the whole regional hazard resulting from all three seismo-genetic sources.

3.2.2 Echo of the input

The data about population, with the corresponding socio-economic indicators, is specified through the sub-city districts (SCDs), the data about the buildings, in terms of number and typology, is specified by building census areas (BCAs), while the use of the territory is specified by land use plan areas (LUPAs).Fig. 3.5, Fig. 3.6 and Fig. 3.7 show the visualization of these data from the software. All three figures also show the subdivision of the study area into a multi-scale rectangular grid, used to model buildings. The software automatically discretizes the study region starting with a user-defined large-size meshing (even only a single rectangular cell) and refines the mesh locally whenever a grid cell intersects with an “urban polygon” (an SCD, a LUPA, or a BCA) up to a user-defined number of times (in this example, six). Because the grid is multi-scale, it is possible to accurately project the building data from the different databases and to closely follow the city boundaries, without using an unnecessary fine mesh in rural areas and limiting the overall computational effort. Only the smallest cells are inhabited and thus linked to reference nodes within the different networks. It can be observed that this approach is convergent, upon mesh refinement, to the single building analysis.

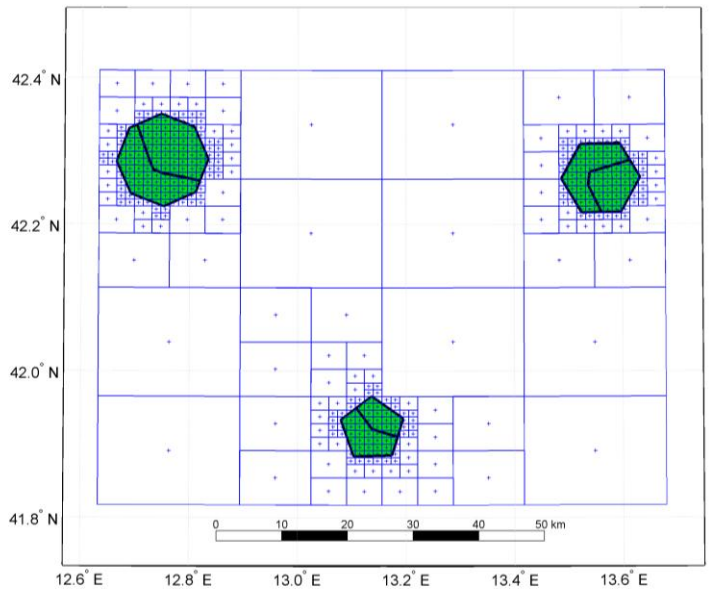

Fig. 3.5 Echo of the input: sub-city districts of each city (see Fig. 3.2), also shown the discretization of the study region into geo-cells with variable size

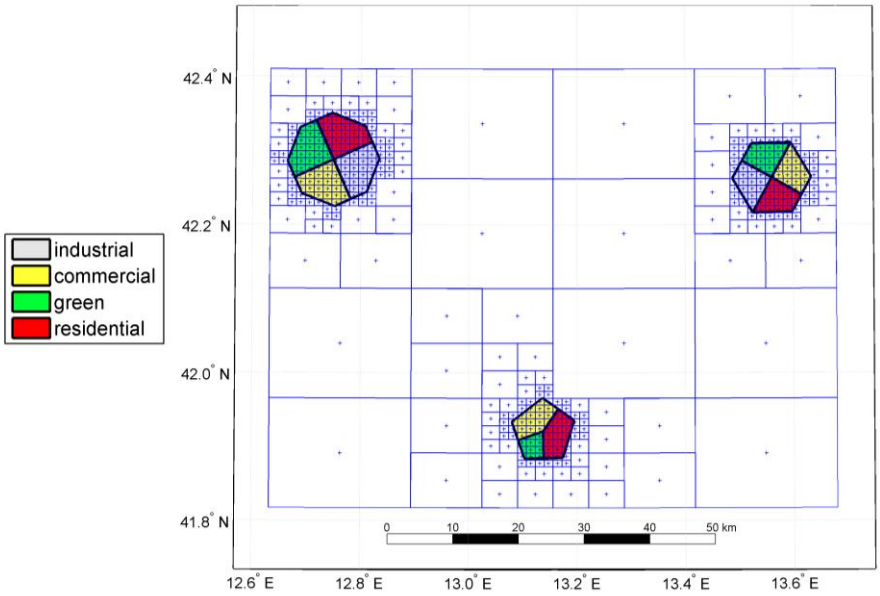

Fig. 3.6 Echo of the input: land-use plan of each city (see Fig. 3.2), also shown the discretization of the study region into geo-cells with variable size

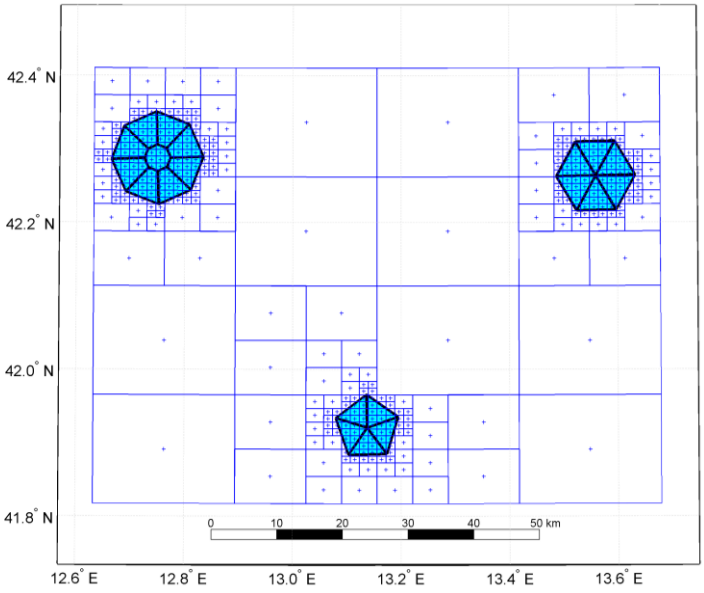

Fig. 3.7 Input echo: Building census (BC) areas of each city (see Fig. 3.2)

The method *projectToGrid* of the *InhabitedArea* class then projects the information from the EUA, BC and LUP onto the square cells. For illustration purposes, Fig. 3.8 shows the resulting map of population density in the study area.

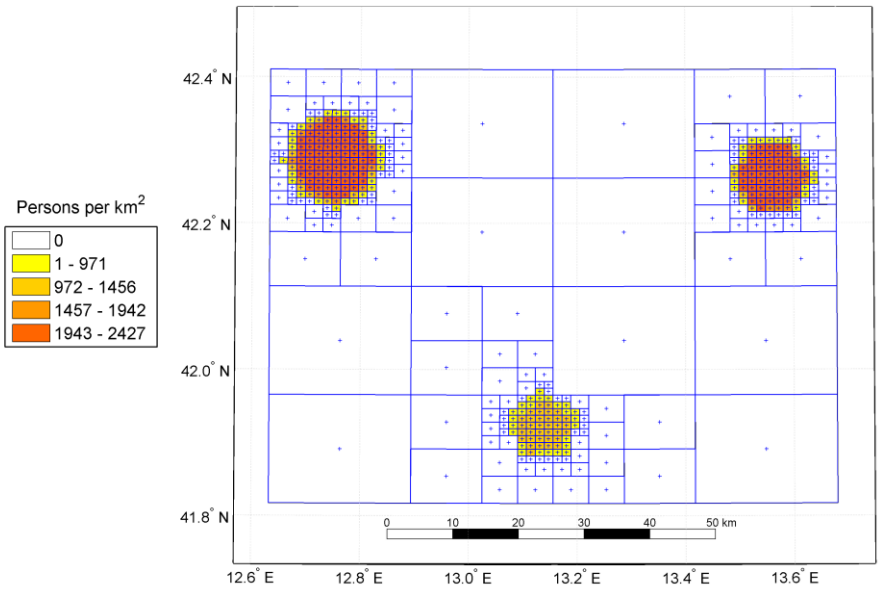

Fig. 3.8 Input echo: population density after projection onto the grid (see Fig. 3.2)

3.2.3 Demand under reference non-seismic conditions

The execution of the analysis starts with the evaluation of the Infrastructure state under the ordinary service conditions, i.e. with undamaged systems.

The demands for potable water and electric power is automatically evaluated as a function of the cell population in each cell, and then aggregated to the corresponding node of the appropriate network before running the flow analysis. Fig. 3.9 and Fig. 3.10 show the demands in each cell for the WSS and the EPN, respectively. It can be noted that the WSS in Fig. 3.9 includes more demand nodes than the network in Fig. 3.3, since for the application the pipes longer than 8 kilometres have been discretized in segments of 8 km each, in order to allow a better description of the earthquake-induced damage along these long pipes. The figures show also the configuration of the two networks, with the location of the various components. The inset in the first figure shows with dashed lines the relation between each cell and its reference node (City A). A red contour encloses the tributary cells of one of the demand nodes.

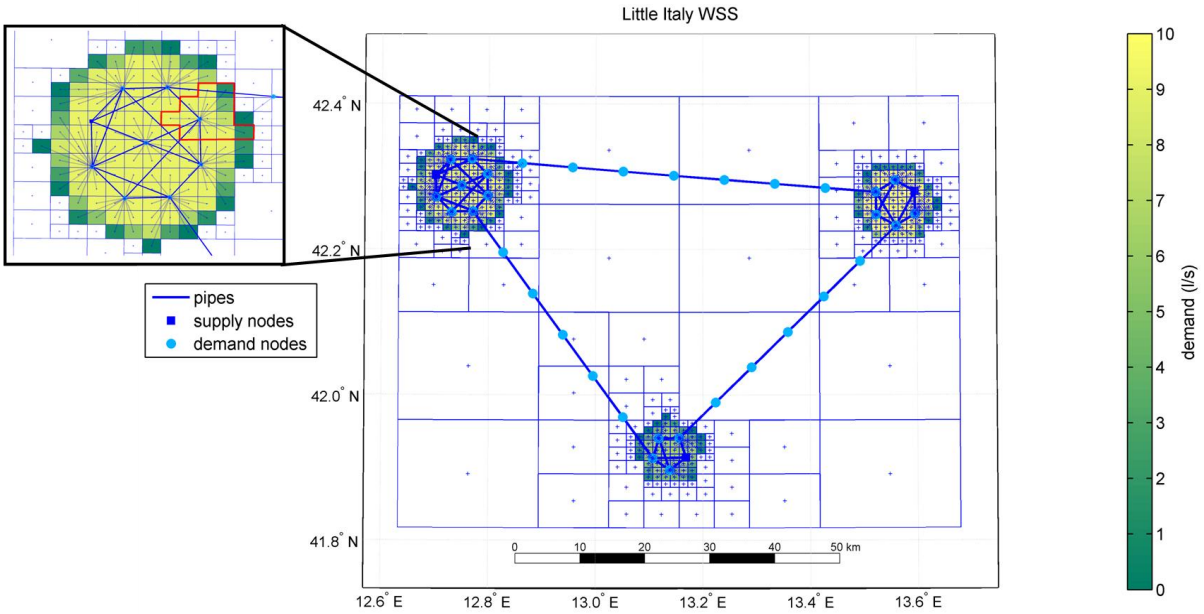

Fig. 3.9 WSS: water demand in each cell after projection onto the grid. Dashed lines show relationship between demand nodes and the tributary grid cells

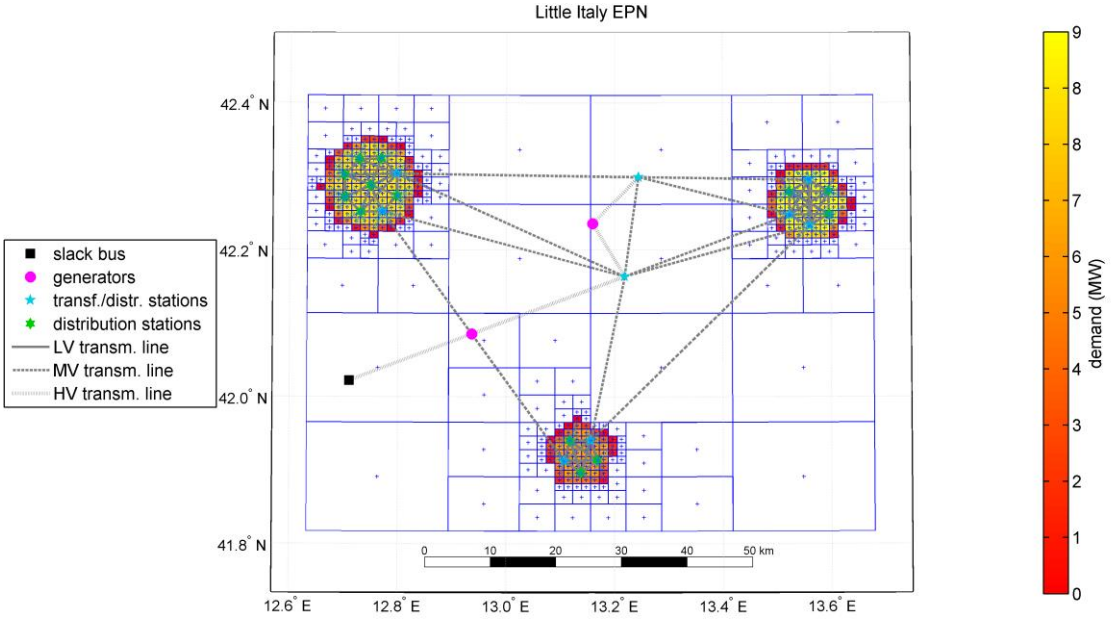

Fig. 3.10 EPN: power demand in each cell after projection onto the grid. Dashed lines show relationship between demand nodes and the tributary grid cells

3.2.4 Response under seismic conditions

Single scenario event

This section presents the results for a simulation where the magnitude and location of the event were held constant and equal to.

Fig. 3.11 shows one simulated *shake-field* of the primary IM (event on source 2, M=7, epicentre at Lat=42.3°, Long=13.7°, identified by a thick dot). Plots (a) to (c) are maps on the study region of the application. In each map the three rectangular areas are the sources. Plot (a) shows the intensity ($10^{(\mu log + \eta)}$) obtained by neglecting the intra-event terms ε, and illustrates the circular nature of the log-mean of the GMPE. Plot (b) shows the map of intra-event residuals, and small circles highlight the tendency of ε values to form cluster of size related to the correlation length. Plot (c) shows the resulting total shake-field. Plot (d) with the IMs values as a function of epicentral distance shows the exponential decay of the average intensity (including or not the inter-event residual), as well as the important intra-event deviations produced by the ε terms.

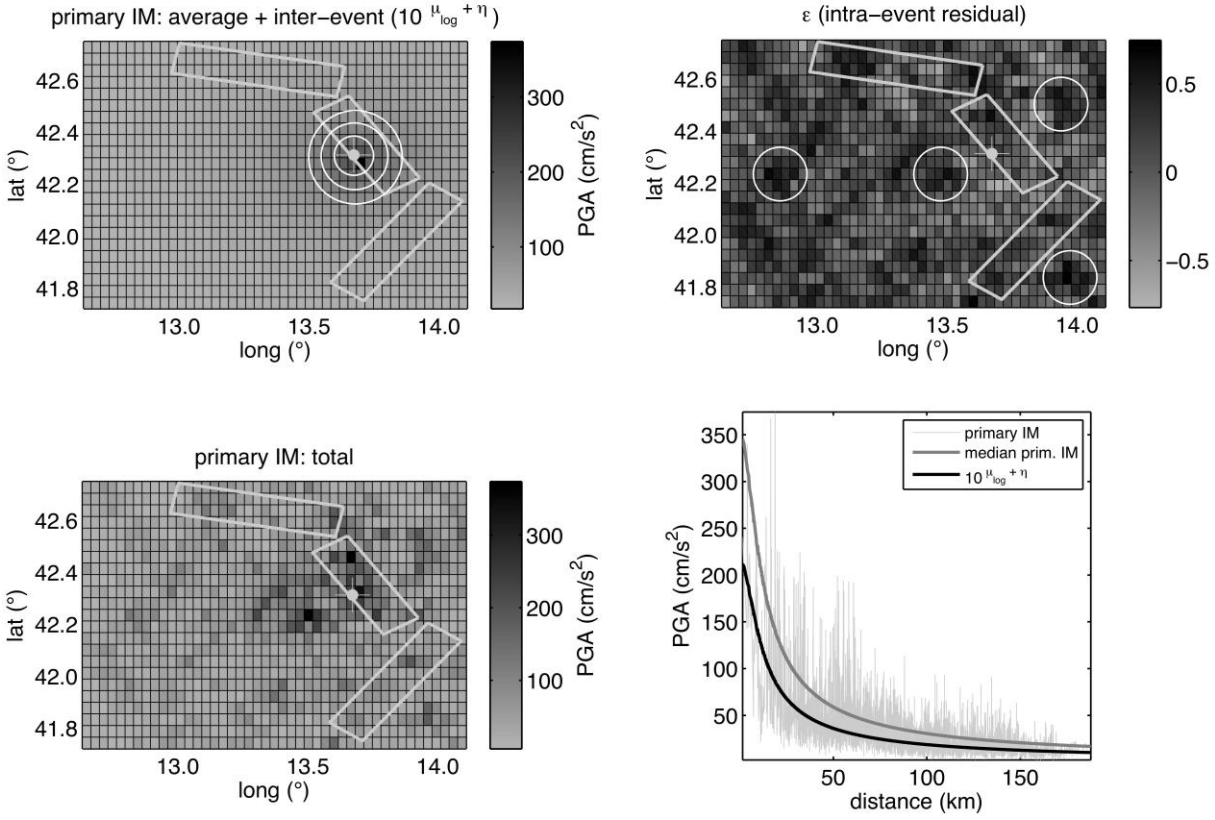

Fig. 3.11 Sample simulation of the primary IM (PGA) for a magnitude 7 event in zone 2: (a) circular decay of the 'average' value (ten to the power of μlog+η); (b) field of intra-event residuals, note the clusters of close values caused by spatial correlation; (c) total shake field; (d) plot of primary IM versus epicentral distance.

Fig. 3.12 shows the map of damage to masonry buildings. Each cell is colour-coded with one of four conditions: the cell has no buildings of the considered typology (white), the typology is present but buildings are undamaged (light grey), have exceeded yield (dark grey) or have collapsed (black). Consistently with the PGA iso-lines, damage is larger closer to the epicentre.

Fig. 3.13 shows the map of damage to RC buildings. Observations similar to the previous ones can be made. It can be further observed how damage is lower to this typology than to masonry buildings, consistently with the employed fragility curves (see Table 3.2).

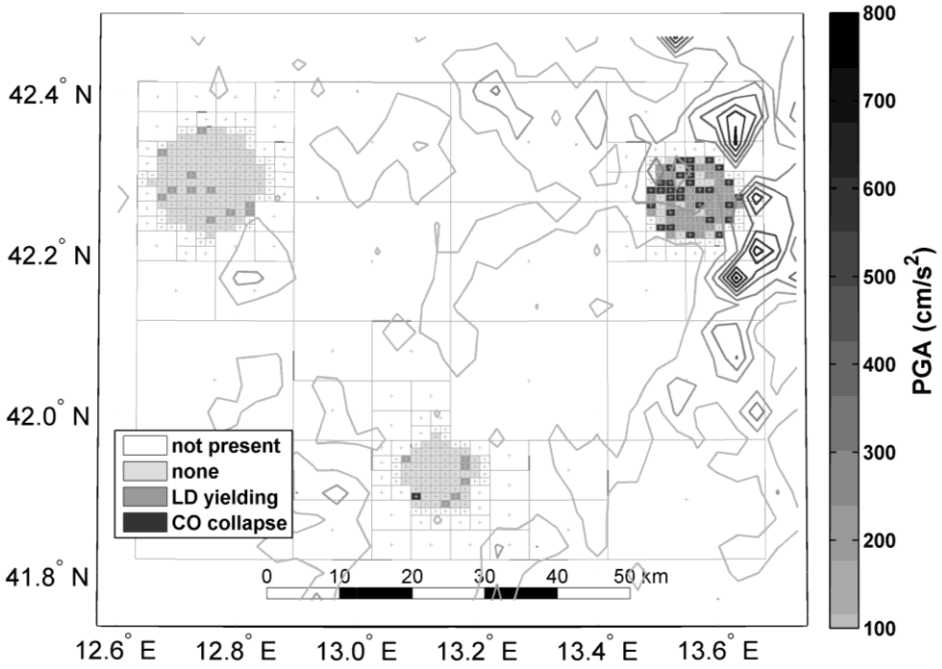

Fig. 3.12 DamageMap to Masonry buildings for one simulation of a M=7 event

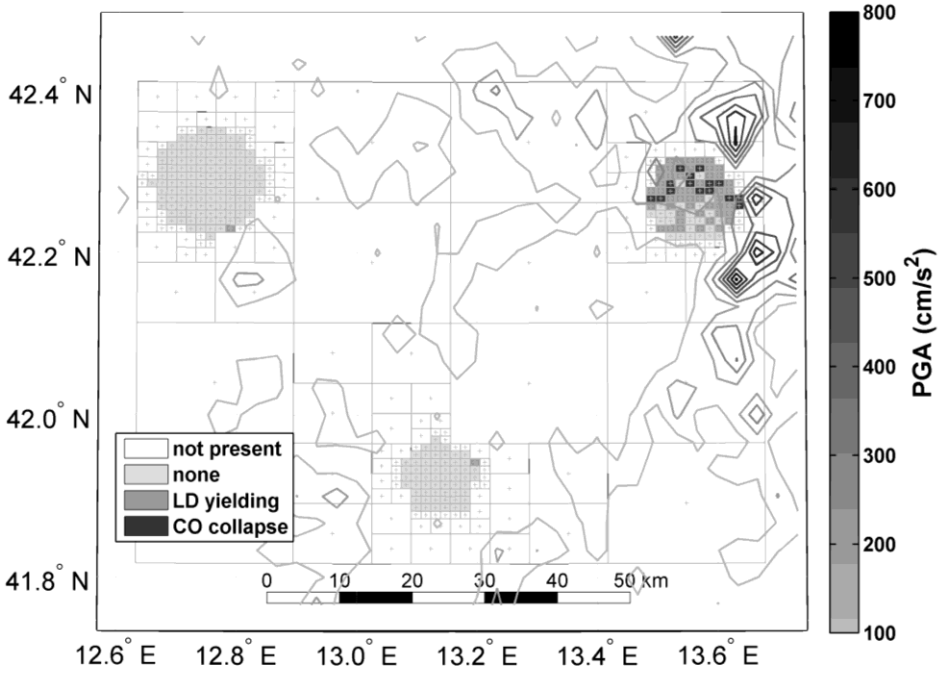

Fig. 3.13 DamageMap to RC buildings for one simulation of a M=7 event

Fig. 3.14 shows the water head ratio HR in all the cells of the grid. All tributary cells of a WSS node have the same colour node corresponding to the HR in that node (as indicated in the close-up for City A). As it can be noted, the water head for some nodes (mostly those of City B, the closest to the epicentre) can drop even to 30% of the reference head.

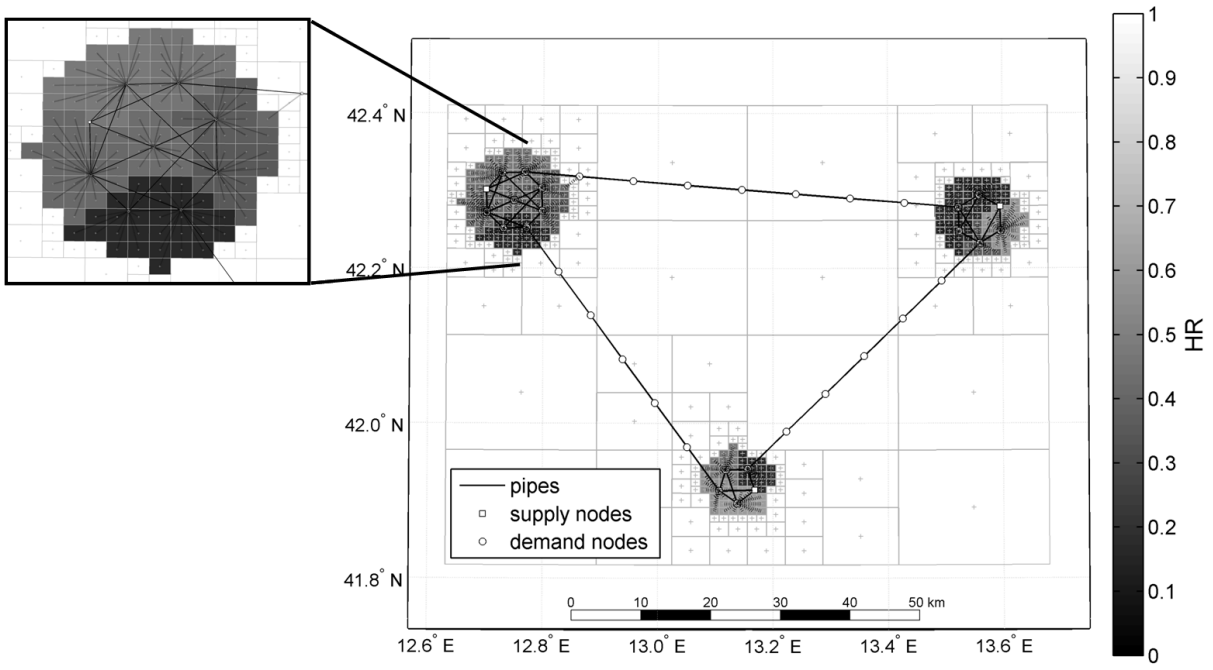

Fig. 3.14 DamageMap to the WSS for one simulation of a M=7 event

Fig. 3.15 and Fig. 3.16 illustrate the damage to the EPN. Both show the voltage ratio VR distribution in the grid cells (between 0 and 1), for two runs where damage to the network occurred (the runs differ for the random GMPE residuals but refer to the same M=7 event on source 2). In one case damage is quite severe, in the other it seems minor, but, actually, what matters is whether the supplied power has a voltage above or below the tolerance threshold, which is usually high (0.9 in this example) since the EPN is a quite stiff system. Hence, even if power is still fed to most nodes in the second run, many of these receive a “qualitatively” insufficient power feed and the corresponding utility loss, for example, would be complete making the cell buildings uninhabitable.

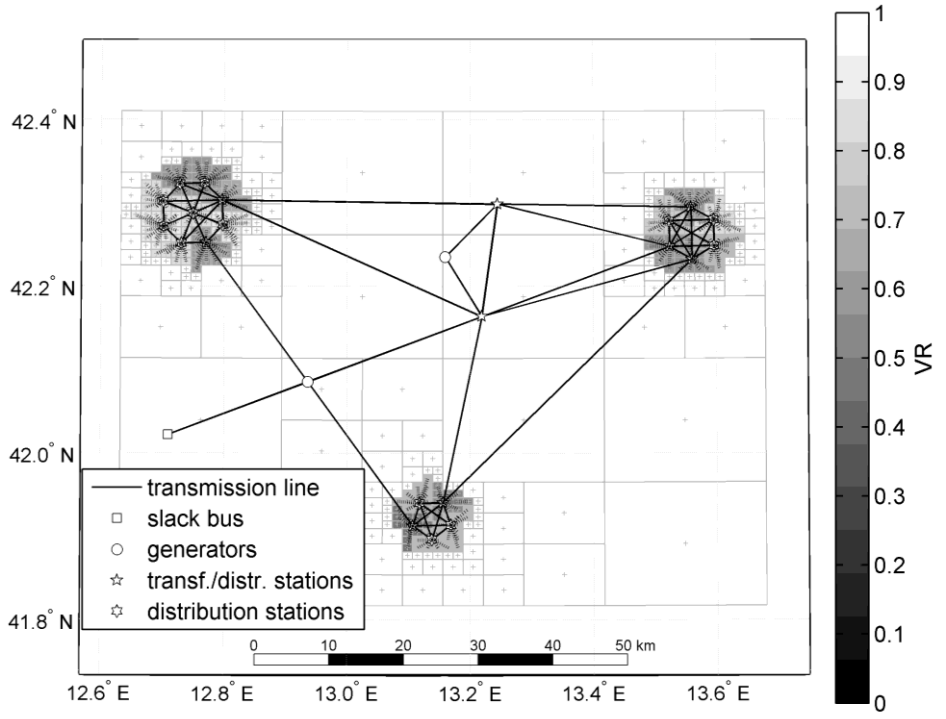

Fig. 3.15 DamageMap to the EPN for one simulation of a M=7 event: Voltage ratio VR in the grid cells (inactive lines are removed from the plot). Damage level is severe

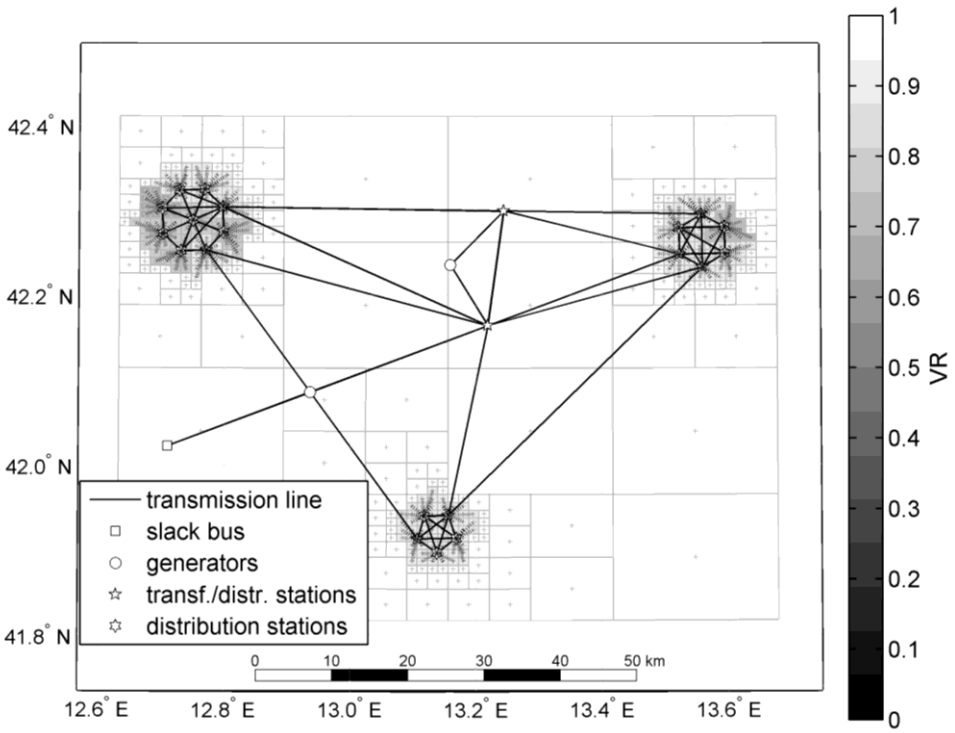

Fig. 3.16 DamageMap to the EPN for one simulation of a M=7 event: Voltage ratio VR in the grid cells (inactive lines are removed from the plot). Damage level is less severe than in Fig. 3.15

The next two figures provide an example of the evaluation of socio-economic performance measures starting from the physical damage to buildings. The model produces estimates of the number of dead people (Fig. 3.17) and displaced people (Fig. 3.18), the latter in good weather conditions. In Fig. 3.18, cells with non-zero (i.e., non-white) values of displaced people are cells that suffered from either building physical damage or reduction of service from utilities.

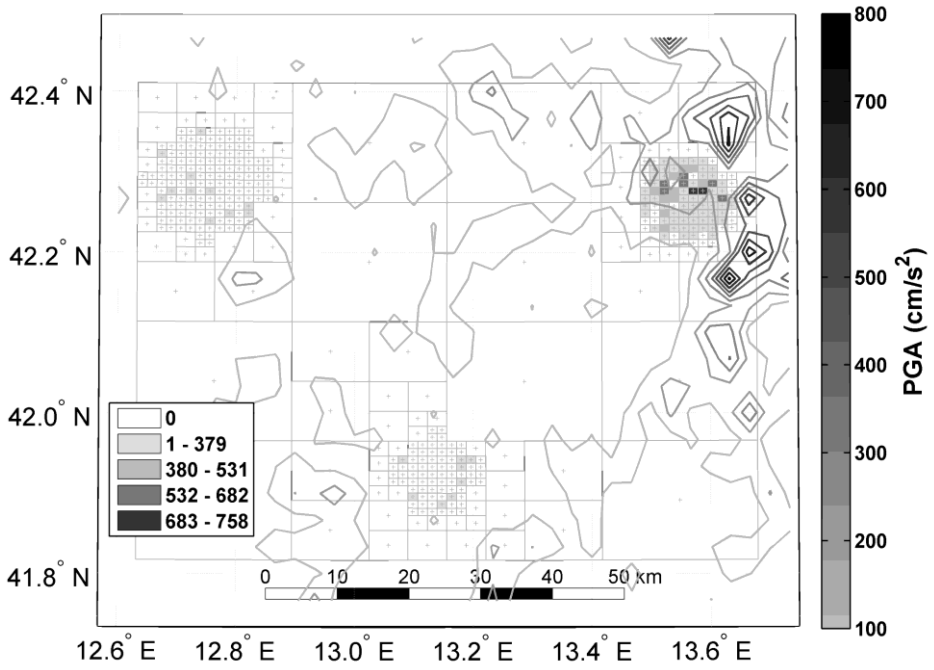

Fig. 3.17 Number of deaths for one simulation of a M=7 event

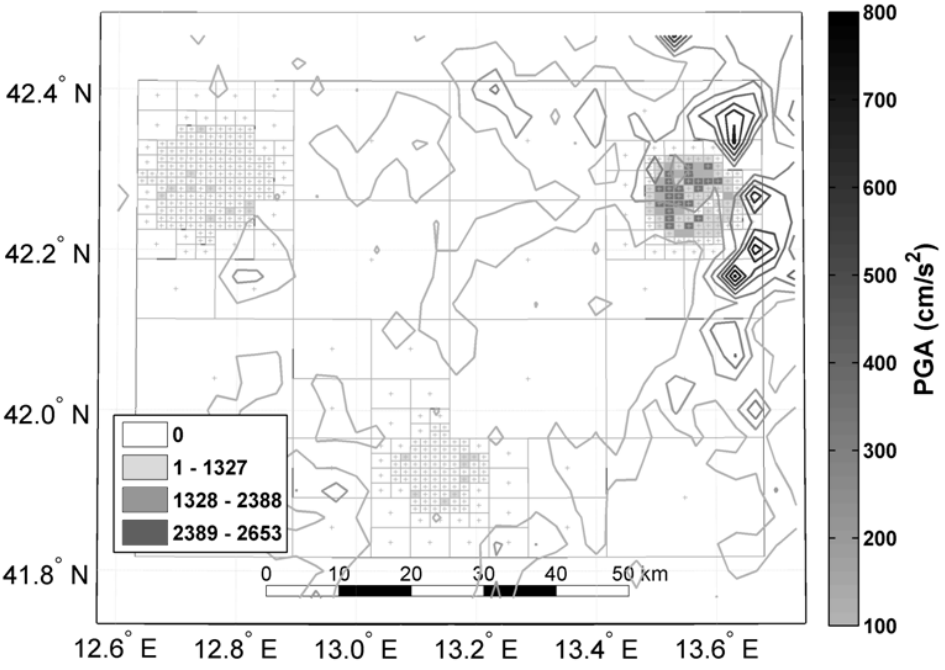

Fig. 3.18 Number of displaced people (good weather conditions) for one simulation of a M=7 event

With the aim of highlighting the influence of weather conditions and utility loss on the number of displaced people, Fig. 3.19 shows a close-up on city B, with raster maps of displaced population computed for good and bad weather conditions. For the bad weather case, the utility loss thresholds have been set to 0.4 and 0.3, for fully and partially usable buildings, respectively; whereas for the good weather case, such thresholds are 1 and 0.9, respectively. In the maps, darker colours mean higher numbers of displaced people. It is noted that the maps for the case of no utility loss (when interaction is neglected by forcing *UL* = 0) are identical for the two weather conditions because they are not affected by the difference on thresholds. On the other hand, the maps in the upper portion are significantly different, indicating the great influence of weather conditions on the number of displaced people. It can also be noted the important role played by the presence of utility loss (i.e., by the damage on utility networks) in increasing the displaced people, especially for bad weather conditions.

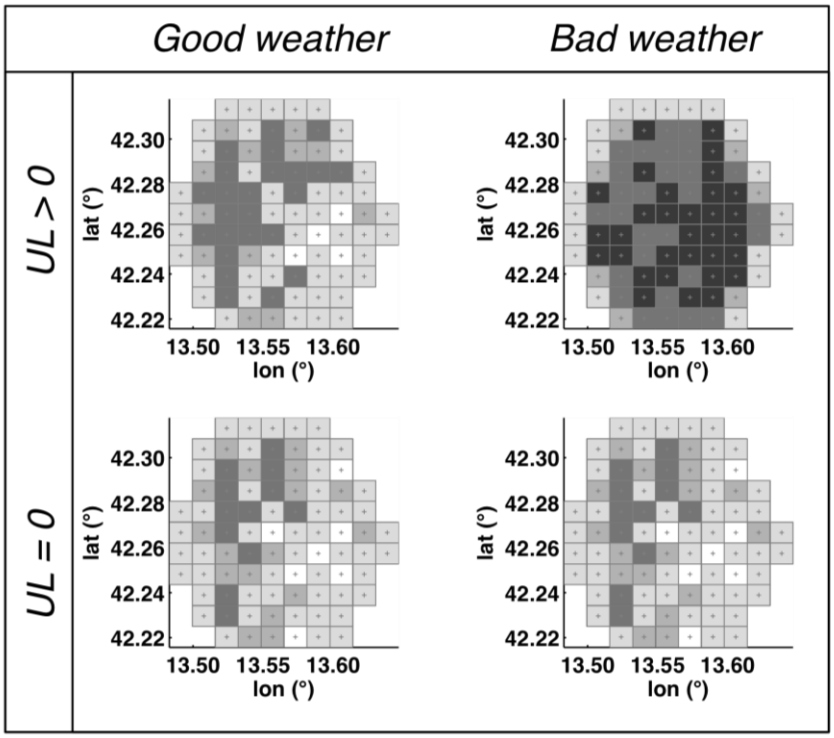

Fig. 3.19 Displaced population in the study area: and close-up on city B (same color code as in Fig. 3.18) for good/bad weather and utility loss present/not present, for the same simulation run as in Fig. 3.18

Integration over all events

This section presents the results for a simulation carried out sampling events from the three sources described in Section 3.1.1.

In the software, the plain Monte Carlo type simulation is stopped when the largest between the coefficient of variations (c.o.v.) of the estimate of the SSI and AHR indices on the WSS network (an arbitrary termination criterion) falls below a target maximum value of, say, 1%. In this case, the c.o.v. has not been monitored, since the chosen number of runs (10,000) showed to yield stable estimates for all considered indicators.

Fig. 3.20 shows a comparison of the target with the experimental distributions (the latter from simulation) for the random variable S (the active source), and for the random variable M, conditional to the active source. The top left plot shows how the simulated events respect the relative frequency of activation (rate of the source over the sum of the rates over all sources) specified in the input, while the remaining plots show that also magnitude is correctly sampled according to the Gutenberg-Richter distribution for each source.

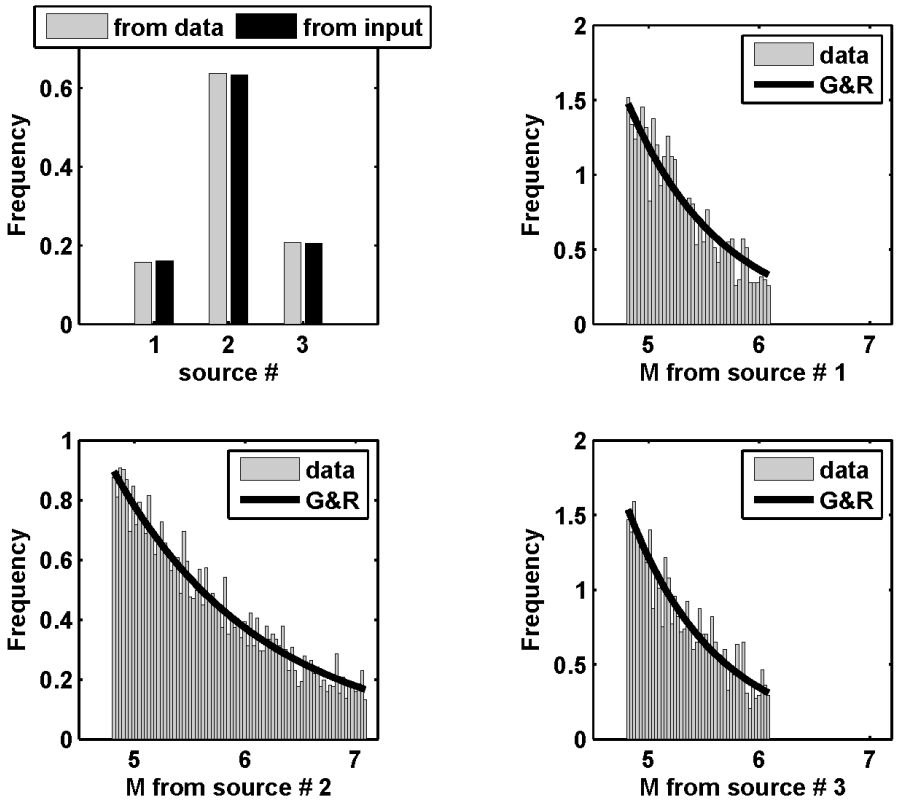

Fig. 3.20 Validation of the event generation portion of the seismic hazard model: top left, relative frequency of activation of the three faults from the simulation (light grey) and as specified in the input (black); top right and bottom plots, magnitude PDF from the Gutenberg-Richter law and the histogram of relative frequencies as obtained from simulation

Coming to results, Fig. 3.21 shows the expected value of the head ratio, estimated through 10,000 runs, in each of the WSS nodes. The left plot refers to the case where interaction between WSS and EPN is disregarded, while the right one refers to the default case of interdependent WSS and EPN. It is evident how the HR value for node # 20, one of the three water sources (which have a HR=1), and in particular the tank fed by a pump (a variableHeadSource object) falls below unity, as a consequence of the physical link existing between the pump and its reference EPN substation: in case the voltage ratio for such substation drops below the adopted threshold (in this case 0.9), the pumping station is not active and the tank is removed from the WSS, bringing node 20 to behave like a demand node. This aspect has of course an impact on the HR values of the nodes close to node 20, values resulting lower in the right plot.

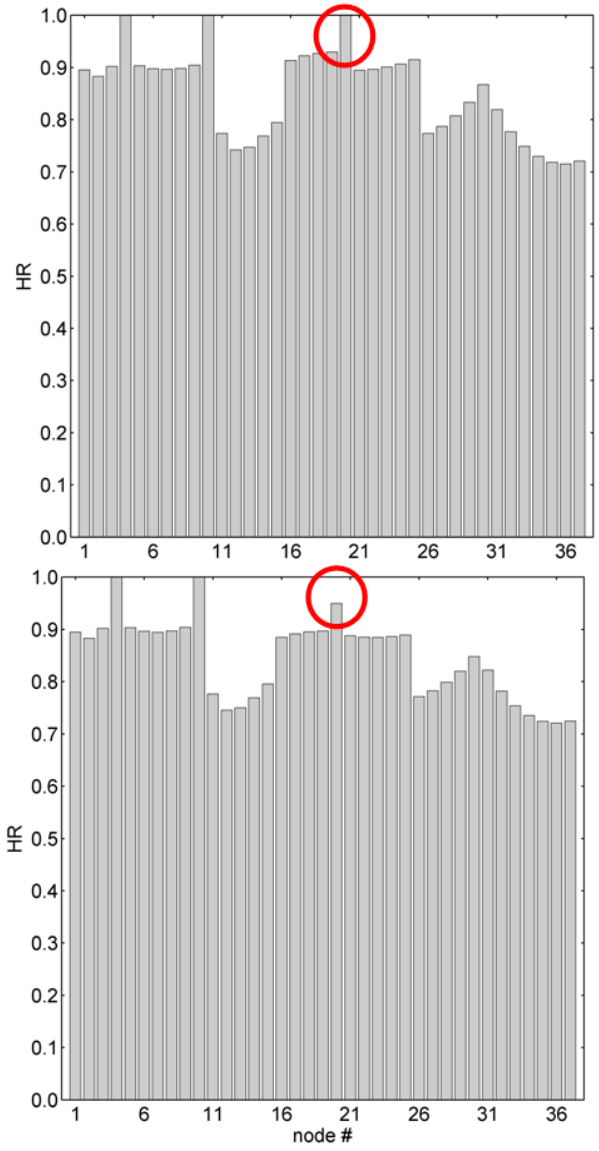

Fig. 3.21 Head ratio for all nodes, values averaged on a 10,000 run simulation: independent lifelines (left) and interdependent lifelines (right)

Fig. 3.22 shows the moving average of the AHR indicator (left) and the SSI indicator (right) for the WSS. These average quantities both stabilize after around 1,000 runs. Being the lifelines interdependent, the jumps visible for the first samples are due to both damage on WSS and damage on EPN, the latter leading to the pump at node 20 not being fed by the closer substation. In the case of independent lifelines, see Fig. 3.23, the jumps are in general smaller, being all three source nodes always present in the WSS.

The final average values for this example, however, are the same both for AHR and for SSI. This can be understood looking at the contour map in Fig. 3.24, which displays the expected values of voltage ratio VR for all EPN nodes. Since the generators are considered not vulnerable, their VR equals unity, so that they appear located in the blue “islands”. For all demand nodes, it can be noted that the expected value of VR is above 0.9, meaning that all substations are expected to deliver the requested power (i.e. the demand), considering this

seismic environment. Hence, on average (expected value), the pump feeding water in the tank at node 20 will be functional.

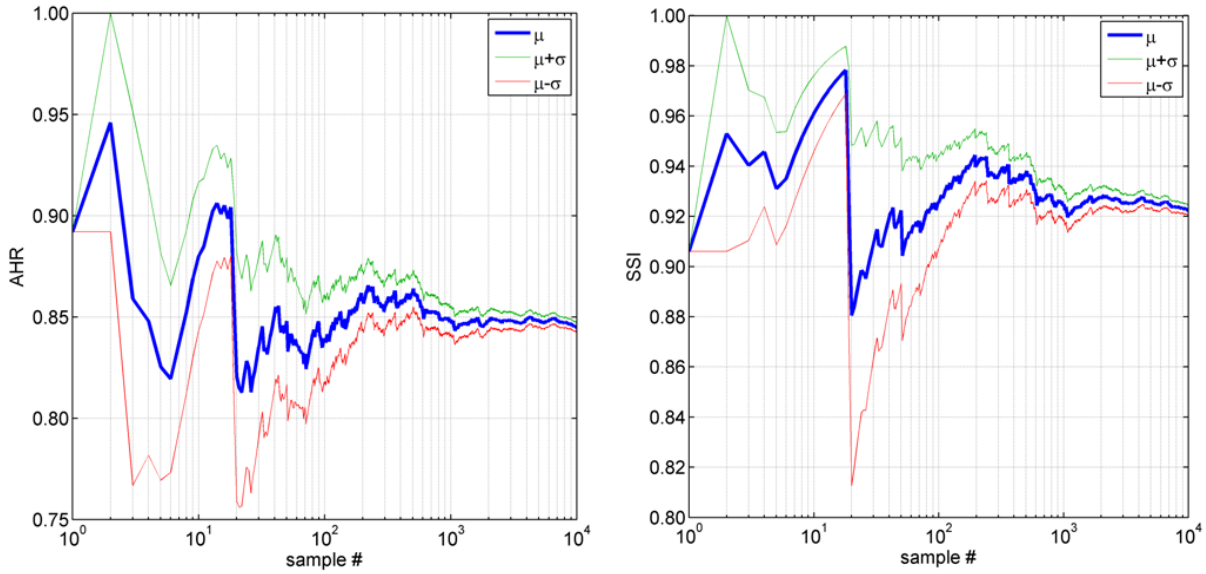

Fig. 3.22 Evolution of the mean of the average head ratio (left) and the system serviceability index (right) vs. number of samples/runs (interdependent lifelines).

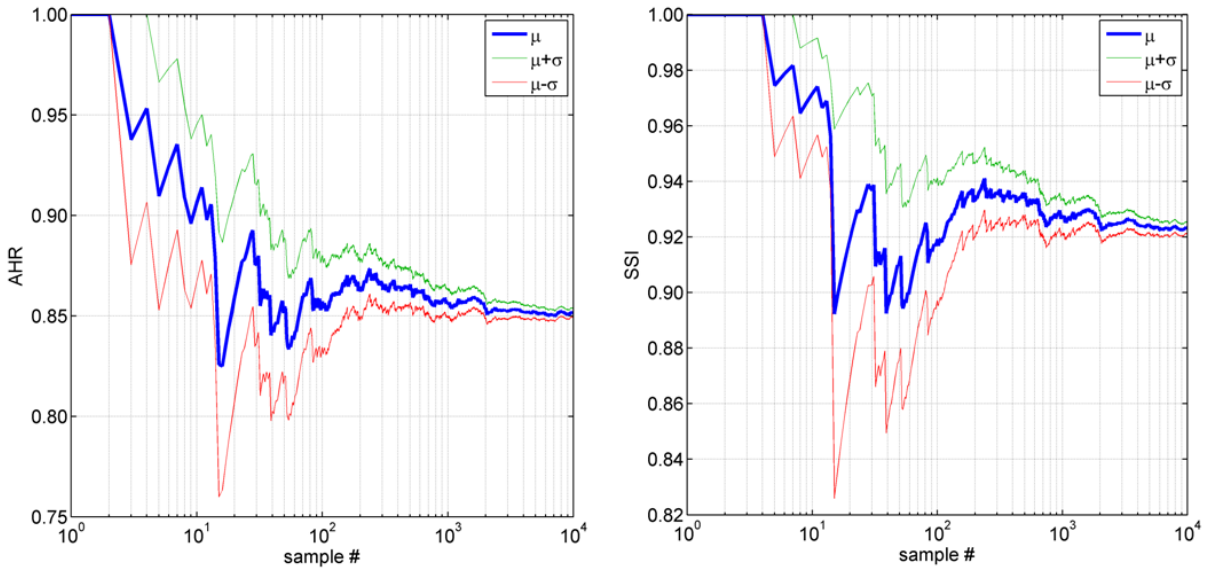

Fig. 3.23 Evolution of the mean of the average head ratio (left) and the system serviceability index (right) vs. number of samples/runs (independent lifelines)

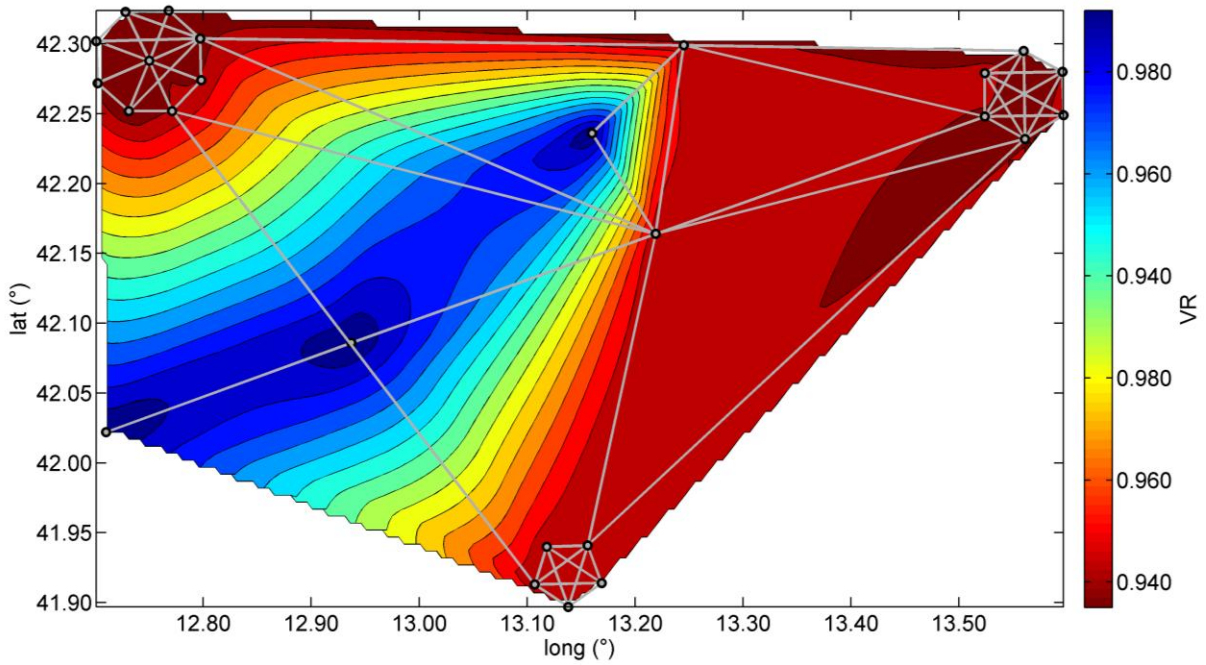

Fig. 3.24 Expected VR contour map; the blue zones indicate the generators' positions

Fig. 3.25 shows again the comparison between the cases of interdependent and independent lifelines, in terms of Mean Annual Frequency (MAF) of exceedance curves of AHR (left) and SSI (right). The influence of the dependance is not so strong with reference to these two performance metrics, in agreement with the similar patterns of moving average curves (see Fig. 3.22 and Fig. 3.23); however, the MAF values for independent lifelines are slightly higher, meaning a (unconservatively) more reliable predicted behaviour of the system.

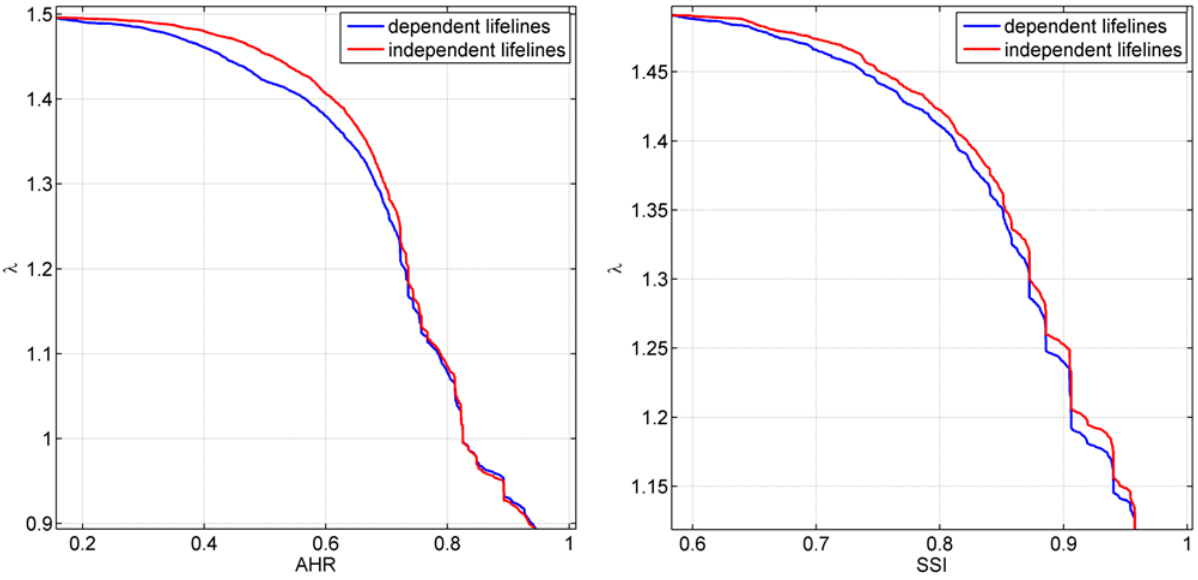

Fig. 3.25 Mean Annual Frequency (MAF) of exceedance curves of AHR (left) and SSI (right), for both cases of dependent and independent lifelines

Fig. 3.26 shows the values of the DCI (left) and UBI (right) indexes, allowing to detect, respectively, the pipes which are most critical for the system's serviceability and those whose upgrade mostly affects the system's performance.

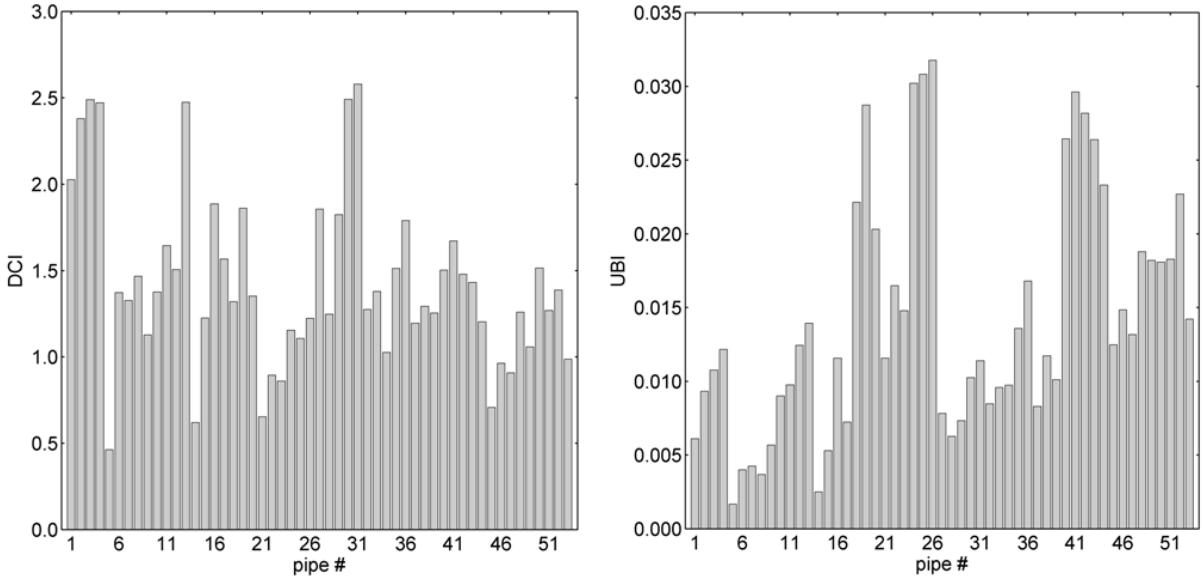

Fig. 3.26 DCI (left) and UBI (right) indexes for the pipes in WSS

Fig. 3.27 shows the MAF of exceedance curves for some socio-economic performance metrics of interest. Plot (a) refers to fatalities. Mean rates are given separately for the three cities and presented in terms of fatalities as a fraction of total population. City B, as expected, has the highest rate. All curves present a smooth behaviour. This is not the case for the MAFs of displaced population, shown in plot (b). Similar to the previous plot, rates are given by city and in terms of the ratio of displaced to total population. All cities, but in particular cities A and C, present a sharp transition close to the 100% value. This is because displaced population is influenced by utility loss, and for this simple example, the EPN is either fully functional or completely non-functional. In the latter case, independent of direct damage, buildings, even usable ones, become non-habitable and occupants are forced to evacuate. This is more apparent in cities A and C where direct physical damage is less likely due to the larger distance from the seismo-genetic sources.

To gain further insight into this effect of interdependencies captured by the model, plot (d) shows the MAF of normalized displaced population for the most affected city B under different modelling assumptions. The solid curve is the same shown in plot (b), that is, the case where utility loss is considered and the lifelines are dependent (WSS on EPN). The dashed line shows what would happen if utility loss was still considered in the evaluation of building habitability, but the interaction between the two systems was disregarded. The MAF would consistently decrease, and, most importantly, the sharp knee at around 100% would be attenuated. This attenuation would be due to the reduced vulnerability of the WSS in case the possibility of EPN-induced failure of the pumps was removed. The knee in the displaced people MAF would completely disappear, and the curve would more closely follow the trend of the fatalities MAF in plot (a) if displaced people were computed only on the basis of direct physical damage (the 'no lifelines' case).

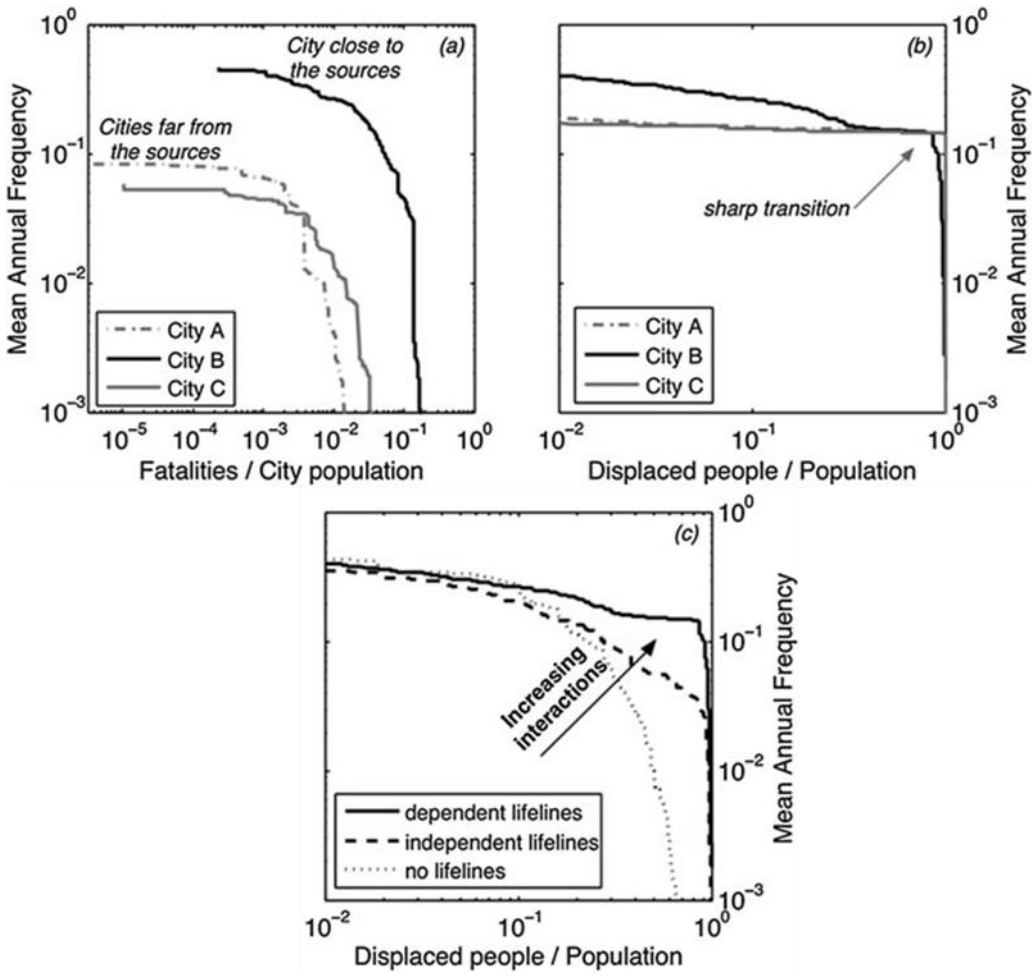

Fig. 3.27 Summary results for the whole simulation (10,000 runs). Mean annual rate of exceedance of (a) fatalities and (b) displaced population, as a ratio of total population; (c) different mean annual rates of exceedance obtained considering various levels of interaction of the normalized displaced population (curves refer to city B)

References

Alexoudi, M. 2003. *Vulnerability assessment of lifelines and essential facilities (WP06): methodological handbook Appendix 8: Electric power utility system.* RISK-UE Report: GTR-RSK 0101-152av7.

Alexoudi, M. and K. Pitilakis. 2003. *Vulnerability assessment of lifelines and essential facilities (WP06): methodological handbook Appendix 7: Gas utility system*. RISK-UE Report: GTR-RSK 0101-152av7.

American Lifelines Alliance 2001. *Seismic Fragility Formulations for Water Systems. Part 1 - Guideline*. ASCE-FEMA, 104 pp.

Applied Technology Council (ATC) 1985. *ATC-13, Earthquake Damage Evaluation Data for California*, Applied Technology Council, Redwood City, CA, 492 pp.

Applied Technology Council (ATC) 1991. *ATC-25, Seismic Vulnerability and Impact of Disruption on Conterminous* United States, Redwood City, California.

Argyroudis S., Monge O., Finazzi D., Pessina V. 2003. Vulnerability assessment of lifelines and essential facilities: methodological handbook, Appendix 1: Roadway transportation system. Report n°GTR-RSK 0101-152av7.

Avşar Ö., Yakut A., Caner A. 2011. Analytical fragility curves for ordinary highway bridges in Turkey. Earthquake Spectra 27(4): 971-996.

Bal, I.E., Bommer, J.J., Stafford, P.J., Crowley, H., Pinho, R. 2010. The Influence of Geographical Resolution of Urban Exposure Data in an Earthquake Loss Model for Istanbul. *Structural Safety* 26(3): 619-634.

Basöz, N., Kiremidjian, A.S. 1996. Risk Assessment for Highway Transportation Systems. Technical Report No. 118, John A. Blume Earthquake Engineering Center, Civil Engineering Department, Stanford University, Stanford, CA.

Bea R., 2003. Lecture notes of CE290A. University of Berkeley, California.

Calvi GM, Pinho R, Magenes G, Bommer JJ, Restrepo-Vélez LF, Crowley H. Development of seismic vulnerability assessment methodologies over the past 30 years. ISET Journal of Earthquake Technology, 2006, 43(3): 75-104.

Charleson, A. (2011) “Review of existing structural taxonomies,” Available from URL: http://www.nexus.globalquakemodel.org/gem-ontology-taxonomy/posts

Coburn A., Spence R., 1992. Earthquake protection. Chichester, England; John Wiley.

Davis D.P., Poste J.C., Hicks T., Polk D., Rymer T.E., Jacoby I, 2005. Hospital bed surge capacity in the event of a mass-casualty incident. *Prehospital Disaster Medicine* 20(3): 169–176.

De Boer J., 1995. An Introduction to Disaster Medicine in Europe. *Journal of Emergency Medicine* 13(2): 212–16.

Erdik M, Sesetyan K, Demircioglu MB, Hancilar U, Zulfikar C. Rapid earthquake loss assessment after damaging earthquakes. Soil Dyn. Earthq. Eng. 2011; 31: 247-266.

Esposito, S., 2011. Systemic seismic risk analysis of gas distribution networks. PhD Thesis, University of Naples Federico II, Italy.

Esposito, S., S. Giovinnazi and I. Iervolino, 2011. D2.4 Definition of system components and the formulation of system functions to evaluate the performance of gas and oil pipeline,

SYNER-G deliverable report D2.4.

Esposito, S. and I. Iervolino, 2011. D5-3 Systemic vulnerability and loss for gas and oil networks, SYNER-G deliverable report D5.3.

Esveld C. 2001. Modern railway track, Delft University of Technology, MRT Productions.

FEMA (1992) *FEMA 178: NEHRP Handbook for the Seismic Evaluation of Existing Buildings*. Federal Emergency Management Agency, Washington, DC.

FEMA (2003) *HAZUS-MH MR4 Technical Manual*, Federal Emergency Management Agency. http://www.fema.gov/plan/prevent/hazus/hz_manuals.shtm

FEMA. 2003. HAZUS MH MR4 Multi-hazard Loss Estimation Methodology – Earthquake Model –Technical Manual. National Institute of Building Sciences (NIBS) 2004. HAZUS-MH: Users's Manual and Technical Manuals. Report prepared for the Federal Emergency Management Agency, Washington, D.C.

Gehl, P., A. Réveillère, N/ Desramaut, H. Modaressi, A. Vagner, K. Kakderi, S. Argyroudis, K. Pitilakis, M. Alexoudi, 2010. D3-4 Fragility functions for gas and oil system networks SYNER-G deliverable reports D3.4.

Grunthal, G. (ed.), (1998) *European Macroseismic Scale 1998 (EMS-98)*. Cahiers du Centre Europeen de Geodynamique et de Seismologie 15, Centre Europeen de Geodynamique et de Seismologie, Luxembourg.

Ichii, K. 2003. *Application of Performance-Based Seismic Design Concept for Caisson-Type Quay Walls*. PhD Dissertation, Kyoto University.

International Navigation Association (PIANC) – Chairman: Iai S. 2001. *Seismic design guidelines for port structures*. Bakelma, 474p.

Jaiswal, K.S., and Wald, D.J. (2008) *Creating a Global Building Inventory for Earthquake Loss Assessment and Risk Management*, U.S. Geological Survey Open-File Report 2008-1160, 103 pp.

Kakderi, K. and K. Pitilakis 2010. Seismic analysis and fragility curves of gravity waterfront structures. In Fifth International Conference on Recent Advances in Geotechnical Earthquake Engineering and Soil Dynamics and Symposium in Honour of Professor I. M. Idriss, San Diego, CA, Paper No. 6.04a.

Kappos, A.J., Panagiotopoulos, Ch., Panagopoulos, G. and Papadopoulos, El. (2003) *RISK-UE: An advanced approach to earthquake risk scenarios with applications to different European towns.* Reinforced Concrete Buildings. Aristotle University of Thessaloniki.

LESSLOSS, 2004-2007. Risk Mitigation for Earthquakes and Landslides. *Research Project*, European Commission, Sixth Framework Programme, Priority 1.1.6.3, Global Change and Ecosystems, Contract Number: GOCE-CT-2003-505448.

Lupoi G., Franchin, P., Lupoi, A., Pinto, P.E. (2006). *Assessment of seismic performance for hospital systems*, 1st European Conference on Earthquake Engineering and Seismology, Geneva, Switzerland, 3-8 September 2006, Paper Number 98.

Lupoi, G., Franchin, P., Lupoi, A., Pinto, P.E., Calvi, G.M., 2008. Probabilistic Seismic Assessment for Hospital and Complex-Social Systems. Research Report No. ROSE-2008/02, IUSS Press, Pavia. www.iusspress.it.

Monge, O., 2003. Vulnerability assessment of lifelines and essential facilities (WP06): methodological handbook Appendix 5: Potable water utility system. RISK-UE report n° GTR-RSK 0101-152av7.

Monge, O., 2003. Vulnerability assessment of lifelines and essential facilities (WP06): methodological handbook Appendix 6: Waste-water utility system. RISK-UE report n° GTR-RSK 0101-152av7.

Monti G. and Nuti C., 1996. A procedure for assessing the functional reliability of hospital systems. *Structural Safety* 18(4): 277-92.

Moschonas, I., Kappos, A., Panetsos, P., Papadopoulos, V., Makarios, T., Thanopoulos, P. 2009. Seismic Fragility Curves for Greek Bridges: Methodology and Case Studies, *Bulletin of Earthquake Engineering*, 7(2): 439-468.

National Institute of Building Sciences (NIBS) 2004. *HAZUS-MH: Users's Manual and Technical Manuals*. Report prepared for the Federal Emergency Management Agency, Washington, D.C.

Nuti C. and Vanzi I., 1998. Assessment of post-earthquake availability of hospital system and upgrading strategies. *Earthquake Engineering & Structural Dynamics*, 27(12): 1403-1423.

PAHO, 1995. Establishing a Mass-casualty Management System. Pan American Health Organisation and World Health Organisation, Washington, DC. http://biblioteca.ucv.cl/recursos/bvd/pdf/english/m0013e/m0013e.htm

PAHO, 2000. Natural Disasters – Protecting the Public's Health. Pan American Health Organisation, Washington, DC. http://www.ops-oms.org/English/Ped/SP575/SP575_prelim.pdf

Penelis, Gr.G., Kappos, A.J., Stylianidis, K.C. and Panagiotopoulos, Ch. (2002) *RISK-UE: An advanced approach to earthquake risk scenarios with applications to different European towns.* Unreinforced Masonry Buildings. Aristotle University of Thessaloniki.

Pinto P.E., Franchin P., Lupoi A. 2009. Metodologia di valutazione del rischio delle opere d'arte. Progetto esecutivo DPC-Eucentre 2009-2012, Progetto d4: Sicurezza della rete viabilistica nazionale.

Pinto, P., F. Cavalieri, P. Franchin and I. Vanzi, 2011. D2.3 – Definition of system components and the formulation of system functions to evaluate the performance of electric power systems. SYNER-G deliverable report D2.3.

Pitilakis et al. 2010. Physical vulnerability of elements at risk to landslides: Methodology for evaluation, fragility curves and damage states for buildings and lifelines. Deliverable 2.5 in EU FP7 research project No 226479 SafeLand: Living with landslide risk in Europe: Assessment, effects of global change, and risk management strategies.

Poljanšek, K., F. Bono and E. Gutiérrez. 2010. GIS-based method to assess seismic vulnerability of interconnected infrastructure. A case of EU gas and electricity networks. JRC Scientific and Technical Reports.

Risk Management Solutions (RMS) 1996. Development of a Standardized Earthquake Loss Estimation Methodology, prepared for the National Institute of Building Sciences by Risk Management Solutions, Inc., Menlo Park, CA.

RISK-UE, 2001-2004. An Advanced Approach to Earthquake Risk Scenarios with Applications to Different European Towns. *Research Project*, European Commission, DG XII2001-2004, CEC Contract Number: EVK4-CT-2000-00014.

Saadi, H. 2002. Power system analysis - second edition. McGraw-Hill Primis Custom Publishing.

Shinozuka M., 2001. Seismic Risk Assessment of Non-structural components in Hospitals. FEMA/USC Hospital Report No. 4, University of Southern California: Los Angeles.

Straub, D., and A. Der Kiureghian. 2008. Improved seismic fragility modeling from empirical data. Structural Safety 30(4), 320–336.

Sundnes K.O. and Birnbaum M.L., 2003. Health and Disaster Management: Guidelines for Evaluation and Research in the Utstein Style. Prehospital and Disaster Medicine 17 (Supplement 3). http://pdm.medicine.wisc.edu/utstein.htm

Thompson N.G., 2001. Gas distribution. Appendix J of corrosion cost and preventative strategies. Final report. http://www.corrosioncost.com/pdf/gas.pdf.

United Nations (1993) *Housing in the World-Graphical presentation of Statistical Data: United Nations*, New York, 177pp.

UN/ISDR, 2004. Living with risk: a Global Review of Disaster Reduction Initiatives. International Strategy for Disaster Reduction. Geneva, UN Publications.

Vanzi, I. 1996. Seismic reliability of electric power networks: methodology and application. Structural Safety 18(4), 311–327.

Vanzi, I. 2000. Structural upgrading strategy for electric power networks under seismic action. Earthquake Engineering and Structural Dynamics 29(7), 1053–1073.

Werner, S. D. 1998. *Seismic guidelines for ports*. TCLEE Monograph No 12, ASCE, 366p.

Werner S.D., Taylor C.E., Cho S., Lavoie J-P., Huyck C., Eitzel C., Chung H., Eguchi R.T. 2006. REDARS 2: Methodology and Software for Seismic Risk Analysis of Highway Systems MCEER-06-SP08.

European Commission
EUR 25884 EN– Joint Research Centre – Institute for the Protection and Security of the Citizen

Title: **Methodology for systemic seismic vulnerability assessment of buildings, infrastructures, networks and socio-economic impacts**

Authors: Paolo Franchin, Amr Elnashai, Fabio Taucer, Ufuk Hancilar

Luxembourg: Publications Office of the European Union

2013 – 164 pp. – 21.0 x 29.7 cm

EUR – Scientific and Technical Research series – ISSN 1831-9424 (online), ISSN 1018-5593 (print)

ISBN 78-92-79-28975-0

doi:10.2788/69238

Abstract
The SYNER-G project aims at developing a methodology to evaluate the vulnerability to earthquakes of a complex system of interconnected infrastructural systems of regional/urban extension. This report describes the developed methodology, which is based on smart simulation of an object-oriented model of the system to account for the uncertainties involved (in the hazard, as well as in the system) and to tackle the complexity of the interactions existing within each system between its components, and across the systems. The methodology integrates within the same framework the hazard, the physical vulnerability and the social consequences/impact. The strength of the object-oriented foundation of the model is that it can be easily expanded and developed step-wise, allowing for multiple choices for each intermediate model. This allows also the integration of previous research results and models within a larger simulation framework for distributed infrastructural systems. The developed methodology is implemented in the SYNER-G software toolbox.

LB-NA25884-EN-N

As the Commission's in-house science service, the Joint Research Centre's mission is to provide EU policies with independent, evidence-based scientific and technical support throughout the whole policy cycle.

Working in close cooperation with policy Directorates-General, the JRC addresses key societal challenges while stimulating innovation through developing new standards, methods and tools, and sharing and transferring its know-how to the Member States and international community.

Key policy areas include: environment and climate change; energy and transport; agriculture and food security; health and consumer protection; information society and digital agenda; safety and security including nuclear; all supported through a cross-cutting and multi-disciplinary approach.

Publications Office

ISBN 978-92-79-28975-0

9 789279 289750